

THESIS

ASSESSING BEST MANAGEMENT PRACTICES FOR THE REMEDIATION OF
SELENIUM IN SURFACE WATER IN
AN IRRIGATED AGRICULTURAL RIVER VALLEY:
SAMPLING, MODELING, AND MULTI-CRITERIA DECISION ANALYSIS

Submitted by

Brent E. Heesemann

Department of Civil and Environmental Engineering

In partial fulfillment of the requirements

for the Degree of Master of Science

Colorado State University

Fort Collins, Colorado

Fall 2016

Master's Committee:

Advisor: Timothy K. Gates

Co-Advisor: Ryan T. Bailey

Dana L. Hoag

Copyright by Brent E. Heesemann 2016

All Rights Reserved

ABSTRACT

ASSESSING BEST MANAGEMENT PRACTICES FOR THE REMEDIATION OF SELENIUM IN SURFACE WATER IN AN IRRIGATED AGRICULTURAL RIVER VALLEY: SAMPLING, MODELING, AND MULTI-CRITERIA DECISION ANALYSIS

The ecological impacts of selenium have been studied for decades and regulatory standards established in an effort to mitigate them. Agricultural activities in regions with high levels of alluvial selenium can lead to in-stream levels that far exceed regulatory limits. Agricultural best management practices (BMPs) are being considered to reduce in-stream selenium concentrations, but exploring the potential effectiveness of these BMPs can only be done after gaining an understanding of the in-stream processes that govern the speciation and transport of selenium in response to loading from irrigation return flows. This study uses extensive field data enhanced by numerical modeling to achieve this. In-stream water and sediment selenium samples, collected over a period of eight years in a region of Colorado's Lower Arkansas River Valley, were analyzed. A sensitivity analysis (SA) was performed on a two part steady-state water quality / solute transport numerical model capable of simulating in-stream selenium processes. The combination of field data and SA was then used to calibrate an unsteady flow version of the model representative of the region to which it was applied. Dissolved and precipitated selenium species concentrations were accurately predicted by the calibrated model. Model simulations indicated that reduced fertilization is the BMP most effective at reducing in-stream SeO_4 and NO_3 concentrations out of the four BMPs examined.

Reduced irrigation, land fallowing, and canal sealing indicated increases in in-stream SeO_4 concentrations, likely caused by a concentration of SeO_4 in the adjacent aquifer. Model results also indicated that the tributaries are impacted more by surface runoff as compared to lateral groundwater flows, while the opposite is true for the River. Although reasonable results were obtained from the model, further investigation into the computational processes and calibrated parameter values is required as part of future work. This study also examines the socio-economic feasibility of various BMPs, through the issuing survey to stakeholders in the study region and its evaluation using analytic hierarchy process multi-criteria decision analysis (MCDA). Reduced irrigation was determined to be the most feasible BMP based on the MCDA, with stakeholders showing a clear preference for economic concerns and placing a higher importance on salinity over SeO_4 or NO_3 concentrations. With model results indicating the effectiveness of various BMPs, and MCDA survey results providing insight into which of the BMPs are most likely to be accepted by stakeholders, it was possible to assess which BMPs are most appropriate for implementation in this study region. In considering both the results from the modeling study and the MCDA, it was determined that reduced fertilization is likely the single best BMP. To date there have been few if any studies utilizing both field data, numerical modeling, and MCDA to so comprehensively describe in-stream selenium processes and the future prospects for selenium remediation in an agricultural region in the western United States.

ACKNOWLEDGEMENTS

I would like to thank my committee members, Dr. Timothy Gates for his continued support, conceptual insight, and motivation, Dr. Ryan Bailey for his support and unwavering willingness to assist with the many technical issues encountered along the way, and Dr. Dana Hoag for his insight and assistance in developing and issuing the survey for stakeholders in the Lower Arkansas River Valley. I would also like to thank Alex Huizenga and Erica Romero for their assistance in gathering and analyzing water quality data. I appreciate Dr. Mike Bartolo at the Colorado State University (CSU) Arkansas Valley Research Center (AVRC) for his assistance in issuing surveys and for providing the resources of the AVRC to use while on sampling trips. I would like to thank Dr. Graham Peers for his assistance and the use of his laboratory at CSU in analyzing water samples for algal concentration. I am grateful for the use of the United States Department of Agriculture (USDA) – Agricultural Research Service (ARS) lab at the Natural Resources Research Center in Fort Collins, CO, along with the expert assistance of Robin Montenieri, to analyze sediment samples. The author also recognizes Dr. Catherine Stewart for her assistance and the use of her laboratory at the USDA-ARS facility in Fort Collins in preparing samples for analysis of algal concentration. This study would not have been possible without the voluntary assistance of more than 120 landowners in Colorado’s Lower Arkansas River Valley. I greatly appreciate their cooperation and interest as well as the financial support and guidance provided by grants from the Colorado Department of Public Health and Environment, the Colorado Agricultural Experiment Station, the Southeastern Colorado Water Conservancy District, the Lower Arkansas Valley Water Conservancy District, and the United States Bureau of Reclamation.

DEDICATION

I dedicate my thesis work to my family and friends, especially my wife Masha, my parents Peter and Cathy Heesemann, my brother Scott Heesemann, and my sister Lauren Gibson. A special feeling of gratitude to my Mom and Dad, whose pride in me always has and always will motivate my life's endeavors, and whose subtle encouragement and voice of reason has repeatedly kept me from straying too far.

TABLE OF CONTENTS

ABSTRACT.....	ii
ACKNOWLEDGEMENTS.....	iv
DEDICATION.....	v
TABLE OF CONTENTS.....	vi
LIST OF TABLES.....	viii
LIST OF FIGURES.....	x
CHAPTER 1: Literature Review and Research Objectives.....	1
1.1 Selenium in the Aqueous Environment.....	1
1.2 Agricultural Best Management Practices to Mitigate Se Pollution.....	6
1.3 Multi-Criteria Decision Analysis.....	9
1.4 Research Objectives.....	12
CHAPTER 2: Methods.....	14
2.1 Site Description.....	14
2.2 Sampling and Analysis of Se and Related Constituent Concentrations in Streams ...	16
2.2.1 Selenium, Uranium, and Irrigation Water Quality.....	16
2.2.2 Algae.....	21
2.2.3 Stream Flow Rate.....	26
2.2.4 Stream Cross-Section Geometry.....	27
2.3 Modeling of Selenium Reactive Transport.....	29
2.3.1 Se In-Stream Water Quality Model (OTIS-QUAL2E-Se).....	29
2.3.2 Coupled Surface Water – Groundwater Reactive Transport Model (RT3D-OTIS)	41
2.4 Multi-Criteria Decision Analysis.....	48
2.4.1 Overview.....	48
2.4.2 The AHP Method.....	50
2.4.3 AHP Applied to the LARV.....	54
CHAPTER 3: Results and Discussion.....	57
3.1 Se and Related Parameters in Water and Sediment Samples.....	57
3.2 Model Predictions of Se in the Stream Network.....	66
3.2.1 OTIS-QUAL2E-Se Sensitivity Analysis.....	66
3.2.2 OTIS-QUAL2E-Se Unsteady Flow Model Calibration.....	75

3.2.3	OTIS-QUAL2E-Se General Observations	83
3.2.4	RT3D-OTIS Testing and Calibration	83
3.2.5	RT3D-OTIS General Observations	89
3.2.6	Best Management Practice Analysis Using RT3D-OTIS	92
3.3	Multi-Criteria Decision Analysis.....	110
3.3.1	Main Criteria for BMP Decision Making	111
3.3.2	Sub-Criteria for BMP Decision Making	113
3.3.3	BMP Ranks	116
3.3.4	General Observations	119
CHAPTER 4: Conclusion		123
APPENDIX A: Supplementary Information		129
REFERENCES		139

LIST OF TABLES

TABLE 2-1. UTM NAD83 COORDINATES OF THE 18 LOCATIONS SAMPLED AS PART OF THIS STUDY.	18
TABLE 2-2. LENGTH OF BASE STATION STATIC DATA OBSERVATION AND ASSOCIATED VERTICAL AND HORIZONTAL ROOT MEAN SQUARED VERTICAL AND HORIZONTAL ERROR FOR THE TOPCON RTK-GPS (WWW.TOPCONPOSITIONING.COM).	28
TABLE 2-3. BMPS EXAMINED USING THE RT3D-OTIS MODEL FOR THE PURPOSE OF LOWERING IN-STREAM SE CONCENTRATIONS IN THE LARV.	45
TABLE 2-4. SAATY SCALE AND ASSOCIATED QUALITATIVE DESCRIPTIONS (ALPHONCE, 1997).	52
TABLE 2-5. RANDOM INDEX (RI) ASSOCIATED WITH AN $N \times N$ SQUARE MATRIX.	54
TABLE 2-6. THE AHP SURVEY STRUCTURE ADMINISTERED IN THE LARV USR.	55
TABLE 2-7. MODIFIED SAATY SCALE USED FOR THE AHP BMP SURVEY IN THE LARV USR.	55
TABLE 3-1. AVERAGE WATER QUALITY DATA COLLECTED FROM LOCATIONS IN THE ARKANSAS RIVER AND ITS TRIBUTARIES FROM 2006-2010.	57
TABLE 3-2. AVERAGE SEDIMENT AND ASSOCIATED WATER QUALITY SELENIUM DATA COLLECTED FROM LOCATIONS IN THE ARKANSAS RIVER AND ITS TRIBUTARIES FROM 2011-2014.	58
TABLE 3-4. CORRELATION COEFFICIENT / LEVEL OF SIGNIFICANCE (R) VALUES BETWEEN SE SPECIES AND OTHER DISSOLVED IONS. STATISTICALLY SIGNIFICANT CORRELATIONS (≥ 0.50 OR ≤ -0.50 , CORRESPONDING TO A P-VALUE OF APPROXIMATELY 0.01 OR SMALLER) ARE SHOWN IN BOLD.	63
TABLE 3-5. CORRELATION COEFFICIENT / LEVEL OF SIGNIFICANCE (R) VALUES BETWEEN SE SPECIES AND DISSOLVED NUTRIENTS. STATISTICALLY SIGNIFICANT CORRELATIONS (≥ 0.50 OR ≤ -0.50 , CORRESPONDING TO A P-VALUE OF APPROXIMATELY 0.01 OR SMALLER) ARE SHOWN IN BOLD.	64
TABLE 3-6. CORRELATION COEFFICIENT / LEVEL OF SIGNIFICANCE (R) VALUES BETWEEN SE SPECIES AND OTHER WATER PROPERTIES. STATISTICALLY SIGNIFICANT CORRELATIONS (≥ 0.50 OR ≤ -0.50 , CORRESPONDING TO A P-VALUE OF APPROXIMATELY 0.01 OR SMALLER) ARE SHOWN IN BOLD.	64
TABLE 3-7. CORRELATION COEFFICIENT / LEVEL OF SIGNIFICANCE (R) VALUES BETWEEN SE SPECIES. STATISTICALLY SIGNIFICANT CORRELATIONS (≥ 0.50 OR ≤ -0.50) ARE SHOWN IN BOLD.	64
TABLE 3-8. SENSITIVE MODEL PARAMETERS IDENTIFIED IN THE SA.	67
TABLE 3-9. OBSERVED AND MODEL-PREDICTED MEAN AND COEFFICIENT OF VARIATION (CV) OF CONSTITUENT CONCENTRATIONS FOR SAMPLES GATHERED AT ALL ARKANSAS RIVER AND TRIBUTARY OBSERVATION LOCATIONS.	78
TABLE 3-10. SPATIO-TEMPORALLY AVERAGED OBSERVED AND SIMULATED CONCENTRATIONS OF SeO_4 , SeO_3 , NO_3 , AND DO FOR THE ARKANSAS RIVER.	91

TABLE 3-11. SPATIO-TEMPORALLY AVERAGED OBSERVED AND SIMULATED CONCENTRATIONS OF SEO_4 , SEO_3 , NO_3 , AND DO FOR THE TRIBUTARIES OF THE ARKANSAS RIVER.....	91
TABLE 3-12. CHANGES IN SEO_4 CONCENTRATION ASSOCIATED WITH EACH BMP EXAMINED.	110
TABLE A-1. BASELINE AND STRESSED PARAMETER VALUES USED IN THE OTIS-QUAL2E-SE SA.....	130
TABLE A-2. WATER QUALITY DATA COLLECTED FROM LOCATIONS IN THE ARKANSAS RIVER AND ITS TRIBUTARIES FROM 2006-2010.....	131
TABLE A-3. SEDIMENT AND ASSOCIATED WATER QUALITY SELENIUM DATA COLLECTED FROM LOCATIONS IN THE ARKANSAS RIVER AND ITS TRIBUTARIES FROM 2011-2014.....	133

LIST OF FIGURES

FIGURE 1-1. CONCEPTUAL MODEL FOR IN-STREAM SE CYCLING.....	3
FIGURE 2-1. LOWER ARKANSAS RIVER VALLEY UPSTREAM STUDY REGION (USR) IN SOUTHEASTERN COLORADO, SHOWING CULTIVATED FIELDS, THE ARKANSAS RIVER, TRIBUTARIES, AND STREAM SAMPLING LOCATIONS.....	17
FIGURE 2-2. DH-48 SEDIMENT SAMPLER USED FOR COMPOSITE SE SAMPLING IN THE WATER COLUMN.....	19
FIGURE 2-3. EXAMPLE SYRINGE, GF/F, AND CASSETTE CONFIGURATION USED TO SEPARATE SUSPENDED ALGAE (WWW.FISHERSCI.COM).....	22
FIGURE 2-4. REGRESSION ANALYSIS OF CHL(A) CONCENTRATION AND RFU READING FOR THE TURNER DESIGNS TRILOGY FLUOROMETER.....	23
FIGURE 2-5. TURNER DESIGNS LABORATORY FLUOROMETER USED TO MEASURE THE RELATIVE FLUORESCENCE UNITS OF EXTRACTED CHLOROPHYLL (A) SOLUTIONS.....	24
FIGURE 2-6. LABCONCO FREEZONE 4.5 LITER LYOPHILIZER USED FOR DRYING CHLOROPHYLL (A) SEDIMENT SAMPLES.....	25
FIGURE 2-7. SONTEK FLOWTRACKER HANDHELD ADV (WWW.SONTEK.COM).....	26
FIGURE 2-8. TOPCON RTK-GPS BASE STATION, ROVER, AND ANCILLARY SURVEYING EQUIPMENT.....	27
FIGURE 2-9. MODEL STUDY REGION SHOWING THE MODEL BOUNDARIES AND THE STREAM NETWORK COMPUTATIONAL GRID FOR THE OTIS-QUAL2E-SE MODEL.....	36
FIGURE 2-10. GENERAL AHP STRUCTURE, INCLUDING MAIN CRITERIA (C1, C2), SUB-CRITERIA (SC1,1, SC1,2, SC2,1, SC2,2), AND ALTERNATIVES (A1, A2, A3, A4, A5). THE HIERARCHICAL STRUCTURE OF THE AHP IS SHOWN, WHEREBY PAIRWISE COMPARISONS ARE MADE AT EACH LEVEL (ARROWS) WITH RESPECT TO THE CRITERIA PRECEDING THEM (LINES).....	51
FIGURE 2-11. THE SET OF POSSIBLE RANKS WHEN QUANTIFYING THE PREFERENCE FOR ONE CRITERIA OR ALTERNATIVE OVER ANOTHER (ALPHONCE ,1997).....	52
FIGURE 2-12. PAIRWISE COMPARISON MATRIX ‘A’ CONTAINING THE SCORES ASSOCIATED WITH ALL POSSIBLE PAIRWISE COMPARISONS AT A GIVEN LEVEL OF AN AHP HIERARCHY.....	52
FIGURE 3-1. MAXIMUM, MINIMUM, MEDIAN, AND 1ST AND 3RD QUARTILES OF (A) TOTAL DISSOLVED SE SAMPLES COLLECTED FROM 2006-2014 IN THE ARKANSAS RIVER (95 SAMPLES) AND TRIBUTARIES (57 SAMPLES), (B) TOTAL PARTICULATE SE SAMPLES COLLECTED FROM 2007-2014 IN THE ARKANSAS RIVER (17 SAMPLES) AND TRIBUTARIES (3 SAMPLES), (C) SORBED SE SAMPLES COLLECTED FROM 2011-2014 IN THE ARKANSAS RIVER (28 SAMPLES) AND TRIBUTARIES (18 SAMPLES), (D) PRECIPITATED AND ORGANIC SE SAMPLES COLLECTED FROM 2011-2014 IN THE ARKANSAS RIVER (25 SAMPLES) AND TRIBUTARIES (17 SAMPLES), (E) NO ₃ SAMPLES COLLECTED FROM 2006-2014 IN THE ARKANSAS RIVER (71 SAMPLES) AND TRIBUTARIES (39 SAMPLES), (F) DO SAMPLES	

COLLECTED FROM 2006-2014 IN THE ARKANSAS RIVER (72 SAMPLES) AND TRIBUTARIES (40 SAMPLES), (G) PH SAMPLES COLLECTED FROM 2013-2014 IN THE ARKANSAS RIVER (24 SAMPLES) AND TRIBUTARIES (16 SAMPLES), (H) EC SAMPLES COLLECTED FROM 2013-2014 IN THE ARKANSAS RIVER (20 SAMPLES) AND TRIBUTARIES (15 SAMPLES), (I) ORP SAMPLES COLLECTED FROM 2013-2014 IN THE ARKANSAS RIVER (20 SAMPLES) AND TRIBUTARIES (15 SAMPLES), AND (J) SUSPENDED ALGAE SAMPLES COLLECTED FROM 2013-2014 IN THE ARKANSAS RIVER (84 SAMPLES) AND TRIBUTARIES (104 SAMPLES). 61

FIGURE 3-2. PLOTS OF SOLUTE AND SORBED/REDUCED SE PREDICTED BY THE STEADY-FLOW MODEL FOR AUGUST 11, 2006 FOR (A) DISSOLVED SeO_4 , (B) DISSOLVED SeO_3 , (C) TOTAL SORBED SeO_4 AND SeO_3 , (D) Se^0 , (E) NO_3 , AND (F) DO. 66

FIGURE 3-3. CONCENTRATIONS OF DISSOLVED SeO_4 , DISSOLVED SeO_3 , NO_3 , AND DO AT A LOCATION ALONG THE ARKANSAS RIVER (ARK12) (A-D) AND AT A LOCATION ALONG TIMPAS CREEK (TIMPAS CREEK 2) (E-H) PREDICTED BY THE STEADY-FLOW MODEL THROUGH THE 2-YEAR SIMULATION PERIOD. 67

FIGURE 3-4. NORMALIZED MODEL RESPONSE TO PARAMETER STRESS FOR IDENTIFIED INFLUENTIAL PARAMETERS FOR IN-STREAM (A) DO, (B) NO_3 , AND (C) ALGAE CONCENTRATIONS, AND THE RELATIONSHIP BETWEEN PARAMETER VALUE AND MODEL OUTPUT FOR IDENTIFIED INFLUENTIAL PARAMETERS FOR IN-STREAM (D) DO, (E) NO_3 , AND (F) ALGAE CONCENTRATIONS. PARAMETER $\lambda_{Alg_{max}}$ WAS NOT SHOWN IN (A) OR (C) DUE TO THE MAGNITUDE OF THE NORMALIZED MODEL RESPONSE TO ITS STRESS. 69

FIGURE 3-5. NORMALIZED SPATIO-TEMPORAL AVERAGED BASELINE MODEL RESPONSE TO PARAMETER STRESSES FOR IN-STREAM (A) DISSOLVED SeO_4 AND SeO_3 , (B) SORBED SeO_4 AND SeO_3 , AND (C) Se^0 AND Se^{2-} . CORRESPONDING RESULTS FOR THE LOW- NO_3 BASELINE MODEL SIMULATION ARE SHOWN IN (D), (E), AND (F). 70

FIGURE 3-6. SENSITIVITY TRENDS AND RANKING OF INFLUENTIAL PARAMETERS FOR IN-STREAM (A) DISSOLVED SeO_4 , (B) DISSOLVED SeO_3 , (C) SORBED SeO_4 , (D) SORBED SeO_3 , (E) Se^0 , AND (F) Se^{2-} . MODEL RESPONSES ARE CALCULATED USING SPATIO-TEMPORAL AVERAGED MODEL OUTPUT. 72

FIGURE 3-7. OBSERVED AND MODFLOW-SFR PREDICTED FLOW RATES IN THE ARKANSAS RIVER AT LOCATIONS (A) ARK12 AT ROCKY FORD AND (B) ARK95 AT LA JUNTA. 77

FIGURE 3-8. OBSERVED AND SIMULATED DISSOLVED SeO_4 , DISSOLVED SeO_3 , NO_3 , AND DO FOR (A) ARK 164, (B) PATTERSON HOLLOW, (C) CROOKED ARROYO 2, AND (D) ARK 95. 78

FIGURE 3-9. SIMULATED VERSUS OBSERVED VALUES FOR (A) DISSOLVED SeO_4 , (B) DISSOLVED SeO_3 , (C) NO_3 , AND (D) DO AT LOCATIONS IN THE ARKANSAS RIVER AND TRIBUTARIES. 80

FIGURE 3-10. OBSERVED AND SIMULATED SPATIO-TEMPORAL AVERAGED SE PARTITIONING IN SEDIMENT FOR (A) THE ARKANSAS RIVER AND (B) ITS TRIBUTARIES. 82

FIGURE 3-11. RT3D-OTIS SIMULATED AND OBSERVED DO CONCENTRATIONS USING DEFAULT RT3D-OTIS PARAMETERS AT OBSERVATION LOCATIONS (A) ARK164, (B) TIMPAS2, AND (C) ARK95.....	85
FIGURE 3-12. BASELINE RT3D-OTIS SIMULATED AND OBSERVED VALUES AT OBSERVATION LOCATION CROOKED 2 FOR (A) SeO_4 AND (B) AND (C) NO_3	86
FIGURE 3-13. RT3D-OTIS SIMULATED AND OBSERVED CONCENTRATIONS USING PARAMETER VALUES FROM THE OTIS-QUAL2E-SE MODEL AT OBSERVATION LOCATION CROOKED ARROYO 2 FOR (A) SeO_4 AND (B) NO_3	87
FIGURE 3-14. RT3D-OTIS BASELINE SIMULATED VALUES OF SeO_4 , SIMULATED VALUES OF SeO_4 WITH INCREASED λ_{SeO_4RH} , AND OBSERVED VALUES OF SeO_4 AT OBSERVATION LOCATION ARK 127.....	89
FIGURE 3-15. RT3D-OTIS BASELINE SIMULATIONS, SIMULATIONS USING SA PARAMETER VALUES, AND SIMULATIONS USING CALIBRATED PARAMETER VALUES AT OBSERVATION LOCATION ARK 127 FOR (A) SeO_4 AND (B) NO_3	90
FIGURE 3-16. RT3D-OTIS BASELINE SIMULATIONS, SIMULATIONS USING SA PARAMETER VALUES, AND SIMULATIONS USING CALIBRATED PARAMETER VALUES AT OBSERVATION LOCATION ARK 95 FOR (A) SeO_4 AND (B) NO_3	90
FIGURE 3-18. PERCENT CHANGE FROM THE SPATIO-TEMPORAL AVERAGED BASELINE SeO_4 GROUNDWATER (GW) CONCENTRATION, RUNOFF (RO) CONCENTRATION, GW MASS LOADING, RO MASS LOADING, GW LATERAL FLOW, AND RO LATERAL FLOW SIMULATED BY RT3D-OTIS UNDER THE RF BMPS ALONG THE (A) ARKANSAS RIVER, (B) TRIBUTARIES, AND (C) ENTIRE STREAM SYSTEM.	94
FIGURE 3-19. TEMPORALLY AVERAGED (A) SeO_4 CONCENTRATION, (B) SeO_3 CONCENTRATION, (C) NO_3 CONCENTRATION, (D) DO CONCENTRATION, AND (E) FLOW RATE SIMULATED BY RT3D-OTIS AT EACH OBSERVATION LOCATION FOR THE BASELINE AND FOR THE RF BMPS.....	95
FIGURE 3-21. PERCENT CHANGE FROM THE SPATIO-TEMPORAL AVERAGED BASELINE SeO_4 GROUNDWATER (GW) CONCENTRATION, RUNOFF (RO) CONCENTRATION, GW MASS LOADING, RO MASS LOADING, GW LATERAL FLOW, AND RO LATERAL FLOW SIMULATED BY RT3D-OTIS UNDER THE RI BMPS ALONG THE (A) TRIBUTARIES, (B) ARKANSAS RIVER, AND (C) ENTIRE STREAM SYSTEM.	98
FIGURE 3-22. TEMPORALLY AVERAGED (A) SeO_4 CONCENTRATION, (B) SeO_3 CONCENTRATION, (C) NO_3 CONCENTRATION, (D) DO CONCENTRATION, AND (E) FLOW RATE SIMULATED BY RT3D-OTIS AT EACH OBSERVATION LOCATION FOR THE BASELINE AND RI BMP SCENARIOS.....	100
FIGURE 3-23. PERCENT CHANGE FROM THE SPATIO-TEMPORAL AVERAGED BASELINE SeO_4 , SeO_3 , NO_3 , AND DO CONCENTRATIONS SIMULATED BY RT3D-OTIS UNDER THE LAND FOLLOWING BMPS IN THE (A) ARKANSAS RIVER, (B) TRIBUTARIES, AND (C) ENTIRE STREAM SYSTEM.....	102
FIGURE 3-24. PERCENT CHANGE FROM THE SPATIO-TEMPORAL AVERAGED BASELINE SeO_4 GROUNDWATER (GW) CONCENTRATION, RUNOFF (RO) CONCENTRATION, GW MASS LOADING, RO MASS LOADING, GW LATERAL FLOW, AND RO LATERAL FLOW SIMULATED BY RT3D-OTIS UNDER THE LF BMPS ALONG THE (A) ARKANSAS RIVER, (B) TRIBUTARIES, AND (C) THE ENTIRE STREAM SYSTEM.....	103

FIGURE 3-25. TEMPORALLY AVERAGED (A) SEO_4 CONCENTRATION, (B) SEO_3 CONCENTRATION, (C) NO_3 CONCENTRATION, (D) DO CONCENTRATION, AND (E) FLOW RATE SIMULATED BY RT3D-OTIS AT EACH OBSERVATION LOCATION FOR THE BASELINE AND LF BMP SCENARIOS.	104
FIGURE 3-26. PERCENT CHANGE FROM THE SPATIO-TEMPORAL AVERAGED BASELINE SEO_4 , SEO_3 , NO_3 , AND DO CONCENTRATIONS SIMULATED BY RT3D-OTIS UNDER THE CANAL SEALING BMPS IN THE (A) ARKANSAS RIVER, (B) TRIBUTARIES, AND (C) THE ENTIRE STREAM SYSTEM.....	106
FIGURE 3-27. PERCENT CHANGE FROM THE SPATIO-TEMPORAL AVERAGED BASELINE SEO_4 GROUNDWATER (GW) CONCENTRATION, RUNOFF (RO) CONCENTRATION, GW MASS LOADING, RO MASS LOADING, GW LATERAL FLOW, AND RO LATERAL FLOW SIMULATED BY RT3D-OTIS UNDER THE CS BMPS ALONG THE (A) ARKANSAS RIVER, (B) TRIBUTARIES, AND (C) ENTIRE STREAM SYSTEM.	107
FIGURE 3-28. TEMPORALLY AVERAGED (A) SEO_4 CONCENTRATION, (B) SEO_3 CONCENTRATION, (C) NO_3 CONCENTRATION, (D) DO CONCENTRATION, AND (E) FLOW RATE SIMULATED BY RT3D-OTIS AT EACH OBSERVATION LOCATION FOR THE BASELINE AND CS BMP SCENARIOS.	108
FIGURE 3-29. RELATIVE IMPORTANCE SCORES AND MOE BY SURVEYED STAKEHOLDERS OF THE MAIN CRITERIA FOR BMP DECISION MAKING, WITH HIGHER SCORES BEING MORE PREFERRED.	112
FIGURE 3-30. AVERAGE SUB-CRITERIA SCORES BY SURVEYED STAKEHOLDERS FOR (A) COST, (B) EASE OF IMPLEMENTATION, (C) ECONOMIC BENEFITS, AND (D) ENVIRONMENTAL BENEFITS, WITH HIGHER SCORES BEING MORE PREFERRED.	113
FIGURE 3-31. AVERAGE OVERALL RANK OF BMPS BY SURVEYED STAKEHOLDERS, WITH HIGHER SCORES BEING MORE PREFERRED.	116
FIGURE 3-32. RELATIVE IMPORTANCE OF BMPS BY SURVEYED STAKEHOLDERS WITH RESPECT TO (A) COST, (B) EASE OF IMPLEMENTATION, (C) ECONOMIC BENEFITS, AND (D) ENVIRONMENTAL BENEFITS, WITH HIGHER SCORES BEING MORE PREFERRED.	117
FIGURE 3-33. AVERAGE MAIN CRITERIA RELATIVE IMPORTANCE SCORES WITH ERROR BARS ASSOCIATED WITH A 95% CONFIDENCE INTERVAL.	119
FIGURE 3-34. AVERAGE SUB-CRITERIA RANKS WITH ERROR BARS ASSOCIATED WITH A 95% CONFIDENCE INTERVAL.....	120
FIGURE 3-35. AVERAGE BMP RANKS WITH ERROR BARS ASSOCIATED WITH A 95% CONFIDENCE INTERVAL.	121
FIGURE 3-36. EXAMPLE OF TRACEABILITY FOR THE REDUCED IRRIGATION AND ENHANCED RIPARIAN BUFFER BMPS SHOWING (A) RELATIVE IMPORTANCE OF MAIN CRITERIA, (B) AVERAGE BMP RANKS WITH RESPECT TO ECONOMIC BENEFITS, AND (C) THE AVERAGE OVERALL BMP RANKS.	121
FIGURE A-1. REDUCED FERTILIZER TIME SERIES PLOTS SHOWING BASELINE, RF10, RF20, AND RF30 MODEL OUTPUT OF DISSOLVED SEO_4 IN THE (A) RIVER AND (B) TRIBUTARIES, DISSOLVED SEO_3 IN THE (C) RIVER AND (D) TRIBUTARIES, NO_3 IN THE (E) RIVER AND (F) TRIBUTARIES, DO IN THE (G) RIVER AND (H) TRIBUTARIES, DISCHARGE IN THE (I) RIVER AND (J) TRIBUTARIES, SEO_4 MASS LOADING FROM GROUNDWATER ALONG THE (K) RIVER AND (L) TRIBUTARIES,	

SEO₄ MASS LOADING FROM SURFACE RUNOFF ALONG THE (M) RIVER AND (N) TRIBUTARIES, RETURN FLOW FROM GROUNDWATER ALONG THE (O) RIVER AND (P) TRIBUTARIES, RETURN FLOW FROM SURFACE RUNOFF ALONG THE (Q) RIVER AND (R) TRIBUTARIES, SEO₄ CONCENTRATION IN GROUNDWATER RETURN FLOW ALONG THE (S) RIVER AND (T) TRIBUTARIES, AND SEO₄ CONCENTRATION IN SURFACE RUNOFF RETURN FLOW ALONG THE (U) RIVER AND (V) TRIBUTARIES.

..... 135

FIGURE A-2. REDUCED IRRIGATION TIME SERIES PLOTS SHOWING BASELINE, RI10, RI20, AND RI30 MODEL OUTPUT OF DISSOLVED SEO₄ IN THE (A) RIVER AND (B) TRIBUTARIES, DISSOLVED SEO₃ IN THE (C) RIVER AND (D) TRIBUTARIES, NO₃ IN THE (E) RIVER AND (F) TRIBUTARIES, DO IN THE (G) RIVER AND (H) TRIBUTARIES, DISCHARGE IN THE (I) RIVER AND (J) TRIBUTARIES, SEO₄ MASS LOADING FROM GROUNDWATER ALONG THE (K) RIVER AND (L) TRIBUTARIES, SEO₄ MASS LOADING FROM SURFACE RUNOFF ALONG THE (M) RIVER AND (N) TRIBUTARIES, RETURN FLOW FROM GROUNDWATER ALONG THE (O) RIVER AND (P) TRIBUTARIES, RETURN FLOW FROM SURFACE RUNOFF ALONG THE (Q) RIVER AND (R) TRIBUTARIES, SEO₄ CONCENTRATION IN GROUNDWATER RETURN FLOW ALONG THE (S) RIVER AND (T) TRIBUTARIES, AND SEO₄ CONCENTRATION IN SURFACE RUNOFF RETURN FLOW ALONG THE (U) RIVER AND (V) TRIBUTARIES.

..... 136

FIGURE A-4. CANAL SEALING TIME SERIES PLOTS SHOWING BASELINE, CS20, CS40, AND CS80 MODEL OUTPUT OF DISSOLVED SEO₄ IN THE (A) RIVER AND (B) TRIBUTARIES, DISSOLVED SEO₃ IN THE (C) RIVER AND (D) TRIBUTARIES, NO₃ IN THE (E) RIVER AND (F) TRIBUTARIES, DO IN THE (G) RIVER AND (H) TRIBUTARIES, DISCHARGE IN THE (I) RIVER AND (J) TRIBUTARIES, SEO₄ MASS LOADING FROM GROUNDWATER ALONG THE (K) RIVER AND (L) TRIBUTARIES, SEO₄ MASS LOADING FROM SURFACE RUNOFF ALONG THE (M) RIVER AND (N) TRIBUTARIES, RETURN FLOW FROM GROUNDWATER ALONG THE (O) RIVER AND (P) TRIBUTARIES, RETURN FLOW FROM SURFACE RUNOFF ALONG THE (Q) RIVER AND (R) TRIBUTARIES, SEO₄ CONCENTRATION IN GROUNDWATER RETURN FLOW ALONG THE (S) RIVER AND (T) TRIBUTARIES, AND SEO₄ CONCENTRATION IN SURFACE RUNOFF RETURN FLOW ALONG THE (U) RIVER AND (V) TRIBUTARIES.

..... 138

CHAPTER 1: Literature Review and Research Objectives

1.1 Selenium in the Aqueous Environment

Environmental impacts associated with elevated in-stream selenium (Se) concentrations have been well documented (Hamilton, 2004). Due to the ability of Se to bioaccumulate, elevated levels of Se in surface water has resulted in Se toxicosis in aquatic fauna, leading to mortality and to developmental and reproductive defects (Presser et al., 1994; Nolan and Clark, 1997). Bedrock is the main source of Se in many terrestrial systems. The concentration of Se in the soils overlying bedrock within alluvial formations commonly is influenced most by the Se concentration in the parent bedrock material (Fernandez-Martinez and Charlet, 2009). As such, in regions with high concentrations of Se in bedrock, it can be expected that the alluvium, comprising mostly of weathered parent material, also will contain high Se concentrations. Although Se occurs naturally in the Cretaceous sediments of the western United States, agricultural activities including irrigation and fertilization can accelerate the natural oxidation and leaching of soluble Se from geological formations into streams and rivers (Nolan and Clark, 1997). In agricultural regions with high Se concentrations in the alluvium, the presence of high levels of dissolved oxygen (DO) and nitrate (NO_3) in groundwater can both accelerate the dissolution of Se and inhibit the chemical reduction of Se species (Bailey et al., 2012, 2015). As a result of these processes, rivers and tributaries in regions receiving agricultural drain water can experience toxic levels of Se.

Se can exist in environmental water systems in four oxidation states: selenate (SeO_4) [Se(VI)], selenite (SeO_3) [Se(IV)], elemental Se (Se^0) [Se(0)], and selenide (Se^{2-}) [Se(-II)] (Masscheleyn and Patrick, 1993). Selenide can be present in multiple forms, for example as

organic selenomethionine (SeMet) and as gaseous Dimethylselenide (DMSe). SeO_4 , SeO_3 , and SeMet are soluble species, with SeO_4 being a weak sorbent to sediment (Ahlrichs and Hossner, 1987) and SeO_3 being a strong sorbent (Balistrieri and Chao, 1987). SeO_4 typically accounts for the vast majority of soluble Se (Gates et al., 2009; Gerla et al., 2011; Masscheleyn et al., 1989) and as such often is targeted for removal from the aqueous phase.

SeO_4 can be transformed to SeO_3 via microbial-mediated chemical reduction (Oremland et al., 1990; Masscheleyn and Patrick, 1993; Ellis and Salt, 2003), with further reduction to Se^0 and Se^{2-} possible. These processes, however, are inhibited by the presence of DO and NO_3 (Weres et al., 1990; White et al., 1991; Zhang and Moore, 1997) due to microbial preference for higher-redox species. This inhibition is particularly significant in agricultural areas, wherein irrigation-induced drainage water discharging to streams can be high in both DO and NO_3 . Within stream environments, release of Se to the atmosphere can occur through volatilization (Lemly, 1999). Dissolved Se can be taken up by algae (Bennett et al., 1986; Riedel et al., 1996; Baines et al., 2004), with organic Se released upon algal respiration. Settling of Se species mass to the stream sediment bed also can occur, with further chemical reduction of these species occurring within the stream sediments. The processes that govern in-stream Se cycling with major sources and sinks for each Se species are summarized in Figure 1-1. Although oxidation of Se species can occur, the dominant Se species transformation in natural systems is chemical reduction, as indicated by the “Net Reduction” term in Figure 1-1 (Masscheleyn and Patrick, 1993; Lemly, 1999; Chapman et al., 2010).

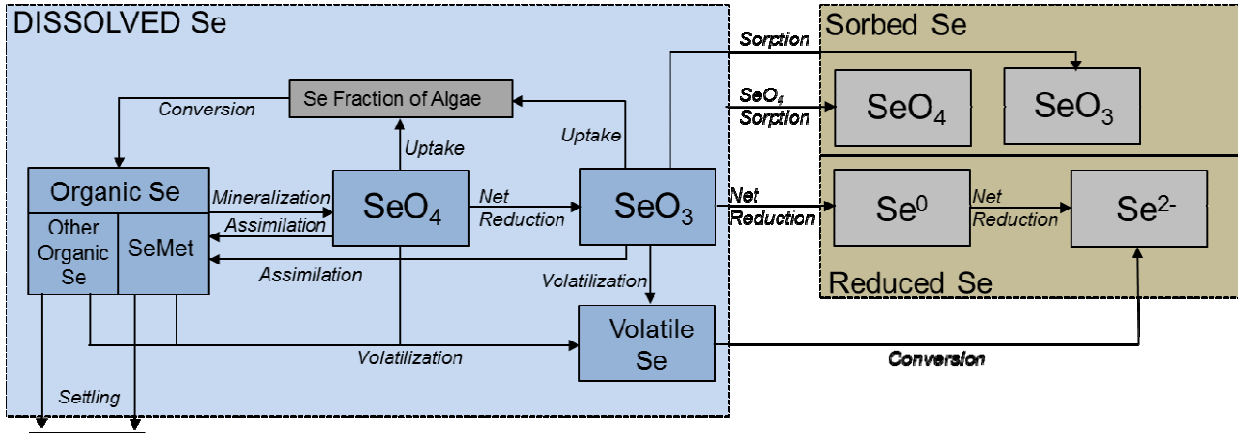


Figure 1-1. Conceptual model for in-stream Se cycling.

- The pool of organic Se (Se_{org}) gains mass from the conversion of algal Se biomass, and loses mass due to settling, mineralization to SeO_4 , and volatilization;
- SeO_4 gains mass from microbial-mediated mineralization of Se_{org} and selenomethionine ($SeMet$), and loses mass due to algal uptake, chemical reduction to SeO_3 , assimilation to $SeMet$, and volatilization;
- SeO_3 gains mass from SeO_4 reduction, and loses mass due to algal uptake, chemical reduction to Se^0 , assimilation to $SeMet$, and volatilization;
- Se^0 gains mass from SeO_3 reduction, and loses mass due to chemical reduction to Se^{2-} ;
- Se^{2-} gains mass from Se^0 chemical reduction and from conversion to Se^{2-} ;
- Volatile Se (Se_{vol}) gains mass from volatilized Se_{org} , SeO_4 , SeO_3 , and $SeMet$, and loses mass from conversion to Se^{2-} ;
- $SeMet$ gains mass from conversion of algal Se biomass, and loses mass due to settling, volatilization, and mineralization to SeO_4 ; and
- Se in sediment gains mass from the sorption of SeO_4 and SeO_3 , and the precipitation of Se^0 and Se^{2-}

Over recent decades, a number of studies have been conducted in an effort to understand the processes that govern the release of Se into the aquatic environment, its transformation in the aquatic environment, its toxicity to aquatic fauna, and various methods to mitigate elevated Se concentrations in surface water. Some of the first attempts to describe the chemical processes that govern Se transformation in surface water were carried out through the collection of field data (Sugimura et al., 1976; Cooke and Bruland, 1987). The study by Conde and Alaejos (1997) examined the results of over 100 Se sampling studies of river water alone. Studies have examined aquatic Se speciation and cycling (Cooke and Bruland, 1987; Cutter, 1989; Canton and Van Derveer, 1997; Conde and Alaejos, 1997; Van Derveer and Canton, 1997; Gao et al., 2000; Oram et al., 2008), redox Se reactions and the conditions that govern them (Oremland et al., 1989; Oremland et al., 1990; Tokunaga et al., 1997; Fernandez-Martinez and Charlet, 2009), sorption of mobile Se species to sediment (Ahlrichs and Hossner, 1987), the inhibition of the reduction of Se species by the presence of NO_3 and DO (Weres et al., 1990; Stillings and Amacher, 2010; Bailey et al., 2012), and the chemical kinetics of Se in various environments (Losi and Frankenberger, 1998; Guo et al., 1999).

In addition to the aforementioned studies examining the physical chemistry of Se in aqueous systems, modeling studies have been conducted to better understand the chemical processes that govern Se reactions and/or to predict Se concentrations. Some of the earliest attempts to model Se chemistry in natural systems were conducted using one-dimensional models representing saturated (Guo et al., 1999) and unsaturated (Alemi et al., 1991) soil columns. More recent modeling efforts include the study of Tayfur et al. (2010), which utilized a two-dimensional finite-element model to simulate Se transport in saturated and unsaturated soil zones, as well as

the study of Bailey et al. (2013) which also examined Se transport in variably saturated soil zones but did so using a three-dimensional model.

Although Se models have been developed for variably saturated transport in alluvial aquifer systems, few numerical models have been developed for Se species fate and transport in streams. However, a number of in-stream water quality models are widely used to assess the impacts of point source and non-point source mass loadings of nutrients (principally nitrogen) associated with agricultural basins, including QUAL2E (Brown and Barnwell, 1987), QUAL2K (Chapra et al., 2008), QUASAR (Whitehead et al., 1997), Q² (Cox and Whitehead, 2005), EPD-RIV1 (Martin and Wool, 2002), and a recently developed model that combines the one-dimensional inflow and storage model OTIS (Runkel, 1998) with QUAL2E for application in a regional stream network (Bailey and Ahmadi, 2014). Such models are used to simulate the transport and cycling of water quality indicators, including DO and NO₃, in a one-dimensional stream setting, and include processes such as advection, longitudinal dispersion, sources/sinks, and chemical reactions. In the model used by Bailey and Ahmadi (2014), sources and sinks include channel inflow/outflow with associated chemical species concentrations, lateral inflow/outflow representing stream-aquifer interactions and associated chemical species concentrations, and the settling of particulates out of the water column, while chemical reactions and cycling of chemical species include chemical reduction, oxidation, volatilization, settling, algal growth and decay, and sediment demand.

Although Se sampling and modeling efforts have occurred separately over recent years, few studies to date have been carried out in a combined effort to both gather field data and use numerical models capable of simulating the transport and transformation of in-stream Se species on a regional scale, in this study being a surface water system comprised of a primary river reach

with multiple tributaries.. Additionally, in cases where these studies have been conducted, their application is limited. The study of Myers (2013) applied a 3-D water quality transport model at the regional scale, but examined only Se discharges from groundwater under various remediation scenarios. The study of Hamer et al. (2012) used the 3-D water quality transport model LAKEVIEW in conjunction with field data and applied it to a region impacted by mining. The majority of regional-scale modeling efforts have been directed toward nutrient modeling, including the studies of Frind et al. (1990), Addiscott and Mirza (1998), Molenat and Gascuel-Odoux (2002), and Conan et al. (2003), all of which examined the transport of NO₃ in regional-scale groundwater systems. The study of Bailey et al. (2015) modeled Se processes in groundwater at the regional scale, but like the studies of Molenat and Gascuel-Odoux (2002) and Conan et al. (2003), groundwater concentrations and loading to surface waters were not translated to surface water concentrations despite highly interconnected surface water – groundwater systems. The studies of Runkel et al. (1998), McKnight et al. (2002), Azzellino et al. (2006), and Boyer et al. (2006) applied solute transport models to stream networks draining catchments on the regional scale (10³ km²), but examined only nutrients and/or other non-Se chemical species. There is an apparent gap in the literature regarding surface water quality transport models capable of predicting water column and sediment Se concentrations applied in an agricultural setting at the regional scale that is enhanced by a field data.

1.2 Agricultural Best Management Practices to Mitigate Se Pollution

Many of the aforementioned Se studies have been conducted ancillary to examining possible groundwater and/or surface water remediation strategies in the form of land and water best management practices (BMPs) (Addiscott and Mirza, 1998; Molenat and Gascuel-Odoux,

2002). However, as with past water quality modeling efforts, the primary focus of best management practice (BMP) studies to date have been focused on nutrient remediation (Buchleiter et al., 1995; Hunsaker and Levine, 1995; Molenat and Gascoul-Oudou, 2002; Chaplot et al., 2004; Morari et al., 2004; Almasri and Kaluarachchi, 2007; Lee et al., 2010; Rong and Xuefeng, 2011; Zhang et al., 2012). Specific nutrient remediation BMPs that have been examined include reducing the amount of irrigation water (Rong and Xuefeng, 2011) and fertilizer (Lee et al., 2010; Zhang et al., 2012) applied to fields, enhancing riparian buffer zones due to their ability to increase chemical reaction rates for denitrification (Heathwaite et al., 1998; Hefting and de Klein, 1998; Spruill, 2000; Vache et al., 2002; Sahu and Gu, 2009), and constructed flow-through wetlands (Gao et al., 2003; Lin and Terry, 2003).

A number of these studies have examined BMPs in the context of agricultural practices. The studies of Ledoux et al. (2007), Almasri and Klamuarachchi (2007), and Lee et al. (2010) used reductions in fertilizer application in the range of 20% to 40%, while the studies of Buchleiter at al. (1995), Ma et al. (2003), and Rong and Xuefeng (2011) examined a reduction in the volume of irrigation water applied to cultivated fields. Although these studies have examined the impacts of agricultural BMPs on nitrate and other nutrients in groundwater, the study of Tong and Naramngam (2007) went further and modeled the changes in both groundwater and surface water quality as a result of agricultural BMP implementation in the Little Miami River Basin, Ohio.

Studies that examine BMPs with respect to Se remediation include Myers (2013), which used a groundwater flow model to explore Se remediation scenarios in the Blackfoot watershed in Idaho, which had been impacted by mining activities. The study of Gao et al. (2000) and Lin and Terry (2003) examined the effectiveness of flow-through constructed wetlands to remove Se

from agricultural drainage water in Central California. The study of Bailey et al. (2015) evaluated BMPs including reduced irrigation, reduced fertilization, irrigation canal sealing, land fallowing, and enhancing riparian buffers to examine changes in Se and nutrient loading from cultivated land to the Arkansas River and its tributaries in Southeastern Colorado. These studies suggest that a number of BMPs are effective at reducing Se loading to rivers which affect in-stream Se concentrations.

An area where the previously mentioned BMP studies, applied to both nutrients and Se, fall short is with regard to stakeholder engagement. For example, although these studies discuss the degrees of effectiveness of a number of BMPs with respect to improving water quality, most were conducted without direct input from stakeholders regarding their willingness to implement the BMPs being examined. This is of particular importance when considering agricultural BMPs such as reduced fertilizer application and reduced irrigation, as most agricultural BMPs must ultimately be implemented directly by individual stakeholders at their discretion. Over the past two decades, the involvement of stakeholders in environmental management decision making in the form of multi-sector collaboration, more of a “grass roots” approach, has been increasing and replacing the previous public hierarchical environmental management model, being a “top down” approach (Koontz and Thomas, 2006). This shift from a “top down” environmental management approach to a collaborative management approach has resulted in the adoption of various forms of multi-criteria decision analysis (MCDA) techniques, which attempts to account for the varying and often conflicting concerns of different groups of stakeholders (Davies et al., 2013).

1.3 Multi-Criteria Decision Analysis

Multi-criteria decision analysis (MCDA) is a sub-discipline of operations research used to solve problems involving multiple criteria that cannot be directly compared. Since the criteria examined under MCDA often cannot be directly compared, unique optimal solutions do not exist for MCDA problems, and therefore the decision maker's preferences are used to weight alternatives to arrive at the "best" solution. MCDA has been used for decades to aid in decision making in complex applications such as natural resource management, environment, health care, and business (Roy and Vincke, 1981; Belton, 1986; Boender et al., 1989). Multi-criteria decision analysis (MCDA) has become widely used in environmental applications over the past few decades. In an effort to collaborate environmental decisions between different groups of stakeholders, MCDA has been applied in at least 113 water resources studies from 34 countries prior to 2006 (Hajkowicz and Collins, 2007). The study of Davies et al. (2013) noted that when using MCDA in environmental decision making, decisions become more transparent, mistrust between various groups is attenuated, dialogue between stakeholders is encouraged, and both human and environmental aspects of decisions are transformed into a form that makes them directly comparable.

Despite the extensive use of MCDA in recent decades, general deficiencies in the literature still remain. The first is the use of the analytic hierarchy process (AHP) MCDA method even though it contains certain advantages over other MCDA methods. The AHP is a form of MCDA whereby the preferred solution is arrived at through a series of pairwise comparisons of criteria (Saaty, 1987). Although the choice of an MCDA method is ultimately up to the researcher and there is no MCDA "super method" exclusively appropriate for a given application, there are clear advantages to using the AHP as opposed to other forms of MCDA in

environmental applications (Guitouni and Martel, 1997). In the study of Moran et al. (2007), two methods for determining agri-environmental policy in Scotland, being the AHP and choice experiments (CE), were compared and advantages of the AHP were discussed. It was noted in this study that respondents had comparable assessments of the level of difficulty in completing the two different types of surveys, even though the AHP required them to answer three times as many questions as the CE. Moran et al. (2007) suggests that since the two MCDA methods had similar levels of reported difficulty, the AHP format, while requiring far more questions to be answered, often can be a more intuitive way to value criteria and/or alternatives.

Also highlighting the advantages of using the AHP is the study by Yong et al. (1994), which used AHP to assign weights to nitrate risk-management strategies. Yong et al. noted two main advantages to using the AHP over other weighting methods, the first being that it is simpler to compare items in pairs as opposed to comparing the entire set of items at once. The second advantage noted is that the AHP allows for the consistency of comparisons to be checked, thus allowing for inconsistent responses to be reassessed or discarded. Ying et al. (2007) added that the AHP was advantageous over other MCDA methods due to its ability to decompose ill-structured problems into workable ones by breaking them down into simple pairwise comparisons. These qualities of the AHP are particularly important when making environmental decisions as they are typically highly complex, ill-structured, and involve both qualitative and quantitative considerations from groups of stakeholders with varying interests (Kiker et al., 2005).

Although MCDA has been applied to agricultural decision making in a number of countries including Germany, Thailand, Scotland, New Zealand, Philippines, Australia, Belgium, Italy, Japan, Senegal, Spain, India, Egypt, Greece, Chile, Nigeria, Indonesia, and the United

States, MCDA has been applied specifically to agriculture relatively few times (Ahrens et al., 2007; Tiwari et al., 1999; Moran et al., 2007; Dooley et al., 2009; Hayashi, 2000). The study of Behzadian et al. (2010) reviewed 217 MCDA studies from 100 journals, only two of which were specifically related to agriculture. Additionally, according to a broad MCDA study by Hayashi (2000), of 35 selected MCDA studies applied to agriculture prior to 2000, only three took place in the United States and none used the AHP.

Despite the relatively few examples of AHP applied to agricultural problems in the United States to date, AHP has been applied in settings similar to those that are the focus of this study. The study of Shrestha et al. (2004) used AHP to examine the adoption of silvopasture, a ranching BMP that combines the use of trees and pasture with cattle operations to maximize land sustainability. However, the scope of this study was very limited in that it only examined one BMP. A more traditional application of the AHP is in the study of Toledo et al. (2010), which sought to prioritize four distinct risk factors associated with agricultural activities, being climate, price and cost variability, human risk, and commercialization. The four risk factors served as main criteria, which were broken down further into sub-criteria. One limitation of this study was the number and diversity of participants, as only 15 people were surveyed and included only growers (eight) and agricultural consultants (seven). Another limitation of this study was the lack of “traceability” in criteria weights, whereby it is easy to determine precisely how criteria weights were arrived at (Koontz et al., 2012). Although the use of sub-criteria does shed some light on criteria weights, a more simple ranking method (i.e. direct ranking of sub-criteria) could have been used in combination with the AHP in an effort to more completely capture the intricacies of the weights of the main criteria.

When MCDA has been used to examine environmental concerns, results are often conflicting and/or counterintuitive. The study of Rezaei-Moghaddam and Karami (2008) used AHP to examine sustainable agricultural development models in Iran. The results of this study showed that “environmental protection”, “wise use of resources”, and “product quality” were consistently ranked as the top three criteria, while “profitability”, “employment”, and “productivity” were consistently ranked last amongst the nine criteria considered. The agricultural AHP study of Tiwari et al. (1999), conducted in Thailand, showed that “environmental cost” ranked higher than “farmer’s net present value”. However, the study of Toledo et al. (2010) found the opposite to be true, with “price and cost variability” having the highest rank and “climate” having the lowest rank. In general, results from various AHP MCDA studies applied to agricultural settings are variable and no obvious conclusions can be drawn from these studies that can be universally applied. Therefore, when using AHP in agricultural decision-making, a study designed specifically for the region of interest should be implemented.

1.4 Research Objectives

In considering the environmental threats that Se can pose in natural systems and the potential for agricultural BMPs to remediate Se in surface water, the primary goals of this study are to assess the extent of Se contamination in surface water within a representative region of an irrigated agricultural river valley and to examine the potential effectiveness and feasibility of BMPs being considered to remediate Se. Toward satisfying these goals, the main objectives of this research effort are as follows:

- i. Assess the speciation and concentration of dissolved, precipitated, and sorbed Se species, as well as other chemical species that potentially affect Se cycling through collecting and analyzing field data from an irrigated agricultural river valley.
- ii. Perform a sensitivity analysis using a steady and unsteady flow surface water quality transport model for Se to identify key processes affecting Se chemistry in a stream network receiving irrigation return flows and loads.
- iii. Apply results from the Se sampling and sensitivity analysis efforts to calibrate a coupled groundwater-surface water quality model.
- iv. Use the calibrated coupled groundwater-surface water quality model to predict changes in loadings and in-stream concentrations of Se species when implementing various BMPs.
- v. Issue an AHP MCDA survey to stakeholders in the region to identify the most socio-economically feasible agricultural BMPs.
- vi. Summarize conclusions and make recommendations to guide future studies.

CHAPTER 2: Methods

2.1 Site Description

The Lower Arkansas River Valley (LARV) is located in southeast Colorado between Pueblo and the Kansas state border, as shown in Figure 2-1. The upstream study region (USR), also shown in Figure 2-1, is the focus of this research and ranges from near the town of Manzanola eastward to near Las Animas. For over one hundred and forty years, the LARV has been the site of irrigated farming and currently grows (in order of planted acres) alfalfa, corn, grass hay, wheat, sorghum, dry beans, cantaloupe, watermelon, and onions (USDA NASS Colorado Field Office, 2009).

The LARV features more than 1,000 miles of main canals that divert water from the Arkansas River (River) and approximately 2,400 pumping wells that support approximately 270,000 irrigated acres. Due to Colorado's prior appropriation water law, which makes providing the relatively constant supply of water required by sprinklers or drip lines difficult for junior water rights holders, the vast majority of fields are irrigated using relatively inefficient surface irrigation methods with ten to fifteen percent irrigated with more efficient sprinkler or drip lines (Bailey et al., 2015).

The LARV is broad and relatively thin (average alluvium thickness of about 10 meters), is composed of a series of Cambrian to Tertiary-age sedimentary formations, and is underlain by bedrock formed mostly of marine-derived shale (Pierre, Niobrara, Carlisle, and Graneros) and limestone (Scott, 1968; Sharps, 1976). At a number of locations throughout the LARV, this shale is present at the surface in the form of outcrops. Previous studies reveal that a variety of salts, Se, and uranium are dissolved from these rocks and from their weathered residuum by the

action of natural and irrigation flows (Zielinski et al 1995, 1997; Gates et al 2009, Bailey et al 2012). As irrigation water is applied to cultivated fields, the amount that is in excess of crop evapotranspiration (ET) percolates down through the alluvium and forms a high groundwater table. Additionally, as groundwater flows through the alluvium, it dissolves Se from the alluvium and carries it to the local stream network where it then contributes to increased concentrations of Se in surface water. This phenomenon is exacerbated when percolated groundwater contains elevated levels of dissolved oxygen (DO), or O₂, and/or NO₃ from fertilizer, as DO and NO₃ can both increase the rate at which Se is mobilized from parent material and decrease the rate at which it is reduced to less toxic forms (Bailey et al., 2015). Excess irrigation surface water runoff, which can experience tailwater NO₃ concentrations up to eight times those of the headwater concentrations (Miller et al., 1977; Ciotti, 2005), is an additional source of NO₃ to surface water in the LARV. The result of the described irrigation practices, coupled with elevated levels of Se in the alluvium and NO₃ in groundwater and surface water, has resulted in in-stream Se concentrations in the Arkansas River and its tributaries that regularly exceed Colorado's aquatic life chronic standard of 4.6 µg/L (85th percentile), often by a factor of three (Gates et al., 2009, 2016). The accumulation and transport of dissolved Se species in groundwater and overland return flows have resulted in all segments of the Lower Arkansas River being designated in 2004 as "water quality limited" with respect to Se and placed on the current Clean Water Act 303(d) list for Total Maximum Daily Load (TMDL) development. River concentrations measured in the USR and another region further downstream along the river amount to between 1.4 and 3.7 times, respectively, the chronic standard for total dissolved Se (Gates et al 2009, Gates et al 2016). The study of Miller et al. (2010) showed that in-stream concentrations of dissolved Se tripled when moving downstream from Pueblo to Avondale

(upstream of the USR), from a median concentration of 3 µg/L to 6 µg/L, as more agriculture-impacted return flows with high Se concentrations are introduced to the river moving downstream. The same study reported in-stream concentrations in the LARV as high as 754 µg/L. The study of Ivahnenko et al. (2013) reported a similar trend, with Se concentrations increasing while moving downstream from Avondale to Las Animas. Median in-stream dissolved Se concentrations reported in that study ranged from 8.4 µg/L to 12.2 µg/L over the same reach of the Arkansas River.

2.2 Sampling and Analysis of Se and Related Constituent Concentrations in Streams

2.2.1 Selenium, Uranium, and Irrigation Water Quality

Samples that were collected as part of this study were collected from four locations in the River (ARK 164, ARK 127, ARK 95, and ARK 201) and four locations in the tributaries (Patterson, Timpas 2, Crooked 2, and Horse). Samples that were collected prior to this study but were used in later sections of this study include 11 locations in the River (ARK Cat., ARK 164, ARK 141, ARK 12, ARK 127, ARK Crk./And., ARK 95, ARK King, ARK 162, ARK 209, and ARK 201) and seven locations in the tributaries (Patterson, Timpas 1, Timpas 2, Crooked 1, Crooked 2, Anderson, and Horse) as shown in Figure 2-1 below.

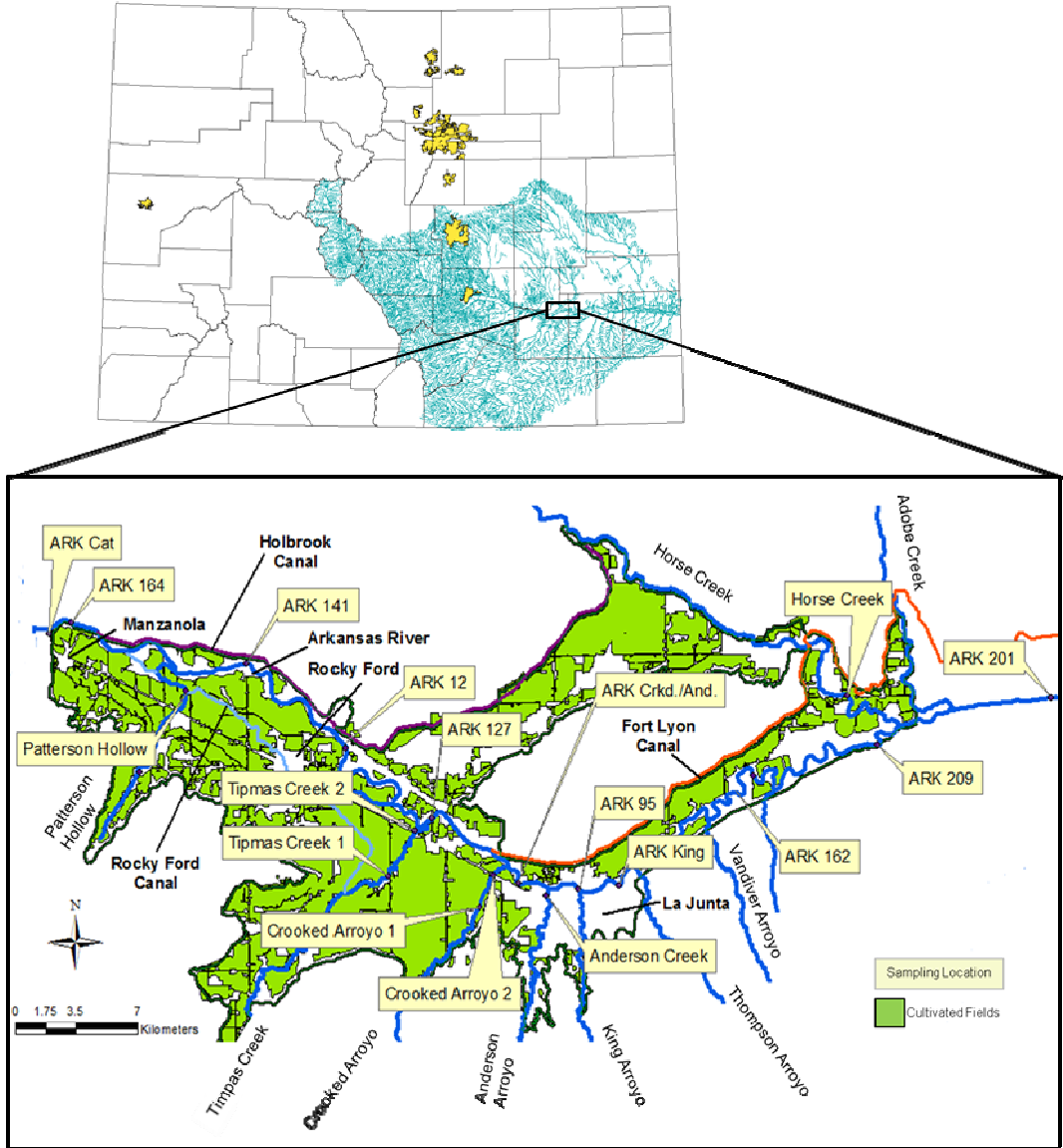


Figure 2-1. Lower Arkansas River Valley upstream study region (USR) in southeastern Colorado, showing cultivated fields, the Arkansas River, tributaries, and stream sampling locations.

The Universal Transverse Mercator (UTM) North American Datum of 1983 (NAD83) coordinated of the 18 locations sampled as part of this study are included in Table 2-1 below.

Table 2-1. UTM NAD83 coordinates of the 18 locations sampled as part of this study.

Location ID	Easting (m)	Northing (m)
ARK Cat	592,524.06	4,220,405.40
ARK 164	599,750.51	4,220,537.70
Patterson Hollow	606,402.31	4,216,810.10
ARK 141	609,874.97	4,218,298.38
ARK 12	615,398.16	4,213,602.02
Timpas Creek 1	617,977.86	4,206,524.40
Timpas Creek 2	619,433.07	4,209,071.02
ARK 127	620,425.26	4,209,699.40
Crooked Arroyo 1	623,137.24	4,204,903.82
Crooked Arroyo 2	623,997.14	4,206,623.62
ARK Crkd. / And.	625,419.28	4,206,127.52
Anderson Creek	627,039.85	4,205,432.99
ARK 95	628,891.94	4,205,829.87
ARK King	631,190.51	4,206,028.30
ARK 162	638,962.66	4,212,113.73
ARK 209	646,106.25	4,213,790.17
Horse Creek	644,435.92	4,216,534.80
ARK 201	656,040.57	4,216,407.80

The first step in stream sample collection was establishing cross-sections. Cross-sections were established in locations where samples could be collected perpendicular to the direction of flow and the cross-sections did not traverse any mid-channel bars. Establishing a cross-section included driving posts into the left and right channel banks and securing a taut rope between them over the water surface. The rope was then marked at 20 evenly spaced locations between the left and right banks, being the number of readings required by the Acoustic Doppler Velocimeter (ADV) (discussed in Section 2.2.3). Additional preparatory steps included recording the date and time, sketching a cross-section profile and a map of the sample location, and placing a staff gage along the cross-section to ensure that there was not any significant change in flow depth over the period it took to collect the samples/measurements.

With the cross section established at a stream location, Se samples were collected from the water column at six to ten locations along the cross-section using a DH-48 sediment sampler, also known as the “fish”, shown in Figure 2-2. Samples were collected by inserting one 16 oz. bottle into the fish for each location and pushing the fish vertically downward from the water surface to the channel bottom to collect a composite water sample representative of the entire water column depth for each sample location.



Figure 2-2. DH-48 sediment sampler used for composite Se sampling in the water column.

With six to ten water samples collected from a given cross-section, water from each sample was poured into a churn and thoroughly mixed to yield a single one-dimensional cross-section averaged composite sample. Water was pumped from the churn using a peristaltic pump into five Nalgene bottles: one 250 mL bottle containing an unfiltered sample to be analyzed for total recoverable Se; one 250 mL bottle containing a filtered sample to be analyzed for total dissolved Se and SeO_3 ; one 250 mL bottle containing a filtered sample to be analyzed for irrigation water quality; one 100 mL bottle containing a filtered sample to be analyzed for uranium (U); and an extra 1 L bottle containing an unfiltered sample as backup. Se samples were sent to South Dakota Agricultural Laboratories (SDAL) in Brookings, SD, irrigation water quality samples were sent to Ward Laboratories in Kearney, NE, and U samples were sent to Test

America in Earth City, MO. Water samples to be analyzed for Se and U were preserved with 0.0001 M nitric acid. Filtered samples were filtered in the field by pumping through 0.45 μm disposable filters. All samples were preserved with ice and/or refrigerated from the time of collection until they were analyzed. Non-disposable equipment was cleaned between sampling sites in four buckets containing approximately 0.0008 M HCl, approximately 0.008 M detergent, and two buckets of distilled water for two minutes in each bucket.

Total dissolved Se and total recoverable Se were measured at SDAL using standard method SM3500-Se-C (fluorometric), while dissolved SeO_3 was measured using a spectrometer. Samples for U analyzed at Test America were measured using United States Environmental Protection Agency (USEPA) Method 200.8. Irrigation water quality samples sent to Ward Labs were analyzed for NH_4 (USEPA), NO_3 (USEPA 1983, Method 353.2), and NO_2 (USEPA 1983, Method 353.2); and other solutes such as Na (USEPA 1983, Method 273.1), Ca (USEPA 1983, Method 215.1), Mg (USEPA 1983, Method 242.1), SO_4 (USEPA 1983, Method 375.4), Cl (USEPA 1983, Method 325.1), CO_3 (APHA 1992, Method 2320-B), HCO_3 (APHA 1992, Method 2320-B), and B (APHA 1992, Method 4500-B-D).

Bed sediment samples were collected from four locations along each cross-section. Samples were collected using a two inch diameter plastic sleeve, which was forced into the stream bed to a depth of up to approximately one foot depending on refusal. Plastic end caps were placed on each end of the sleeve to hold the captured sediment in place. Once back from the field, sediment samples were spread onto disposable plates, with one plate per sample, in order to speed up the drying process. Samples were allowed to air dry for one week, after which they were pulverized to allow them to pass through a #30 sieve. The four samples collected from

the same cross-section then were combined in equal amounts by weight to create a single composite sediment sample for each cross-section.

A sorption analysis was performed on each of the composite sediment samples to determine concentrations of sorbed SeO_4 , sorbed SeO_3 , and reduced (particulate and organic) Se species. Five grams of each composite sediment sample were mixed with a 0.1 M dipotassium phosphate (K_2HPO_4) solution in a centrifuge tube and shaken for 24 hours to remove sorbed SeO_3 and SeO_4 from sediment particles to be dissolved in the K_2HPO_4 solution. Samples then were centrifuged for 15 minutes to separate particulates, after which the supernatant was decanted into vials and sent to SDAL to be analyzed for total recoverable Se and SeO_3 . It was assumed that previously-sorbed SeO_4 and previously-sorbed SeO_3 accounted for all of the total recoverable Se from the decanted K_2HPO_4 solution. Then, five grams of dried and homogenized sediment were sent to SDAL and analyzed for total Se. Precipitated and organic Se was assumed to be the difference between the total Se present in the dried and homogenized sediment and the total recoverable Se from the decanted K_2HPO_4 solution.

2.2.2 Algae

Due to the role of algae in Se cycling in surface water (Figure 1-1 and Section 1.1), chlorophyll (a) samples were collected from each of the eight stream cross-sections in an effort to determine algae concentrations in the water and bed sediment. Algae suspended in the water column, known as phytoplankton, were sampled by collecting five cross-section averaged water samples in a 60 mL Luer-Lok syringe and filtering them through a Whatman 0.7 μm glass microfiber filter (GF/F) enclosed in a Swinnex Luer-Lok cassette. Depending on the turbidity of the sample, in some cases not all of the 60 mL collected in the syringe could be filtered. By

filtering the water through the 0.7 μm GF/F, phytoplankton was trapped on the “upstream” side of the filter. Filters were folded onto themselves to prevent loss of organic material by contact with the aluminum foil that they were immediately wrapped in to prevent light exposure and subsequent chl(a) degradation. Samples were immediately placed in a cooler for preservation and frozen after returning from the field until analysis. Due to the relative consistency between the five samples collected at each cross-section during the first sampling event in March 2014, subsequent phytoplankton sampling events only included three samples from each cross-section. An example of the syringe, GF/F, and cassette configuration used in this study is shown in Figure 2-3 below.



Figure 2-3. Example syringe, GF/F, and cassette configuration used to separate suspended algae (www.fishersci.com).

Phytoplankton chl(a) samples were collected and analyzed based on USEPA Method 445.0 (Arar and Collins, 1997). 10 mL of a 90% acetone / 10% milli-q water solution was added to a 15 mL centrifuge tube using a pipette. The frozen filter samples were removed from the freezer and, using forceps, each filter was placed into its own 15 mL centrifuge tube with acetone solution in order to extract the chl(a) from the phytoplankton. Ensuring that the filters were

completely submerged in acetone, the samples were placed back in the freezer and allowed to extract for 24 hours.

Prior to conducting chl(a) measurements, a standard curve had to be created for the fluorometer to be used. A standard curve provides an empirical relationship between a fluorometer reading in relative fluorescence units (RFU) and chl(a) concentration in mg/L. The standard curve for the fluorometer used in this analysis, being a Turner Designs Trilogy Fluorometer (Figure 2-5), was determined by systematically diluting a chl(a) solution of known concentration and obtaining an associated RFU reading for each concentration. A linear regression function was then fit to the plot of chl(a) concentration versus RFU reading. This relationship was used to correlate RFU measurements to chl(a) concentrations for this device. Figure 2-4 below illustrates the relationship between chl(a) concentration and RFU measurement for the device used in this study.

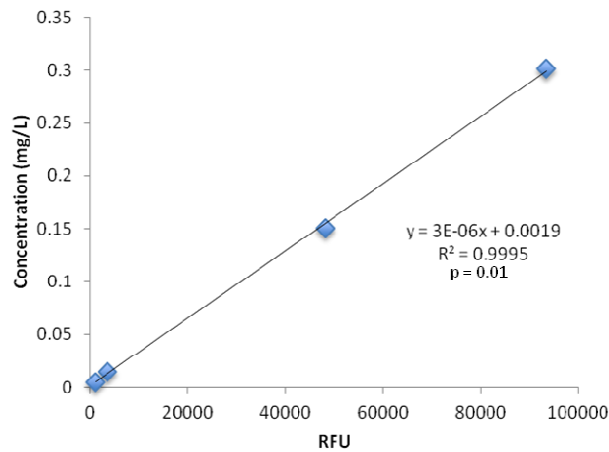


Figure 2-4. Regression analysis of chl(a) concentration and RFU reading for the Turner Designs Trilogy Fluorometer.



Figure 2-5. Turner Designs Laboratory Fluorometer used to measure the relative fluorescence units of extracted chlorophyll (a) solutions.

With chl(a) extracted from the phytoplankton and a standard function developed for the fluorometer, it was possible to obtain chl(a) estimates for the extraction solution for each of the phytoplankton samples. Using a pipette, 1 mL of extraction solution was added to a fluorometer cuvette and an RFU reading obtained. Using the standard regression equation for the fluorometer, this was converted into a concentration of chl(a) in mg/L. In converting chl(a) concentration to an equivalent algae concentration, it was assumed that the collected algae was comprised of 5% chl(a) by mass (Voros and Padisak, 1991).

Algae in the sediment, known as microphytobenthos, also was sampled from each of the eight cross-sections. Samples were collected from three locations (at approximately 25%, 50%, and 75% of the channel width) along each cross-section by pressing an upside-down 100 mm diameter by 15 mm deep petri dish into the sediment until the bottom of the petri dish was flush with the top of the sediment. The lid to the petri dish was slid carefully beneath the sediment and directly under the petri dish to encase the sediment trapped in the inverted petri dish. The sediment sample was lifted carefully to the surface, where it was then poured into a 50 mL conical centrifuge tube. The centrifuge tube then was immediately wrapped in aluminum foil to

prevent light exposure and subsequent chl(a) degradation. Samples were immediately placed in a cooler for preservation and frozen once back from the field until analysis.

Microphytobenthos samples were collected and analyzed in adaptation of USEPA Method 445.0, as no other studies/methods to determining chl(a) concentrations from sediment using an extraction/fluorometric technique could be found. The frozen sediment samples were placed in a lyophilizer (Labconco 4.5 liter FreeZone), shown in Figure 2-6, to be freeze dried for approximately five days in order to dry the sample without degrading the chl(a).



Figure 2-6. Labconco FreeZone 4.5 liter lyophilizer used for drying chlorophyll (a) sediment samples.

Once completely dry, approximately three grams of dried sediment was weighed and placed in 15 mL centrifuge tubes. 10 mL of a 90% acetone / 10% milli-q water solution was added to each 15 mL centrifuge tube using a pipette. Following this step, the extraction and measurement methods for the microphytobenthos samples were the same as for the phytoplankton samples.

2.2.4 Stream Cross-Section Geometry

Six of the eight stream cross-sections sampled were surveyed for cross-section geometry (Crooked Arroyo was excluded due to access issues, while ARK 164 was excluded due to a large error in static data collection and a lack of a benchmark). Surveys were collected using a Topcon Real Time Kinematic Global Positioning System (RTK-GPS), shown in Figure 2-8.



Figure 2-8. Topcon RTK-GPS base station, rover, and ancillary surveying equipment.

At each cross-section, the base station was first set up and allowed to collect static GPS data for at least one hour to improve survey accuracy. The accuracy associated with base station static data is shown in Table 2-2.

Table 2-2. Length of base station static data observation and associated vertical and horizontal root mean squared vertical and horizontal error for the Topcon RTK-GPS (www.topconpositioning.com).

Length of static data observation (hours)	Vertical RMS (ft)		Horizontal RMS (ft)	
	feet	meter	feet	meter
1	0.1214	0.0370	0.0328	0.0100
2	0.0858	0.0262	0.0232	0.0071
3	0.0701	0.0214	0.0189	0.0058
4	0.0607	0.0185	0.0164	0.0050
5	0.0543	0.0166	0.0147	0.0045
6	0.0496	0.0151	0.0134	0.0041
7	0.0459	0.0140	0.0124	0.0038
8	0.0429	0.0131	0.0116	0.0035
9	0.0405	0.0123	0.0109	0.0033
10	0.0384	0.0117	0.0104	0.0032
11	0.0366	0.0112	0.0099	0.0030
12	0.035	0.0107	0.0095	0.0029
13	0.0337	0.0103	0.0091	0.0028
14	0.0324	0.0099	0.0088	0.0027
15	0.0313	0.0095	0.0085	0.0026
16	0.0303	0.0092	0.0082	0.0025
17	0.0294	0.0090	0.008	0.0024
18	0.0286	0.0087	0.0077	0.0023
19	0.0278	0.0085	0.0075	0.0023
20	0.0271	0.0083	0.0073	0.0022
21	0.0265	0.0081	0.0072	0.0022
22	0.0259	0.0079	0.007	0.0021
23	0.0253	0.0077	0.0068	0.0021
24	0.0248	0.0076	0.0067	0.0020

Although accuracy increases with static data collection time, it was not possible to allow the base station to collect static data for more than one hour in most cases due to time constraints. Following one hour of static data collection, the rover was used to collect latitude, longitude, and elevation data at approximately 20 locations along each cross-section, depending on physical channel characteristics. Upon returning from the field, static data were uploaded to the National Oceanic and Atmospheric Administration (NOAA) Online Positioning User Service (OPUS) website to correct for base error. Additionally, National Geodetic Survey vertical control marks were surveyed at each cross-section to correct for rover error. Both the base error from OPUS and the rover error from the surveyed vertical control marks were used to correct for error in the cross-section surveys.

2.3 Modeling of Selenium Reactive Transport

The modeling tools used in this study include a surface water quality transport model and a coupled groundwater/surface water reactive transport model for selenium and nitrogen species. Whereas the surface water quality model has been tested previously for nitrogen transport (Bailey and Ahmaid, 2014) and the groundwater model has been tested previously for selenium reactive transport in the region, the development of a selenium module for the surface water model and the coupling of this model with the groundwater model are key aspects of this thesis. Sensitivity analysis and parameter estimation methods were used to identify key system factors and test the models against collected field data. The models then were used to assess the impact of various BMPs on groundwater Se concentration and on in-stream Se concentrations.

2.3.1 Se In-Stream Water Quality Model (OTIS-QUAL2E-Se)

2.3.1.1 Model Development

The base numerical models for the Se in-stream fate and transport model are OTIS and QUAL2E, with OTIS used as the advection-dispersion solute transport engine and QUAL2E providing the basic in-stream water quality processes for Se species, DO, N species, and algae (Bailey and Ahmadi, 2014). The inclusion of DO and N species in the Se species model is essential for accurate simulation of Se fate and transport due to the inhibition of Se chemical reduction processes in the presence of DO and NO_3 (e.g. Weres et al., 1990; White et al., 1991). QUAL2E is used to simulate the reactive behavior of DO, organic N, ammonia (NH_3), nitrite (NO_2), NO_3 , algae, and carbonaceous biological oxygen demand (CBOD) in a 1D stream network setting, with major reactions governing N cycling, DO fate, algal growth and respiration, and algal uptake of N and DO. Specific processes included in the model are

atmospheric reaeration, algal respiration, sediment oxygen demand, nitrification of NH₃, and oxidation of NO₂. Algal growth rate is a function of the availability of nutrients, light (solar radiation), and water temperature. Reactions are simulated using first-order kinetics, with terms included to condition reaction rates on the presence or absence of DO, depending on the reaction. For 1D transport (i.e. solute concentration varies only in the longitudinal direction) that accounts for advection, dispersion, lateral inflow, lateral outflow, sorption, and biochemical reaction processes, the following partial differential equation (Runkel and Broshears, 1991; Runkel, 1998) is used for each solute, with additional equations for the sorbate on the streambed (Bencala, 1983) and the solid-phase species in the streambed:

Solute in the stream channel:

$$\frac{\partial C_j}{\partial t} = -\frac{Q}{A} \frac{\partial C_j}{\partial x} + \frac{1}{A} \frac{\partial}{\partial x} \left(AD \frac{\partial C_j}{\partial x} \right) + \frac{q_L}{A} (C_{L_j} - C_j) + S_j + R_j \quad j = 1, \dots, n \quad (1)$$

$$S_j = \bar{\rho} \lambda_{s_j} (C_j^* - K_{d_j} C_j) \quad (2)$$

Sorbate in the streambed:

$$\frac{\partial C_j^*}{\partial t} = -\frac{S_j}{\bar{\rho}} \quad (3)$$

Solid-phase species in the streambed:

$$\frac{\partial C_k^s}{\partial t} = R_k \quad k = 1, \dots, m \quad (4)$$

where n is the number of dissolved-phase species, m is the number of solid-phase species in the streambed, C_j is the main channel solute concentration of the j^{th} dissolved-phase species [ML⁻³], C_k^s is the main channel solute concentration of the k^{th} solid-phase species [MM⁻¹], t is time [T], Q is the volumetric flow rate [L³T⁻¹], A is the channel cross-sectional area of flow [L²], x is

distance [L], D is the dispersion coefficient [L^2T^{-1}], q_L is the lateral inflow rate [$L^3T^{-1}L^{-1}$], C_{L_j} is the lateral inflow solute concentration of the j^{th} species [ML^{-3}], $\bar{\rho}$ is the mass of accessible sediment per volume of stream water [ML^{-3}], λ_s is the first order sorption rate coefficient [T^{-1}], C^* is the solute concentration in streambed sediment [MM^{-1}], K_d is the distribution coefficient [L^3M^{-1}], and R represents the change in solute mass due to biochemical reactions [$ML^{-3}T^{-1}$].

For representation of the Se biochemical processes (algal uptake, algal biomass conversion to organic Se, settling, mineralization and assimilation, volatilization, chemical reduction) presented in Section 1.1 and Figure 1-1, first-order reaction rate laws similar in form to those used in QUAL2E are adopted. The equations used to simulate DO, N species, and algal chemical processes in the model can be found elsewhere (Brown and Barnwell, 1987; Chapra et al., 2008) and are not shown here. For the current study, denitrification has been added as a first-order kinetic reaction, which proceeds at near-maximum rates when C_{O_2} (DO) is low. Se_{org} , SeO_4 , SeO_3 , Se_{vol} , and $SeMet$ are treated as dissolved-phase species, with fate and reactive transport simulated using Equation (1), whereas Se^0 and Se^{2-} are treated as solid-phase species in the streambed, with transformations simulated using Equation (4). Solute mass exchange between the water column and the streambed due to sorption is represented by Equation (2), and is operative only for SeO_4 and SeO_3 . Concentrations of sorbed SeO_4 and sorbed SeO_3 are calculated using Equation (3). In this study, it was assumed that once Se species take on a particulate form (i.e. solid-phase or sorbed to sediment), they immediately drop out of suspension, becoming part of the streambed and are not transported downstream. The rate of change in mass due to biochemical reactions (R) in Equations (1) and (4) for Se_{org} , SeO_4 , SeO_3 , Se^0 , Se^{2-} , Se_{vol} , and $SeMet$ is quantified by the following equations (see Figure 1-1 for transformation pathways) using first-order reaction rates:

$$R_{Se_{org}} = \left(\alpha_{Se} C_{alg} \gamma_{alg} \right) - \left(\sigma_{Se_{org}} C_{Se_{org}} \right) - \left(\lambda_{Se_{org}}^{min} C_{Se_{org}} \right) - \left(\lambda_{Se_{org}}^{vol} C_{Se_{org}} \right) \quad (5)$$

$$R_{Se_{O_4}} = \left[\left(\lambda_{Se_{org}}^{min} C_{Se_{org}} \right) + \left(\lambda_{SeMet}^{min} C_{SeMet} \right) - \left(fr_{Se_{O_4}} \alpha_{Se} \mu_{alg} C_{alg} \right) - \left(\lambda_{Se_{O_4}} C_{Se_{O_4}} \right) - \left(\lambda_{Se_{O_4}}^{assim} C_{Se_{O_4}} \right) - \left(\lambda_{Se_{O_4}}^{vol} C_{Se_{O_4}} \right) \right] \quad (6)$$

$$R_{Se_{O_3}} = \left(\lambda_{Se_{O_4}} C_{Se_{O_4}} \right) - \left[\left(1 - fr_{Se_{O_4}} \right) \alpha_{Se} \mu_{alg} C_{alg} \right] - \left(\lambda_{Se_{O_3}} C_{Se_{O_3}} \right) - \left(\lambda_{Se_{O_3}}^{vol} C_{Se_{O_3}} \right) - \left(\lambda_{Se_{O_3}}^{assim} C_{Se_{O_3}} \right) \quad (7)$$

$$R_{Se^0} = \left(\lambda_{Se_{O_3}} C_{Se_{O_3}} \right)^s - \left(\lambda_{Se^0} C_{Se^0}^s \right) \quad (8)$$

$$R_{Se^{-2}} = \left(\lambda_{Se^0} C_{Se^0}^s \right) + \left(\lambda_{Se_{vol}} C_{Se_{vol}} \right) \quad (9)$$

$$R_{Se_{vol}} = \left(\lambda_{Se_{org}}^{vol} C_{Se_{org}} \right) + \left(\lambda_{Se_{O_4}}^{vol} C_{Se_{O_4}} \right) + \left(\lambda_{Se_{O_3}}^{vol} C_{Se_{O_3}} \right) + \left(\lambda_{SeMet}^{vol} C_{SeMet} \right) - \left(\lambda_{Se_{vol}} C_{Se_{vol}} \right) \quad (10)$$

$$R_{SeMet} = \left(\alpha_{Se}^{SeMet} C_{alg} \gamma_{alg} \right) - \left(\sigma_{SeMet} C_{SeMet} \right) - \left(\lambda_{SeMet}^{vol} C_{SeMet} \right) - \left(\lambda_{SeMet}^{min} C_{SeMet} \right) \quad (11)$$

where $R_{Se_{org}}$ is the change in organic Se mass [MT⁻¹], $R_{Se_{O_4}}$ is the change in SeO₄ mass [MT⁻¹], $R_{Se_{O_3}}$ is the change in SeO₃ mass [MT⁻¹], R_{Se^0} is the change in Se⁰ mass [MT⁻¹], $R_{Se^{-2}}$ is the change in Se⁻² mass [MT⁻¹], $R_{Se_{vol}}$ is the change in volatile Se mass [MT⁻¹], R_{SeMet} is the change in SeMet mass [MT⁻¹], α_{Se} is the fraction of algal biomass that is Se [MM⁻¹], C_{alg} is the mass of algae in the water column [M], γ_{alg} is the rate at which algal Se is converted to organic Se [T⁻¹], $\sigma_{Se_{org}}$ is the settling rate of organic Se [T⁻¹], $C_{Se_{org}}$ is the mass of organic Se in the water column [M], $\lambda_{Se_{org}}^{min}$ is the mineralization rate of organic Se [T⁻¹], $\lambda_{Se_{org}}^{vol}$ is the volatilization rate of organic Se [T⁻¹], λ_{SeMet}^{min} is the mineralization rate of SeMet [T⁻¹], C_{SeMet} is the mass of SeMet in the water column [M], $fr_{Se_{O_4}}$ is the algal preference factor SeO₄, μ_{alg} is the SeO₄ algal uptake rate [T⁻¹], $\lambda_{Se_{O_4}}$ is the rate at which SeO₄ is reduced to SeO₃ [T⁻¹], $C_{Se_{O_4}}$ is the mass of SeO₄ in the water column [M], $\lambda_{Se_{O_4}}^{assim}$ assimilation rate to SeMet [T⁻¹], $\lambda_{Se_{O_4}}^{vol}$ is the volatilization rate of SeO₄ [T⁻¹], $\lambda_{Se_{O_3}}$ is the

rate at which SeO_3 is reduced to Se^0 [T^{-1}], C_{SeO_3} is the mass of SeO_3 in the water column [M], $\lambda_{\text{SeO}_3}^{\text{vol}}$ is the volatilization rate of SeO_3 [T^{-1}], $\lambda_{\text{SeO}_3}^{\text{assim}}$ is the assimilation rate to SeMet [T^{-1}], λ_{Se^0} is the rate at which Se^0 is reduced to Se^{-2} [T^{-1}], $C_{\text{Se}^0}^s$ is the mass of Se^0 in sediment [M], $\lambda_{\text{Se}^0}^{\text{vol}}$ is the rate at which volatile Se is converted to Se^{-2} [T^{-1}], $C_{\text{Se}^0}^{\text{vol}}$ is the mass of volatile Se in the water column [M], $\lambda_{\text{SeMet}}^{\text{vol}}$ is the rate at which SeMet is volatilized [T^{-1}], C_{SeMet} is the mass of SeMet in the water column [M], $\alpha_{\text{Se}}^{\text{SeMet}}$ is the fraction of algal Se that is SeMet [MM $^{-1}$], σ_{SeMet} is the settling rate of SeMet [T^{-1}], and $\lambda_{\text{SeMet}}^{\text{min}}$ is the mineralization rate of SeMet [T^{-1}].

Each first-order rate coefficient λ shown in Equations (5)-(11) is modified from a base value λ_{20} (at $T = 20$ °C) according to the water temperature T_{water} of the current day of the simulation (Brown and Barnwell, 1987):

$$\lambda = \lambda_{20} 1.083^{(T_{\text{water}} - 20)} \quad (12)$$

The fraction of algal Se uptake corresponding to SeO_4 uptake in Equation (6) is calculated according to the following equation, where f_{SeO_4} is the algal preference factor for SeO_4 (as opposed to SeO_3):

$$f_{\text{SeO}_4}^{\text{algal}} = \frac{f_{\text{SeO}_4} C_{\text{SeO}_4}}{(f_{\text{SeO}_4} C_{\text{SeO}_4} + (1 - f_{\text{SeO}_4}) C_{\text{SeO}_3})} \quad (13)$$

The chemical reduction of SeO_4 , SeO_3 , Se^0 , and Se_{vol} is tempered by the presence of DO and NO_3 using inhibition constants, which impede the rate of Se reduction. For SeO_4 reduction, the base rate constant is modified according to:

$$\lambda_{SeO_4} = \lambda_{SeO_4,20} \left(\frac{I_{O_2}}{I_{O_2} + C_{O_2}} \right) \left(\frac{I_{NO_3}}{I_{NO_3} + C_{NO_3}} \right) \quad (14)$$

where I_{O_2} and I_{NO_3} are the DO and NO_3 inhibition constants [ML^{-3}], and indicate the concentrations of DO and NO_3 at which λ_{SeO_4} is half of its base value. Similar equations are used for λ_{SeO_3} , λ_{Se^0} , and $\lambda_{Se_{vol}}$.

Both Se^0 and Se^{-2} are solid-phase species contained in the streambed sediment. The mass of Se that is transferred from dissolved-phase SeO_3 to solid-phase Se^0 via chemical reduction is converted to a solid concentration ($\mu g/g$) using the volume of stream water, the volume of accessible bed sediment, and the bulk density of the sediment. This is indicated by the s superscript for the SeO_3 reduction term in Equation (8).

2.3.1.2 Model Code Development and Solution Strategy

The FORTRAN modeling code for OTIS is used as the underpinning computer code, with subroutines defining QUAL2E and Se in-stream processes imbedded within the code. The advection-dispersion equation (Equation 1) is solved using a Crank-Nicolson finite-difference scheme (Runkel, 1998), with the stream network divided into physically-uniform reaches and each reach divided into segments, with each segment representing a finite-difference cell. Whereas the original OTIS model can be applied to a single stream and account only for multiple, non-interacting species (Runkel, 1998), the modeling code for this study was modified to simulate the fate of multiple interacting chemical species in a multi-stream network (Bailey and Ahmadi, 2014). For multiple interacting chemical species, the 4th-order Runge-Kutta method was implemented to solve the system of ordinary differential equations required for simulating the kinetics of interacting species (Chapra, 1997), and hence be able to solve the QUAL2E and

Se species' mass-balance equations. To implement OTIS in a multi-stream network, mass balance mixing calculations were implemented at stream junctions, with physical parameters and reach lengths of each stream designated in input files.

Model parameters are defined reach by reach, with each reach divided into a specified number of stream segments (finite-difference cells). The length of each reach is specified. The concentration for each solute is specified at the upstream end of the main stem streams (i.e. streams not fed exclusively by groundwater). The model can operate under either steady or unsteady flow conditions. For steady, non-uniform flow, lateral inflow/outflow rates q_L are set to desired values in the input files, with associated concentration values C_L for each solute. For a multi-stream network, flow rates are provided for each stream, with flow accumulating as tributaries discharge to the main stem of the channel. Water diverted into irrigation canals from the main stem is subtracted from the main stem flow and not present in the finite-difference cell immediately downstream of the cell from which the diversion occurred. Water left over in the irrigation canals (i.e. water not applied to fields or lost to non-beneficial use such as canal seepage) is returned to the main stem or tributaries and accumulated as described above. For unsteady, non-uniform flow, segment-by-segment flow rates, lateral inflow/outflow rates, and cross-section areas are provided by a streamflow routing model.

2.3.1.3 Model Implementation

2.3.1.3.1 Steady Flow Model

For the steady flow model, the Arkansas River and tributaries are divided into reaches that are approximately 250 m in length, with each reach further divided into five finite difference cells. The model grid representing the stream network is shown in Figure 2-9.

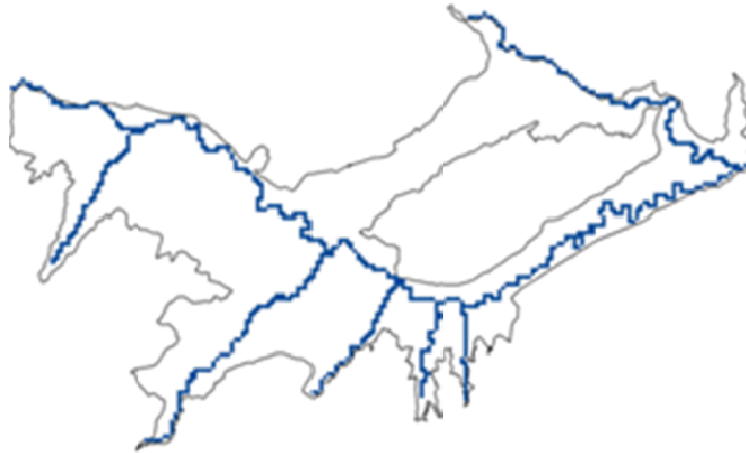


Figure 2-9. Model study region showing the model boundaries and the stream network computational grid for the OTIS-QUAL2E-Se model.

Values of daily air temperature ($^{\circ}\text{C}$) and hourly solar radiation ($\text{MJ m}^{-2} \text{m}^{-1}$) were obtained from the climate station at the La Junta airport near the town of La Junta (Figure 2-1), and daily daylight hours for the region were obtained from the U.S. Naval Observatory. Simulations are run for two years using hourly time steps, with data for air temperature, solar radiation, daily daylight hours, and streamflow corresponding to the years 2006-2007. Average field measurements were used to set the stream width, stream depth, and channel bed slope to 60 m, 0.75 m, and 0.0016 m m^{-1} , respectively. Using this channel geometry and observed stream gage flow rates at the upstream end of the Arkansas River, Patterson Hollow, Timpas Creek, Crooked Arroyo, Anderson Creek, and Horse Creek of 29.16, 1.00, 1.94, 0.47, 1.00, and $0.56 \text{ m}^3 \text{ sec}^{-1}$, respectively, an average calibrated Manning's roughness coefficient (n) of 0.042 was used to produce predicted stream flow rates that correspond closely to observed the data.

Lateral groundwater flows to the Arkansas River ($1.19 \text{ m}^3 \text{ day}^{-1} \text{ m}^{-1}$ to $3.57 \text{ m}^3 \text{ day}^{-1} \text{ m}^{-1}$) and the tributaries are based on average simulation results from the groundwater modeling study of Morway et al. (2013) for the time period 1999-2009, and concentration values of DO and NO_3 in the lateral inflow (2.0 mg/L to 10.0 mg/L and 0.1 mg/L to 10.0 mg/L , respectively) are based

on average simulation results from the calibrated Se and N groundwater reactive solute transport model of Bailey et al. (2014) for the years 2006-2009. In-stream DO and C_{NO_3} at the upstream end of the Arkansas River are based on field data collected in the region (Gates et al., 2009). To reflect the hydrologic patterns of tributary flow, i.e., streamflow is groundwater-driven, C_{DO} and C_{NO_3} at the upstream end of the tributaries are set to 0.0 mg/L and solute mass enters the tributary stream channels only via groundwater discharge. Evaporation from the water surface was assumed to be negligible and was ignored in both the steady and unsteady flow models.

2.3.1.3.2 Unsteady Flow Model

The OTIS-QUAL2E-Se model was applied to the 2006-2009 time period for model corroboration against field data, with simulated spatial- and temporal-varying flow rates in the Arkansas River and tributaries used to provide accurate flow conditions for solute transport. Spatial- and temporal-varying flow rates for the OTIS-QUAL2E-Se simulation using unsteady streamflow were provided by a MODFLOW groundwater flow model employing the Streamflow-Routing (SFR) package, which simulates streams in a model through addition and subtraction of water to streams from runoff, precipitation, and evapotranspiration, as well as the interaction between streams and aquifers (Prudic et al., 2004). The original calibrated and tested groundwater model for the region (Morway et al., 2013) is run through 2009. The model, which used the River package to simulate groundwater-surface water interactions, was modified to use the SFR package along the grid cells representing the Arkansas River and its tributaries (Figure 2-1). Streambed elevation (range: 1195 m amsl to 1315 m), stream length (avg. = 245 m), streambed slope (avg. = 0.003 m/m), thickness, streambed hydraulic conductivity (avg. = 0.12 m/day), and saturated water content (avg. = 0.30) and specific yield (avg. = 0.19) of the alluvial

material underlying the stream were specified for each SFR cell. Manning's roughness coefficient values (0.03 to 0.06) (Barnes, 1967), inflow (avg. = 13.8 m³/s) and outflow volumetric flow rates were specified for each stream segment, i.e. a collection of SFR cells that corresponds to reaches of the OTIS-QUAL2E-Se grid. Inflows at the upstream end of the stream network were provided by a stream gage, with outflows specified along certain segments to represent measured diversions to irrigation canals. Three irrigation canals (Fort Lyon, Holbrook, Rocky Ford) divert water from the Arkansas River within the study region, with average diversion rates of 8.9 m³/s, 1.8 m³/s, and 1.2 m³/s during the study period. Although the Fort Lyon Storage and Las Animas Consolidated canals also divert water from the USR, they were erroneously excluded from this study but will be included in future work. The model was run using weekly time steps (Morway et al., 2013), with model output consisting of weekly streamflow, groundwater inflow/outflow, and stream depth for each grid cell, with output prepared to provide Q , A , and q_L (Equation 1) for the OTIS-QUAL2E-Se simulation. No additional modification of model parameters (e.g. streambed hydraulic conductivity, specific yield) in the MODFLOW model was performed.

2.3.1.4 OTIS-QUAL2E-Se Model Sensitivity Analysis

Models that account for in-stream advection, dispersion, and chemical chemical reactions can be used not only to simulate in-stream solute concentrations, but also to investigate the environmental factors that govern these concentrations through sensitivity analysis (SA) (Beck, 1987; Campolongo and Saltelli, 1997; Saltelli et al., 2000; Saltelli, 2002; Bailey and Ahmadi, 2014) and thereby to elucidate fate and transport control for a given stream system. Due to the large number of parameters associated with the processes that govern Se transformations in the

OTIS-QUAL2E-Se water quality model, it was desired to quantify the sensitivity of these parameters both to explore the key processes governing Se cycling and to identify the parameters best suited for model calibration. To do this, a SA was performed in two parts: first, each model parameter was stressed by one order of magnitude from the baseline value using the one-at-a-time (OAT) method (Hamby, 1994; Campolongo and Saltelli, 1997), with model output compared to baseline model output. Second, a more detailed relationship between parameter value and model output was explored to discover the most influential model parameters, with the parameter values stressed over a range of 0.1 to 10 times the baseline value. By doing so, the behavior of multiple parameters could be explored relative to the water quality indicators, thereby testing parameters for non-linearity and providing a rank of parameter influence. Parameter values for the baseline model simulation were taken from the literature and from a previous modeling study of the stream network (Bailey and Ahmadi, 2014). These values are presented in Appendix A Table A-1.

The first part of the SA was performed under two baseline conditions: one in which in-stream NO₃ concentration is specified at average historical levels (2.0 mg/L), and one in which NO₃ concentration is specified at a lower level (0.6 mg/L, a decrease of 70%) to represent implementation of reduced fertilizer application, a practice being considered for the region (Bailey et al., 2015). These two conditions were analyzed due to the influence of NO₃ on Se speciation, with lower concentrations of NO₃ allowing for more chemical reduction of SeO₄ to SeO₃ and from SeO₃ to Se⁰. For the second part of the SA, the most influential parameters were identified by the following criteria:

$$\frac{\% \Delta \text{ in Output from Baseline}}{\% \Delta \text{ in Input from Baseline}} \geq 0.10 \quad (15)$$

or

$$\frac{\% \Delta \text{ in Output from Baseline}}{\% \Delta \text{ in Input from Baseline}} \leq -0.05 \quad (16)$$

wherein %Δ represents percent change and with either Equation (15) or (16) used depending on whether the parameter caused an increase or decrease in in-stream solute concentration.

2.3.1.5 OTIS-QUAL2E-Se Model Testing using Unsteady Flow Conditions

The unsteady OTIS-QUAL2E-Se model was used for corroboration due to the more realistic representation of the natural system as compared to the steady-state model. Simulation results were compared against observed values of DO, NO₃, dissolved SeO₄, dissolved SeO₃, sorbed SeO₄, sorbed SeO₃, and reduced and organic Se. Model reaction rate parameters identified as influential in the SA were modified within realistic ranges to provide reasonable matches between simulated and observed data. Boundary conditions and forcing terms (e.g., upstream-end inflow solute concentration, groundwater inflow solute concentration, solar radiation, etc.) were not modified from baseline values. All other parameter values were designated as the baseline values (Appendix A Table A-1). Water samples collected from the Arkansas River and tributaries during the model simulation time period (2006-2009) were analyzed for total dissolved Se. To provide in-stream concentrations of SeO₄ and SeO₃, the average partitioning of total Se into SeO₄ and SeO₃ (82% SeO₄, 18% SeO₃) observed from water samples collected during 2011-2014 (Appendix A Table A-3) from the targeted stream cross-sections (Section 2.2) was applied to the value of total Se observed from 2006-2010 (Section 3.1 Table 3-1). Observed values of DO, NO₃, total Se, dissolved SeO₄, and dissolved SeO₃ are provided in Tables A-2 and A-3 in Appendix A. Simulated sorbed SeO₄, sorbed SeO₃, and reduced and organic Se were compared to values measured during the 2011-2014 sampling period, with the assumption that streambed conditions for the sampling period are similar to

those of the simulation period (2006-2009). Since the measured field data do not distinguish between various forms of reduced and organic Se, simulated Se^0 concentrations were compared to the total residual Se in the streambed samples.

Comparison between observed and simulated streamflow at two gages (Rocky Ford, La Junta) along the Arkansas River demonstrates reasonable accuracy of the model, as discussed in Section 3.2.2. Solute concentrations C_{L_j} in the groundwater inflow were provided by a calibrated and tested UZF-RT3D model (Bailey et al., 2013) for groundwater transport of Se and N in the region (Bailey et al., 2014), with daily model-calculated groundwater concentrations of DO, NH_3 , NO_3 , SeO_4 , SeO_3 , and SeMet averaged on a weekly basis to coincide with the weekly MODFLOW q_L values.

2.3.2 Coupled Surface Water – Groundwater Reactive Transport Model (RT3D-OTIS)

Discrepancies were discovered between predicted and observed concentrations in the tributaries (see Section 3.2.3) as seen in the OTIS-QUAL2E-Se model described in Section 2.3.1. It was determined that a dynamic link between the groundwater flow model UZF-RT3D (Bailey et al., 2013) and the in-stream water quality model OTIS-QUAL2E-Se (Bailey and Ahmadi, 2014) might improve model performance since the tributaries were fed largely by groundwater. As such, the model code was modified to simulate chemical interactions between the surface water and groundwater systems by linking the OTIS-QUAL2E-Se model and the UZF-RT3D groundwater model, with the linked model referred to as RT3D-OTIS. By doing this, for a given time step, species concentrations and lateral flows from the previous time step within the OTIS-QUAL2E-Se model are used as input for the UZF-RT3D model. Additionally, after having simulated groundwater chemical reactions in the previous time step, groundwater concentrations

predicted by the UZF-RT3D model are used as input for the OTIS-QUAL2E model. This communication between the surface water and groundwater allows for species concentrations to be more realistically impacted by the dynamics of a highly-correlated surface water/groundwater system. The baseline RT3D-OTIS model used the unsteady streamflow and groundwater heads provided by the calibrated and tested groundwater model for the region (Morway et al., 2013).

2.3.2.1 RT3D-OTIS Model Calibration

The RT3D-OTIS model was calibrated by simulating the period 2006-2009 (described in Section 2.3.1.3.2) which corresponded to a period during which in-stream water quality samples for dissolved SeO_4 , dissolved SeO_3 , DO, and NO_3 had been collected. Samples during this period were collected from six locations along the River and from locations in four tributaries. These locations were assigned as observation cells in the RT3D-OTIS model so that model predicted concentrations could be compared to observed data. The first step of the calibration process was simply to run the RT3D-OTIS model with baseline parameter values. Deviations between predicted and observed solute concentrations were addressed in one of three ways:

1. UZF-RT3D parameter values were adjusted as to modify the simulated concentration of lateral groundwater inflow to surface water;
2. OTIS-QUAL2E-Se parameter values were adjusted as to modify the in-stream reaction rates of solutes;
3. Solute concentrations in irrigation tailwater runoff were adjusted in the RT3D-OTIS model to account for additional sources of solute loads to the system.

The results of the SA, described in Section 3.2.1, were instrumental in identifying key parameters that could be adjusted in the OTIS-QUAL2E-Se portion of the RT3D-OTIS model in

order to drive predicted solute and sediment species concentrations toward observed values. Although a SA was not performed on the parameters governing the UZF-RT3D portion of the RT3D-OTIS model, after targeting only a few parameters it was clear that only a limited number of parameters needed to be adjusted to make the required changes in predicted in-stream concentrations. Due the potential of riparian zones to reduce high valence forms of SeO_4 and NO_3 , the heterotrophic chemical reduction rate of SeO_4 in the riparian zone ($\lambda_{\text{SeO}_4\text{RH}}$) and the heterotrophic chemical reduction rate of NO_3 in the riparian zone ($\lambda_{\text{NO}_3\text{RH}}$) were targeted for calibration (Peterjohn and Correll, 1984; Jacobs and Gilliam, 1985; Cooper, 1990). Additionally, since irrigation tailwater runoff has been reported to contain NO_3 concentrations of up to 3.3-8.0 times those of the irrigation water being applied to fields, a SeO_4 tailwater multiplication factor (TW_{SeO_4}) and a NO_3 tailwater multiplication factor (TW_{NO_3}) were added to the RT3D-OTIS model (Ciotti, 2005; MacKenzie and Viets, 1974) and targeted for calibration. These tailwater multiplication factors determined the concentration of the irrigation tailwater entering surface water as surface return flows by multiplying the concentration of the irrigation water being applied to the fields by the tailwater multiplication factor. Where possible, parameter values were kept within ranges previously reported in the literature.

The RT3D-OTIS model was calibrated using time series plots of predicted and observed concentrations as well as statistics including predicted and observed concentration mean (μ), coefficient of variation (CV), and mean absolute error (MAE) (see Section 3.2.2). Although no specific statistical criteria were used to certify the RT3D-OTIS model was “sufficiently calibrated”, an emphasis was placed on improving the performance of dissolved Se species over other water quality parameters. Additionally, improving the predictive performance within the Arkansas River was preferred over improving the performance within the tributaries. These

trade-offs were necessary in part due to the inability to adjust QUAL2E chemical reduction rates on a spatially targeted basis.

Although no Se sediment data existed over the simulation period from 2006-2009, RT3D-OTIS predicted speciation percentages of sorbed SeO_4 , sorbed SeO_3 , and Se^0 were used to compared to observed speciation percentages of sorbed SeO_4 , sorbed SeO_3 , and reduced and organic Se, respectively, collected after the modeling period. Section 2.3.1.5 describes the justification for comparing model predicted Se^0 to observed values of reduced and organic Se. Additionally, as also described in Section 2.3.1.5, samples collected during the simulation period were not directly analyzed for dissolved SeO_4 and SeO_3 . Instead, dissolved SeO_3 and SeO_4 were assumed to be approximately 18% and 82%, respectively, of total dissolved Se based on fractions from data collected after the calibration period.

2.3.2.2 Modeling Best Management Practices (BMPs)

With the RT3D-OTIS model sufficiently calibrated, it was applied to predict changes in in-stream Se concentrations associated with various BMPs. The model simulation period for BMP analysis was approximately 38 years. To simulate this period of time, the calibrated groundwater flow model for the region (Morway et al., 2013) for the simulation period of 1999-2009 was repeated until 38 years of MODFLOW output was obtained and could be used by the RT3D-OTIS model. After approximately 38 years of weekly output consisting of streamflow, groundwater inflow/outflow, and stream depth for each time step was obtained, the MODFLOW output was prepared for use by the RT3D-OTIS model. First, a baseline MODFLOW / RT3D-OTIS BMP scenario was run using parameter values in the RT3D-OTIS model from the calibration effort described in Section 2.3.2.1. The results from this baseline scenario provided

the in-stream Se concentrations to which the predicted concentrations under each of the simulated BMP scenarios were compared. The BMPs examined as part of this analysis are outlined in Table 2-3.

Table 2-3. BMPs examined using the RT3D-OTIS model for the purpose of lowering in-stream Se concentrations in the LARV.

BMP Description	Amount	Symbol
Reduced Fertilization	10%	RF10
	20%	RF20
	30%	RF30
Reduced Irrigation	10%	RI10
	20%	RI20
	30%	RI30
Land Fallowing	5%	LF5
	15%	LF15
	25%	LF25
Canal Sealing	20%	CS20
	40%	CS40
	80%	CS80

Of the BMPs examined, reduced fertilization (RF) was the simplest to model. Since RF did not involve a change in water management practices, the baseline MODFLOW output could be used in the simulations of all three RF scenarios. Modeling the RF scenarios involved decreasing NH₄ fertilizer application rate for RF 10, RF 20, and RF30 by 10%, 20%, and 30%, respectively. Baseline fertilizer application rates for the LARV are detailed in the study by Bailey et al. (2012).

Reduced irrigation (RI), being a water management BMP, required modifying MODFLOW by reducing the volume of irrigation water applied to each field by 10%, 20%, or 30%. Altering the amount of water applied to each field affected simulated deep percolation from the root zone to the water table aquifer and the associated groundwater heads. In addition, since water applications from the irrigation canals to the fields were decreased, diversions from the River into the canals were decreased by the percentage associated with each RI scenario. The RT3D-OTIS model was then run with new flow output from MODFLOW that reflected the

impacts of both the decrease in irrigation water applied to fields and an equivalent decrease in diversions from the River.

Land fallowing (LF) was modeled in a similar fashion to RI, whereby either 5%, 15%, or 25% of the cultivated fields in the USR were fallowed and therefore irrigation water was no longer applied to those fields. As such, MODLFOW was run such that the RT3D-OTIS model used MODFLOW output reflective of both the decrease in irrigation water applied to fields and an equivalent decrease in water diversions to irrigation canals from the River. Baseline irrigation water application rates are detailed in the study of Bailey (2012).

Canal sealing (CS) was the most difficult of the BMPs to model and required a number of simplifying assumptions. The various degrees of canal sealing modeled, being CS20, CS40, and CS80, represented a decrease in the conductance of irrigation canals in MODFLOW of 20%, 40%, and 80%, respectively. Conductance of irrigation canals or any conveyance channel is a function of the hydraulic conductivity of the bed material and the geometry of the channel, and has a direct impact on the head difference between the stream and the adjacent aquifer.

Streambed conductance (C) is defined as shown in equation (17) (Lackey et al., 2015).

$$C = K \frac{A}{b} \quad (17)$$

where K is the hydraulic conductivity of the streambed [L^2T^{-1}], A is the area of the streambed [L^2], and b is the thickness of the streambed [L].

These reduced conductance values, which result in corresponding reductions in canal seepage, are in line with those reported in the study of Susfalk et al. (2008), which reported seepage reductions of 35%-85% following field application of linear anionic polyacrylamide (LA-PAM) to canals. The same study also reported that as much as 30% of water diverted for irrigation is lost to the aquifer through seepage. To most accurately model the required decreases

in diversion volume associated with each CS scenario, not only would the total decrease in seepage volume for each canal have to be quantified, but the impacts of those seepage volume decreases on lateral groundwater return flows to the Arkansas River would also have to be quantified. This would have to be done as to not impact flows in the Arkansas River. To achieve this, the decreases in diversions for a given canal would have to be timed such that the water remaining in the Arkansas River offsets the decreases in lateral groundwater return flows. However, not only would this approach be prohibitively time-intensive, it would be very difficult to attribute changes in lateral groundwater return flows to a particular canal, as the changes in lateral groundwater return flows could be the result of changes in seepage volumes from more than one canal. Therefore, accurately determining the volume and timing of diversion reductions for a given canal would be extremely difficult. Another approach to quantifying the amount by which diversions to each irrigation canal should be reduced would be to quantify the calculated reduction in seepage volume for each canal for each of the three CS scenarios as compared to the baseline simulation. Then, diversions to each canal for each time step would simply be reduced by an amount proportional to the total seepage reduction over the simulation period. However, this approach would not address the issue of the timing of the return flows to the Arkansas River, and would also be extremely time consuming. To simplify the modeling approach, reductions in diversion volumes were estimated by scaling the reported range in seepage reduction (35%-85%) linearly between CS20, CS40, and CS80, where a 20% decrease in conductance would result in a 35% reduction in seepage volume, a 40% decrease in conductance would result in a 52% reduction in seepage volume, and an 80% decrease in conductance would result in a 85% reduction in seepage volume. Furthermore, the 30% seepage rate reported in the study of Susfalk et al. (2008) was applied to the three canals included in this study. As such, diversion volumes

for each of the CS scenarios examined in this study were determined according to equations (18) through (20) below:

$$Q_{D_{CS20}}=Q_{D_B} - Q_{D_B} * 0.30 * 0.35 \quad (18)$$

$$Q_{D_{CS40}}=Q_{D_B} - Q_{D_B} * 0.30 * 0.52 \quad (19)$$

$$Q_{D_{CS80}}=Q_{D_B} - Q_{D_B} * 0.30 * 0.85 \quad (20)$$

where $Q_{D_{CS20}}$ is the diversion volume for the CS20 scenario, $Q_{D_{CS40}}$ is the diversion volume for the CS40 scenario, $Q_{D_{CS80}}$ is the diversion volume for the CS80 scenario, and Q_{D_B} is the baseline diversion volume.

2.4 Multi-Criteria Decision Analysis

2.4.1 Overview

The use of multi-criteria decision analysis (MCDA) in choosing between courses of action which involve numerous, complex, and often unrelated variables has been in practice for a number of decades, and over that time has become increasingly common. In fact, when considering only the Preference Ranking Organization Method for Enrichment Evaluations (PROMETHEE) MCDA method, at least 217 scholarly papers from 100 journals have been published in disciplines including environmental management, hydrology and water management, business and financial management, chemistry, logistics and transportation, manufacturing and assembly, energy management, agriculture, and government (Behzadian et al., 2010). In the field water resources planning and management, at least 113 MCDA studies from 34 countries have been published in recent years (Hajkowicz and Collins, 2007). The use of MCDA in environmental applications has become particularly widespread due to the nature of environmental issues; that is, where some decisions can be made based solely on social,

economic, or environmental bases, most environmental decisions have to be made with consideration of all of the aforementioned concerns. Additionally, the units by which social, economic, and environmental concerns are quantified vary, making their direct side-by-side comparison difficult (Kiker et al., 2005). Saaty (1990) likened the attempt to compare such differing concerns to comparing “the inch, the pound, the angstrom, and the dollar.” However, when properly utilizing MCDA, such comparisons can be made in a way that lessens ambiguity and provides decision makers with a more transparent solution inclusive of the multi-faceted concerns of stakeholders (Davies et al., 2013).

One of the key components of MCDA is stakeholder engagement. With respect to water resources management, the framework of such engagement can be outlined as follows (Hamalainen et al., 2001):

1. Framing, structuring, and learning the problem

- identification of interest groups
- selection of decision criteria
- defining operational, measurable attributes

2. Identifying Pareto-optimal alternatives

- interactive search of Pareto-optimal alternatives

3. Seeking group consensus

- value tree prioritizations of Pareto-optimal alternatives
- consensus seeking by joint prioritizations

4. Seeking public acceptance

- public evaluation of value tree prioritizations

The outline above is a general framework for how MCDA should be appropriately applied to complex decision making. However, there are multiple MCDA methods which can be used in water resources applications that conform to this framework, including but not limited to fuzzy set analysis, compromise programming (CP), analytic hierarchy process (AHP), ELECTRE (I, II, III, IV, and TRI), PROMETHEE (I, II, V), multi-attribute utility theory (MAUT), multi-criterion analysis (MCQA I, II, and III), EXPROM, MACBETH, weighted summation, and TOPSIS (Hajkowicz and Collins, 2007), with some methods having certain advantages depending on the specific application.

2.4.2 The AHP Method

Of the MCDA methods listed, one of the most widely used is the AHP. Developed by Thomas Saaty in 1980, the AHP has been used in numerous water resources applications, many of which dealt specifically with water quality (Hajkowicz and Collins, 2007). The study of Almasri and Kaluarachchi (2005) used the AHP to prioritize nitrate management alternatives for the Sumas-Blaine aquifer in Washington State, and illustrated the dominant importance of economic factors in weighting alternatives. The study of DeSteiguer et al. (2003) used the AHP in assessing integrated watershed management plans, including the chemical integrity of surface water, and emphasized the effectiveness of the AHP in providing stakeholders' concerns can be considered even though they may not have a clear understanding of various watershed management plans.

The AHP is used to derive rankings of alternatives through comparing alternatives two at a time (pairwise comparisons) based on either actual measurements (i.e. cost, efficiency, etc.) or from relative strength of preferences and feelings (Saaty, 1987). The general structure of the

AHP is hierarchical, which from top to bottom includes the main criteria, sub-criteria, and alternatives, as shown in Figure 2-10.

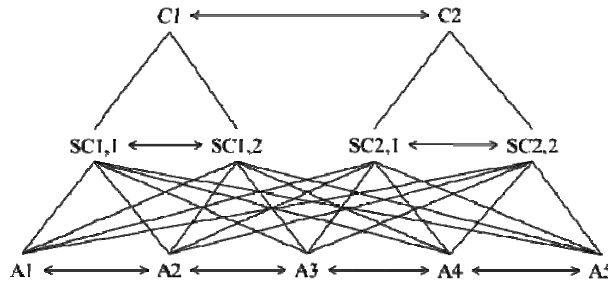


Figure 2-10. General AHP structure, including main criteria (C1, C2), sub-criteria (SC1,1, SC1,2, SC2,1, SC2,2), and alternatives (A1, A2, A3, A4, A5). The hierarchical structure of the AHP is shown, whereby pairwise comparisons are made at each level (arrows) with respect to the criteria preceding them (lines).

The hierarchical structure of the AHP serves to break down the complex relationship between criteria and alternatives into sets of pairs that can be easily compared. It also ensures to the designer of the hierarchy that the elements being compared at each level (i.e. main criteria, sub-criteria, and alternatives) are of the same magnitude and can therefore be reasonably compared in the first place (Saaty, 1990). The operation of the AHP is such that at each level, pairwise comparisons are made between all elements at that level with respect to the preceding criteria (main criteria are compared only amongst themselves as there are no criteria preceding them). For example, using Figure 2-10, a stakeholder might be asked “when considering Criteria 1 (C1), do you prefer sub-criteria 1 (SC1,1) or sub-criteria 2 (SC1,2)?” The same process follows at the alternatives level (A1-5), where all of the alternatives would be compared to each other with respect to each of the four sub-criteria. Regarding quantifying preference of one criteria or alternative over another, Thomas Saaty recommended using a 1-9 scale (Saaty scale) when making pairwise comparisons, wherein assigning a value of 9 to A1 when comparing it to A2, for example, it is implied that A1 is 9 times more preferred than A2 (and therefore A2 is 1/9 as preferred as A1). Although the Saaty scale was recommended by Saaty, others have implemented scales varying in range to aid in simplicity, to encompass comparisons between

elements that are of substantially different magnitude, etc. (Macharis et al., 2004; Steele et al., 2009). Following the traditional Saaty ranking scale, the set of possible ranks when comparing one criterion or alternative to another is shown in Figure 2-11.

$$S = \left\{ \frac{1}{9}, \frac{1}{8}, \frac{1}{7}, \frac{1}{6}, \frac{1}{5}, \frac{1}{4}, \frac{1}{3}, \frac{1}{2}, 1, 2, 3, 4, 5, 6, 7, 8, 9 \right\}$$

Figure 2-11. The set of possible ranks when quantifying the preference for one criteria or alternative over another (Alphonce, 1997).

The Saaty scale corresponds to the word scale shown in Table 2-4.

Table 2-4. Saaty scale and associated qualitative descriptions (Alphonce, 1997).

Importance	Definition	Explanation
1	Equal Importance	Two elements contribute identically to the objective.
3	Weak Dominance	Experience or judgment slightly favors one element over another.
5	Strong Dominance	Experience or judgment strongly favors one element over another.
7	Demonstrated Dominance	An element's dominance is demonstrated in practice.
9	Absolute Dominance	The evidence favoring an element over another is affirmed to the highest possible order.
2,4,6,8	Intermediate Values	Further subdivision or compromise is needed.

In completing all possible pairwise comparisons at each level of the decision hierarchy, a series of matrices are being populated. For example, the numerical score associated with the comparison of element i to element j would be placed in the position a_{ij} as shown in a pairwise comparison matrix A as shown in Figure 2-12 (Alphonce, 1997).

$$A = \begin{bmatrix} a_{11} & a_{12} & \cdot & \cdot & \cdot a_{1n} \\ a_{21} & a_{22} & \cdot & \cdot & \cdot a_{2n} \\ \cdot & & & & \cdot \\ \cdot & & & & \cdot \\ \cdot & & & & \cdot \\ a_{n1} & a_{n2} & \cdot & \cdot & \cdot a_{nn} \end{bmatrix}$$

Figure 2-12. Pairwise comparison matrix 'A' containing the scores associated with all possible pairwise comparisons at a given level of an AHP hierarchy.

There are an infinite number of ways to compute the relative priorities, or ranks, of criteria, sub-criteria, and alternatives from the theoretical matrix shown above. However, the

emphasis on consistency when making comparisons suggests an eigenvalue formulation. There are five general steps in determining the eigenvalue of a given pairwise comparison matrix (Saaty, 1987):

1. Determine the n^{th} root of product values. This is performed by multiplying all values in a given row of the comparison matrix and raising that product to the $1/n$ power, where n is the number of rows or columns in the $n \times n$ comparison matrix. This is repeated for all rows in the matrix such that each of the n elements has its own product value.
2. Determine the eigenvector (w) for each of the n elements in the comparison matrix. This is performed by dividing each of the values determined in step 1 by the sum of the values from step 1. *It should be noted that the eigenvectors of each of the n elements determined in this step serve as the relative priorities used in the final rankings and should always sum to one.*
3. Multiply each of the rows in the $n \times n$ comparison matrix by the $1 \times n$ w matrix determined in step 2.
4. Divide the values from step 3 by the w for that element determined in step 2.
5. The average of the values determined in step 4 is the eigenvalue (λ) for the $n \times n$ comparison matrix.

The consistency of a given comparison matrix is checked using the eigenvalues. First, the consistency index (CI) of an $n \times n$ comparison matrix must be determined according to (Saaty, 1987):

$$CI = \frac{\lambda - n}{n - 1} \tag{21}$$

The consistency ratio (CR) of the $n \times n$ comparison matrix can then be determined using (Saaty, 1987):

$$CR = \frac{CI}{RI} \tag{22}$$

where RI is the random index and varies according the number n of elements in the comparison matrix according to Table 2-5 (Saaty, 1987).

Table 2-5. Random index (RI) associated with an $n \times n$ square matrix.

n	2	3	4	5	6	7	8	9	10
RI	0	0.58	0.90	1.12	1.24	1.32	1.41	1.45	1.51

A comparison matrix is said to be random and therefore results should be ignored if the CR is greater than 10% (Saaty 1987). Final rankings of alternatives are determined by multiplying the eigenvectors of the criteria by the eigenvectors of each of the alternatives with respect to each of the criteria. These weighted products will sum to one, with the alternative with the largest weighted product representing the most preferred alternative.

2.4.3 AHP Applied to the LARV

In an effort to gage the socio-economic perceptions of stakeholders in the LARV regarding the land and water BMPs being considered for the region, an AHP survey was developed. The first step in this process was to conduct qualitative interviews with stakeholders, asking questions that would provide more insight into stakeholder sentiments about the major issues facing the LARV, what is responsible for those issues, and possible solutions. This qualitative survey was conducted in a one-on-one or two-on-one [researcher(s) to stakeholder] setting on May 29, 2014 in Rocky Ford, Colorado. Interviews were held with five farmers and one a water conservancy district employee. Those interviewed varied greatly in years of experience in farming, crops grown, acres farmed, irrigation practices used, water management, geographic location, and ditch company memberships. Although the results of these surveys were not quantified, common sentiment between those interviewed and new ideas were incorporated into the final AHP survey.

In the months that followed the qualitative interview, the final AHP survey was developed and approved by Colorado State University’s Institutional Review Board. The structure of the final survey is illustrated in Table 2-6.

Table 2-6. The AHP survey structure administered in the LARV USR.

Main Criteria	Sub-Criteria	Alternatives (BMPs)
Cost of BMP Implementation	Upfront	Reduced fertilization (RF)
	On-going	Reduced irrigation (RI)
	Service	Canal sealing (CS)
Ease of BMP Implementation	Willingness	Land-fallowing (LF)
	Incentives	Enhanced riparian buffer (ERB)
	Avoiding legal hurdles	
	Cooperation	
Economic Benefits from BMP Implementation	Water efficiency	
	Crop yield	
	Avoiding legal or regulatory restrictions	
Off-farm Environmental Benefits from BMP Implementation	Nitrogen reduction	
	Selenium reduction	
	Salinity reduction	

In an effort to reduce the number of pairwise comparisons that had to be made, the sub-criteria were excluded from the typical hierarchical structure of the AHP. Instead, survey participants were asked simply to provide a strict ranking of sub-criteria (i.e. directly ranking 1-3 or 1-4, with 1 being the most preferred) with respect to the main criteria to which they pertained. By doing this, more data could be collected with respect to each of the main criteria without greatly increasing the cognitive burden and the time required to complete the survey. Survey participants then were asked to rank the main criteria via a series of pairwise comparisons using a modified Saaty scale shown in Table 2-7.

Table 2-7. Modified Saaty scale used for the AHP BMP survey in the LARV USR.

Importance	Definition
1	Equally
2	Somewhat More
3	Much More
4	Very Much More
5	Absolutely More

A modified Saaty scale was adopted for this study in an effort to simplify responses and likely decrease the time required to complete the survey, thereby increasing the chances that surveys would be completed entirely and carefully. This scale was also used to compare the alternative BMPs, whereby survey participants scored each of the pairwise comparisons with respect to each of the main criteria.

The first set of surveys was issued on October 31, 2014, at Colorado State University's Arkansas Valley Research Center (AVRC) in Rocky Ford, Colorado. These initial surveys were conducted on a one-on-one basis, where the content and structure of the surveys was thoroughly explained to participants prior to its completion. This format also allowed for any questions that participants had to be clarified and noted so that the survey could be revised as needed. Eight stakeholders were surveyed anonymously at this meeting. The initial feedback from the participants suggested that only minor text adjustments to the survey were required.

A second set of surveys was issued at the Annual AVRC Advisory Council meeting held on December 16, 2014 in Rocky Ford, CO. These surveys were issued in a large group setting, where they were placed on each table and meeting participants around the table were asked to complete them. Although the content and structure of the surveys were explained before the surveys were distributed, the large number of participants did not allow for questions regarding the structure or content of the survey to be readily addressed. However, it was assumed that given the two preliminary meetings in May and October 2014, any major issues or causes for confusion had been addressed in the survey prior to the December 2014 issuing. Twelve stakeholders from the region were surveyed anonymously at this meeting. Thus, a total of 25 stakeholders from the region were surveyed as part of this overall study.

CHAPTER 3: Results and Discussion

3.1 Se and Related Parameters in Water and Sediment Samples

Water quality data collected from 2006-2010 are summarized in Table 3-1, with a complete listing of data presented in Appendix A Table A-2. Sediment and associated water quality data collected from 2011-2014 are summarized in Table 3-2, with a complete listing of data presented in Appendix A Table A-3.

Table 3-1. Average water quality data collected from locations in the Arkansas River and its tributaries from 2006-2010.

Sample Location	Total Se (µg/L)	Dissolved SeO ₄ ** (µg/L)	Dissolved SeO ₃ * (µg/L)	DO (mg/L)	NO ₃ (mg/L)
ARK 164	7.81	6.41	1.40	9.32	1.57
ARK 167	8.21	6.74	1.47	9.21	1.53
Patterson Hollow	13.12	10.77	2.35	10.90	1.21
ARK 141	8.30	6.81	1.48	9.49	1.47
ARK 12	8.07	6.62	1.44	9.57	1.37
Timpas Creek 2	12.79	10.50	2.29	9.18	2.71
ARK 127	9.03	7.41	1.62	9.33	1.59
Crooked Arroyo 2	11.68	9.59	2.09	9.88	2.25
Anderson Creek	12.86	10.56	2.30	10.27	1.00
ARK 95	9.32	7.65	1.67	9.01	2.14
River	8.46	6.95	1.51	9.32	1.61
Tributaries	12.57	10.32	2.25	9.98	1.92

*Dissolved SeO₄ was estimated as being the difference between total dissolved selenium and SeO₃. **Sorbed SeO₄ was estimated as being the difference between total recoverable selenium and SeO₃ from the decanted 0.1 M K₂HPO₄ solution.

Table 3-2. Average sediment and associated water quality selenium data collected from locations in the Arkansas River and its tributaries from 2011-2014.

Sample Location	Selenium in the Water Column			Selenium in Sediment		
	Total Se (µg/L)	Dissolved SeO ₃ (µg/L)	Dissolved SeO ₄ * (µg/L)	Sorbed SeO ₃ (µg/g)	Sorbed SeO ₄ ** (µg/g)	Precipitated and Organic Se*** (µg/g)
ARK Cat.	NS	NS	NS	0.01	0.01	0.13
ARK 164	11.15	1.70	9.45	0.06	0.06	0.52
Patterson Hollow	17.27	1.51	15.76	0.13	0.14	0.90
ARK 141	9.85	1.78	8.07	0.08	0.06	0.67
ARK 12	9.60	1.93	7.67	0.04	0.03	0.30
Timpas Creek 1	15.30	1.61	13.69	0.26	0.14	1.20
Timpas Creek 2	16.57	1.74	14.83	0.23	0.15	1.15
ARK 127	11.11	1.33	9.79	0.05	0.05	0.40
Crooked Arroyo 1	6.71	2.14	5.24	0.15	0.17	1.03
Crooked Arroyo 2	11.51	1.57	10.20	0.41	0.18	1.47
ARK Crkd./And.	6.85	2.48	4.37	0.12	0.06	0.45
Anderson Creek	NS	NS	NS	0.23	0.18	2.10
ARK 95	11.39	1.67	9.72	0.04	0.04	0.30
ARK King	9.34	1.99	7.36	0.10	0.10	0.76
ARK 162	9.78	2.34	7.43	0.06	0.09	0.63
ARK 209	9.76	1.37	8.39	0.04	0.07	0.63
Horse Creek	10.47	2.51	7.96	0.39	0.18	1.21
ARK 201	11.59	1.50	10.44	0.05	0.06	0.37
River	10.45	1.79	8.74	0.06	0.06	0.45
Tributaries	13.05	1.88	11.30	0.28	0.17	1.27

*Dissolved SeO₄ was estimated as being the difference between total dissolved selenium and SeO₃. **Sorbed SeO₄ was estimated as being the difference between total recoverable selenium and SeO₃ from the decanted 0.1 M K₂HPO₄ solution. ***Precipitated and organic selenium was estimated using the difference between the total selenium present in the sediment and the total recoverable selenium from the decanted 0.1 M K₂HPO₄ solution. Data used to generate these values are included as supplemental data.

In general, Se concentrations were higher in the tributaries than in the Arkansas River.

Average dissolved SeO₄ concentrations from 2006-2010 and 2011-2014 were 7.0 µg/L and 8.7 µg/L, respectively, in the Arkansas River and 10.3 µg/L and 11.3 µg/L, respectively, in the tributaries; average dissolved SeO₃ concentrations from 2006-2010 and 2011-2014 were 1.5 µg/L and 1.8 µg/L, respectively, in the Arkansas River and 2.3 µg/L and 1.9 µg/L, respectively, in the tributaries; total dissolved Se concentrations from 2006-2010 and 2011-2014 were 8.5 µg/L and 10.5 µg/L, respectively, in the Arkansas River and 12.6 µg/L and 13.1 µg/L,

respectively, in the tributaries. The studies of Miller et al (2010) and Ivahnenko et al (2013) also showed dissolved Se concentrations in tributaries higher than those in the Arkansas River, and like this study, had dissolved Se concentrations generally increase when moving downstream. The 85th percentile dissolved SeO₄ concentrations from 2006-2010 and 2011-2014 were 10.3 µg/L and 12.0 µg/L, respectively, in the Arkansas River and 12.8 µg/L and 18.7 µg/L, respectively, in the tributaries; average dissolved SeO₃ concentrations from 2006-2010 and 2011-2014 were 2.3 µg/L and 2.2 µg/L, respectively, in the Arkansas River and 2.8 µg/L and 2.5 µg/L, respectively, in the tributaries; total dissolved Se concentrations from 2006-2010 and 2011-2014 were 12.6 µg/L and 13.4 µg/L, respectively, in the Arkansas River and 15.6 µg/L and 20.1 µg/L, respectively, in the tributaries. Sample data collected between 2006 and 2014 show significant levels of total dissolved Se well above Colorado's aquatic life chronic standard of 4.6 µg/L (85th percentile), up to approximately five times the chronic standard in the tributaries.

Using the concentration values from 2006-2010 and from 2011-2014, dissolved SeO₄ and SeO₃ accounted for 83% and 17%, respectively, of the total dissolved Se mass in the Arkansas River and 84% and 16%, respectively, of the total dissolved Se mass in the tributaries. Van Derveer and Canton (1997) reported SeO₄ and SeO₃ as accounting for approximately 80% and 16%, respectively, of total dissolved Se in the Arkansas River and 85% and 13%, respectively, of total dissolved Se in the tributaries. Other dissolved Se mass in the Van Derveer and Canton (1997) study was organic Se, which was reported as approximately 3% of total dissolved Se mass in the water column.

The results of bed sediment sample analysis from 2011-2014 (Table 3-2) show that Se concentration in tributary sediment was generally higher than in Arkansas River sediment. Average sorbed SeO₄, sorbed SeO₃, and reduced and organic Se concentrations were 0.1 µg/g,

0.1 µg/g, and 0.5 µg/g, respectively, in Arkansas River sediment and 0.2 µg/g, 0.3 µg/g, and 1.3 µg/g, respectively, in tributary sediment. Examining these concentrations on a percentage basis, sorbed SeO₄, sorbed SeO₃, and reduced and organic Se comprised 10%, 10%, and 80%, respectively, of the total Se mass in Arkansas River bed sediment and 10%, 16%, and 74%, respectively, in tributary bed sediment. The study of Van Derveer and Canton (1997) reported similar Se speciation in sediment, with sorbed SeO₄, sorbed SeO₃, and reduced and organic Se comprising 5%, 5%, and 90%, respectively, in Arkansas River bed sediment and 2%, 3%, and 95%, respectively, in tributary bed sediment (the speciation of unaccounted-for Se mass was not reported). Van Derveer and Canton (1997) reported Se⁰ accounting for approximately 43% of the total reduced and organic Se mass in River sediment and approximately 62% of the total reduced and organic Se mass in tributary sediment.

In addition to Se samples, other water quality parameters also were analyzed in samples taken for between 2006 and 2014, including NO₃, DO, pH, electrical conductivity (EC), oxidation/reduction potential (ORP), and suspended algae. Figure 3-1 shows the maximum, minimum, median, and 1st and 3rd quartiles for Se and other water quality parameters.

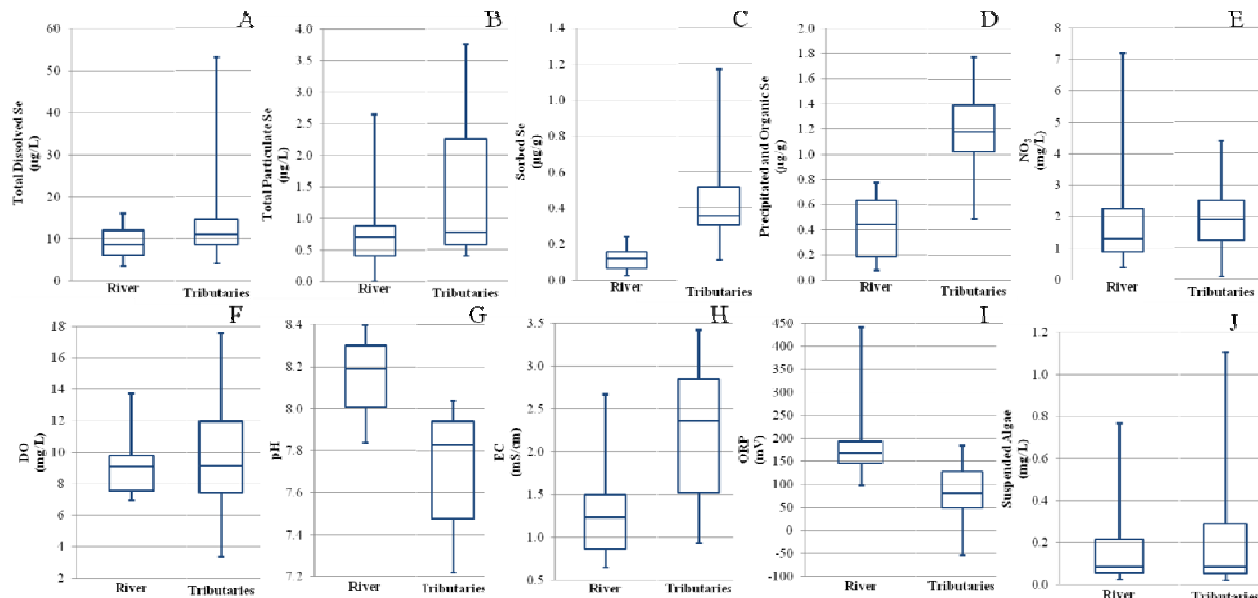


Figure 3-1. Maximum, minimum, median, and 1st and 3rd quartiles of (A) total dissolved Se samples collected from 2006-2014 in the Arkansas River (95 samples) and tributaries (57 samples), (B) total particulate Se samples collected from 2007-2014 in the Arkansas River (17 samples) and tributaries (3 samples), (C) sorbed Se samples collected from 2011-2014 in the Arkansas River (28 samples) and tributaries (18 samples), (D) precipitated and organic Se samples collected from 2011-2014 in the Arkansas River (25 samples) and tributaries (17 samples), (E) NO_3 samples collected from 2006-2014 in the Arkansas River (71 samples) and tributaries (39 samples), (F) DO samples collected from 2006-2014 in the Arkansas River (72 samples) and tributaries (40 samples), (G) pH samples collected from 2013-2014 in the Arkansas River (24 samples) and tributaries (16 samples), (H) EC samples collected from 2013-2014 in the Arkansas River (20 samples) and tributaries (15 samples), (I) ORP samples collected from 2013-2014 in the Arkansas River (20 samples) and tributaries (15 samples), and (J) suspended algae samples collected from 2013-2014 in the Arkansas River (84 samples) and tributaries (104 samples).

Figures 3-1A through 3-1D show that Se concentrations were much higher in the tributaries than the Arkansas River, with median, quartile, and maximum and minimum concentrations in the tributaries exceeding those of the Arkansas River. Additionally, the tributaries displayed a broader range of Se concentration in comparison to the Arkansas River. Although NO_3 concentrations were generally higher in the tributaries than in the Arkansas River, Figure 3-1E shows that the Arkansas River contains a higher maximum sampled NO_3 concentration than the tributaries. Figure 3-1 F shows that DO was generally higher and spanned a wider range in the tributaries in comparison to the Arkansas River. EC and suspended algae show the same characteristics, with both parameters generally higher and more diverse in the tributaries than the River (Figures 3-1H and 3-1J). The opposite is true when examining pH and

ORP. Although pH data spanned a wider range of values in the tributaries as compared to the Arkansas River, pH was generally lower in the tributaries as compared to the Arkansas River (Figure 3-1G). ORP was both lower and less diverse in the tributaries as compared to the Arkansas River (Figure 3-1I).

Higher concentrations of Se and NO_3 in the tributaries as compared to the Arkansas River are expected since the tributary flows are more dominated by flows from the surrounding aquifer than are flows in the Arkansas River. The average concentrations of SeO_4 measured in groundwater samples from the alluvial aquifer that flows to the tributaries and the Arkansas River in the USR is about 56 $\mu\text{g/L}$ (Gates et al., 2009, Gates et al 2016). Observing higher DO concentrations in the tributaries is also expected, as flow in the tributaries tends to be shallower, more mixed, and generally more exposed to the atmosphere on a per-unit volume basis. The presence of generally elevated levels of suspended algae in the tributaries may be due to the shallower flows in the tributaries that allow for a more complete penetration of sunlight through the water column allowing algae to photosynthesize and reproduce over a greater fraction of the flow depth as compared to the Arkansas River. Relatively elevated levels of NO_3 in the tributaries also contribute to greater algal growth.

Figure 3-1I reveals that ORP was almost always positive and was generally higher in the Arkansas River compared to the tributaries. This indicates a net reducing environment, with higher ORP measurements indicate a greater tendency for Se species of higher oxidation state to be chemically reduced. As such, higher observed dissolved SeO_4 concentrations are supported by the lower observed ORP measurements in the tributaries as compared to the Arkansas River. As shown in Figure 3-1G, Arkansas River water typically is more alkaline than tributary water, with median pH values of approximately 8.2 in the River and 7.8 in the tributaries, although samples

from both the Arkansas River and tributaries show generally alkaline water. This alkaline environment decreases the ability for SeO_4 and SeO_3 to sorb to bed sediment, allowing it to remain dissolved and mobile in the water column (Dzombak and Morel, 1990).

A statistical analysis also was performed on the data summarized in Figure 3-1 to identify correlations between the concentrations of various Se species and other parameters and between the Se species themselves. With no prior knowledge of whether or not the correlation between two variables would be positive or negative, a Pearson correlation coefficient two-tailed test was used. The analysis was performed on 26 pairs, being the number of samples for which all concentrations and parameters were available. With a sample size (N) of 26, the degrees of freedom (df) for this sample size was 24 ($N-2$). With df equal to 24, a correlation with a level of significance (r) of ≥ 0.330 or ≤ -0.330 and an associated p-value of ≤ 0.05 is considered a significant correlation. However, to identify only those correlations with a high level of significance, a p-value of 0.01 and a corresponding r of ± 0.453 were targeted. In this study, 0.453 was rounded to 0.50, thus an r of ≥ 0.50 or ≤ -0.50 was used. This r corresponds to a p-value of approximately 0.01 or smaller. (Zuo et al., 2003).

Table 3-4. Correlation coefficient / level of significance (r) values between Se species and other dissolved ions. Statistically significant correlations (≥ 0.50 or ≤ -0.50 , corresponding to a p-value of approximately 0.01 or smaller) are shown in bold.

		Dissolved Ions					
		Calcium (Ca)	Magnesium (Mg)	Boron (B)	Bicarbonate (HCO_3)	Total Hardness (CaCO_3)	Total Alkalinity (CaCO_3)
Selenium	Total Dissolved Se	0.42	0.56	0.52	0.58	0.48	0.61
	Dissolved SeO_3	-0.30	-0.30	-0.18	-0.30	-0.33	-0.25
	Sorbed SeO_3 (bed)	0.38	0.33	0.40	0.30	0.36	0.28
	Sorbed SeO_3 (banks)	0.11	-0.06	-0.03	-0.02	0.02	-0.05
	Sorbed SeO_4 (bed)	0.52	0.45	0.42	0.45	0.50	0.43
	Sorbed SeO_4 (banks)	0.43	0.33	0.23	0.46	0.38	0.43
	Precipitated and Organic Se (bed)	0.57	0.46	0.47	0.45	0.53	0.42
	Precipitated and Organic Se (banks)	0.34	0.26	0.31	0.32	0.31	0.31

Table 3-5. Correlation coefficient / level of significance (r) values between Se species and dissolved nutrients. Statistically significant correlations (≥ 0.50 or ≤ -0.50 , corresponding to a p-value of approximately 0.01 or smaller) are shown in bold.

		Dissolved Nutrients	
		Ammonium (NH ₄ -N)	Nitrate (NO ₃ -N)
Selenium	Total Dissolved Se	-0.06	0.71
	Dissolved SeO ₃	0.15	0.20
	Sorbed SeO ₃ (bed)	0.55	0.19
	Sorbed SeO ₃ (banks)	0.05	-0.22
	Sorbed SeO ₄ (bed)	0.46	0.41
	Sorbed SeO ₄ (banks)	0.03	0.26
	Precipitated and Organic Se (bed)	0.46	0.41
	Precipitated and Organic Se (banks)	0.33	0.17

Table 3-6. Correlation coefficient / level of significance (r) values between Se species and other water properties. Statistically significant correlations (≥ 0.50 or ≤ -0.50 , corresponding to a p-value of approximately 0.01 or smaller) are shown in bold.

		Other Properties		
		ORP	Temperature	pH
Selenium	Total Dissolved Se	-0.27	-0.42	-0.02
	Dissolved SeO ₃	0.26	0.71	0.17
	Sorbed SeO ₃ (bed)	-0.52	0.10	-0.54
	Sorbed SeO ₃ (banks)	-0.20	0.13	-0.24
	Sorbed SeO ₄ (bed)	-0.63	-0.09	-0.65
	Sorbed SeO ₄ (banks)	-0.47	-0.12	-0.23
	Precipitated and Organic Se (bed)	-0.64	0.00	-0.60
	Precipitated and Organic Se (banks)	-0.33	-0.04	-0.36

Table 3-7. Correlation coefficient / level of significance (r) values between Se species. Statistically significant correlations (≥ 0.50 or ≤ -0.50) are shown in bold.

		Selenium			
		Sorbed SeO ₃ (bed)	Sorbed SeO ₄ (bed)	Sorbed SeO ₄ (banks)	Precipitated and Organic Se (bed)
Selenium	Sorbed SeO ₃ (banks)	0.35			
	Sorbed SeO ₄ (bed)	0.83	-		
	Sorbed SeO ₄ (banks)	0.15	0.34	-	
	Precipitated and Organic Se (bed)	0.90	0.90	0.40	-
	Precipitated and Organic Se (banks)	0.66	0.51	0.50	0.59

As shown in Table 3-5, there is a correlation of 0.71 between total dissolved Se and NO₃, highlighting the tendency of NO₃ to both promote the dissolution of Se and inhibit its chemical

reduction to particulate forms (Bailey et al., 2015). The negative (inverse) correlations of sorbed SeO_3 and SeO_4 in bed sediment with pH shown in Table 3-6 support the affect of pH on sorption reported by Dzombak and Morel (1990), indicating that as the water becomes more alkaline, the ability of Se species to sorb to bed sediment is reduced. The correlation of -0.64 between precipitated and organic Se in bed sediment and ORP is somewhat unexpected, since an increase in ORP indicates a more reducing environment where Se species are more likely to be reduced to organic and particulate forms. However, though not statistically significant, the negative correlation between ORP and total dissolved Se (Table 3-6) is expected. Statistically significant correlations also were detected between sorbed SeO_4 and sorbed SeO_3 in bed sediment (0.83), precipitated and organic Se and sorbed SeO_3 in bed sediment (0.90), precipitated and organic Se in bank sediment and sorbed SeO_3 in bed sediment (0.66), precipitated and organic Se and sorbed SeO_4 in bed sediment (0.90), precipitated and organic Se in bank sediment and sorbed SeO_4 in bed sediment (0.51), precipitated and organic Se and sorbed SeO_4 in bank sediment (0.50), and precipitated and organic Se in bank and bed sediment (0.59). The positive correlation between various Se species and the ions shown in Table 3-5 can likely be attributed to the source of Se and various ions in the region, being the alluvium (Van Raij et al., 1986). This positive correlation indicates that both Se and ions from the alluvium are proportionally mobilized by groundwater in the region.

3.2 Model Predictions of Se in the Stream Network

3.2.1 OTIS-QUAL2E-Se Sensitivity Analysis

3.2.1.1 Initial Parameter Stress

Figure 3-2 displays concentrations of dissolved SeO_4 , dissolved SeO_3 , total sorbed SeO_4 and SeO_3 , Se^0 , NO_3 , and DO for August 11, 2006 along the stream network as predicted for baseline conditions using the steady-flow model. Although this specific date was arbitrarily selected, it falls within a period where the impacts from agricultural activities including irrigation and fertilization in surface water are pronounced.

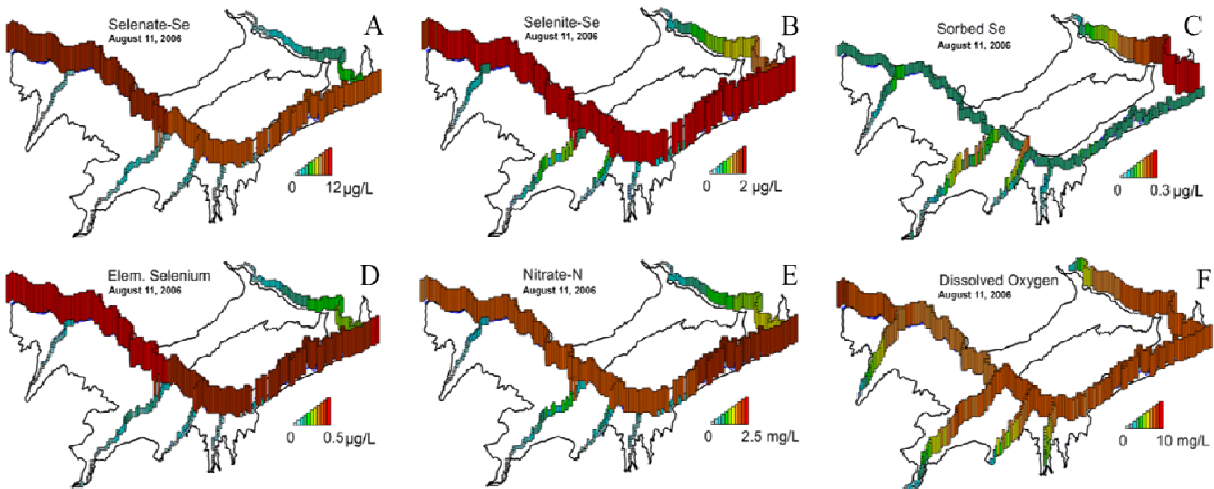


Figure 3-2. Plots of solute and sorbed/reduced Se predicted by the steady-flow model for August 11, 2006 for (A) dissolved SeO_4 , (B) dissolved SeO_3 , (C) total sorbed SeO_4 and SeO_3 , (D) Se^0 , (E) NO_3 , and (F) DO.

For the solute transport time step shown, all predicted values of dissolved SeO_4 were below 12 $\mu\text{g/L}$, all values of dissolved SeO_3 were below 2 $\mu\text{g/L}$, all values of sorbed SeO_4 and SeO_3 were below 0.3 $\mu\text{g/g}$, all values for Se^0 were below 0.5 $\mu\text{g/g}$, all values for NO_3 were below 2.5 mg/L , and all values for DO were below 10 mg/L . Figure 3-3 shows simulated concentrations from the steady-flow model over the 2-year simulation period for dissolved SeO_4 , dissolved SeO_3 , NO_3 , and DO for one location in the River (ARK12) and one tributary location (Timpas

Creek 2). The seasonal fluctuations in solute concentration driven by temperature-dependent and solar radiation-dependent chemical processes can be seen.

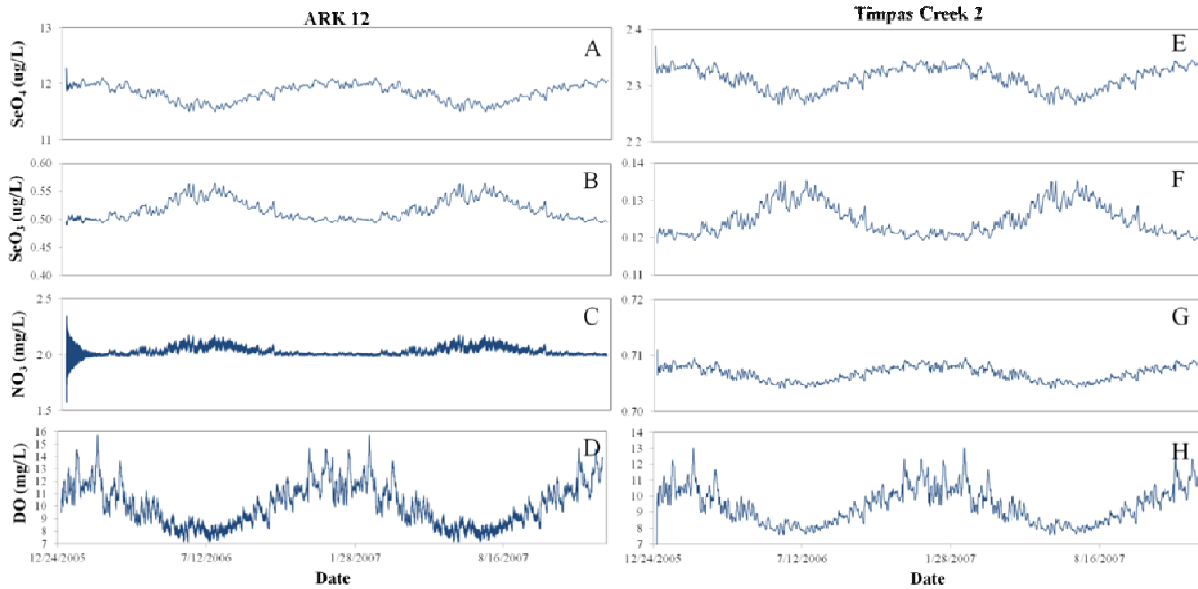


Figure 3-3. Concentrations of dissolved SeO_4 , dissolved SeO_3 , NO_3 , and DO at a location along the Arkansas River (ARK12) (A-D) and at a location along Timpas Creek (Timpas Creek 2) (E-H) predicted by the steady-flow model through the 2-year simulation period.

Of the 54 parameters targeted as part of the SA using the steady-flow model, 17 parameters caused a normalized response in dissolved SeO_4 , dissolved SeO_3 , sorbed SeO_4 , sorbed SeO_3 , Se^0 , Se^{2-} , NO_3 , and/or DO predictions that was either ≥ 0.10 or ≤ -0.05 from the baseline model output. These parameters are listed in Table 3-8.

Table 3-8. Sensitive model parameters identified in the SA.

Model Parameter*	Symbol	Units	Baseline Value
Upstream Conc. of SeO_4	$C_{U_{\text{SeO}_4}}$	$\mu\text{g/L}$	12
Upstream Conc. of SeO_3	$C_{U_{\text{SeO}_3}}$	$\mu\text{g/L}$	0.5
SeO_4 Conc. of Lateral Flow	$C_{L_{\text{SeO}_4}}$	$\mu\text{g/L}$	10
SeO_3 Conc. of Lateral Flow	$C_{L_{\text{SeO}_3}}$	$\mu\text{g/L}$	0.5
SeO_4 partition coefficient in sediment	Kd_{SeO_4}	L/g	0.00007
SeO_3 partition coefficient in sediment	Kd_{SeO_3}	L/g	0.00007
Rate constant for the chemical reduction of SeO_4 to SeO_3	λ_{SeO_4}	day⁻¹	0.2

Rate constant for the volatilization of SeO_4 to species such as dimethylselenide	$\lambda_{\text{SeO}_4}^{\text{vol}}$	day ⁻¹	0.05
Rate constant for the chemical reduction of SeO_3 to Se^0	λ_{SeO_3}	day ⁻¹	0.1
Rate constant for the conversion of volatile Se species to Se^{2-}	$\lambda_{\text{Se}_{\text{vol}}}$	day ⁻¹	0.05
Upstream Conc. of Alg.	$C_{U_{\text{Alg}}}$	mg/L	1.5
Maximum specific algal growth rate	$\lambda_{\text{Alg}_{\text{max}}}$	day ⁻¹	2
Local algal respiration rate	$\lambda_{\text{Alg}_{\text{resp}}}$	day ⁻¹	0.5
Local algal settling rate	σ_{Alg}	m/day	1
Upstream Conc. of DO	$C_{U_{\text{DO}}}$	mg/L	9.72
Upstream Conc. of NO_3	$C_{U_{\text{NO}_3}}$	mg/L	2
NO_3 Conc. of Lateral Flow	$C_{L_{\text{NO}_3}}$	mg/L	3

*Parameters in bold were targeted for model calibration. All 54 parameters included in the initial SA are included in supplemental data.

Of the non-Se constituents, the specified upstream-end concentrations of DO ($C_{U_{\text{DO}}}$), NO_3 ($C_{U_{\text{NO}_3}}$), and algae ($C_{U_{\text{Alg}}}$) were found to strongly govern in-stream DO, NO_3 , and algae, respectively, with the maximum specific algal growth rate ($\lambda_{\text{Alg}_{\text{max}}}$) and the groundwater inflow NO_3 concentration ($C_{L_{\text{NO}_3}}$) also having a strong influence (Figure 3-4). In Figure 3-4, the term “parameter stress” refers to incremental changes from baseline values for independent model parameters. For each parameter stress, the response in in-stream concentrations of DO (Figure 3-4 A and D), NO_3 (Figure 3-4 B and E), algae (Figure 3-4 C and F) were determined and normalized by dividing the percent change in the baseline spatio-temporal averaged concentrations by the percent change from the stressed parameter baseline values.

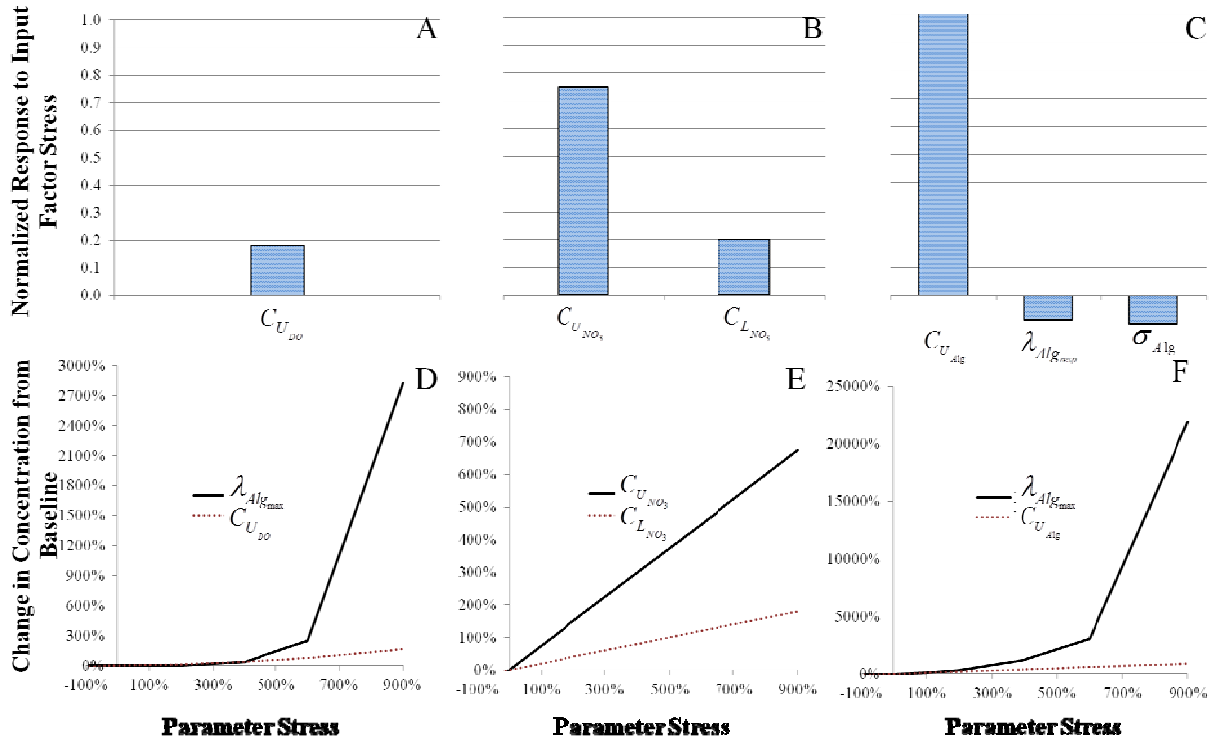


Figure 3-4. Normalized model response to parameter stress for identified influential parameters for in-stream (A) DO, (B) NO₃, and (C) algae concentrations, and the relationship between parameter value and model output for identified influential parameters for in-stream (D) DO, (E) NO₃, and (F) algae concentrations. Parameter $\lambda_{Alg_{max}}$ was not shown in (A) or (C) due to the magnitude of the normalized model response to its stress.

For example, the normalized response of simulated in-stream NO₃ to $C_{U_{NO_3}}$ and $C_{L_{NO_3}}$ is 0.8 and 0.2, respectively. Of these parameters, the change in specified inflow concentrations ($C_{U_{DO}}$, $C_{U_{NO_3}}$, $C_{L_{NO_3}}$, and $C_{U_{alg}}$) were linear or approximately linear over a range of a factor of 0.1 to a factor of 10 times the baseline value (Figure 3-4). With respect to DO and algae concentrations, $\lambda_{Alg_{max}}$ produced a non-linear trend between the parameter value and the change in model results when stressed above 500% of its baseline value and was the most influential parameter with respect to both in-stream DO and algae concentrations. This exponential response of algae concentrations with respect to stresses in $\lambda_{Alg_{max}}$ is reflective of the exponential nature of population growth in general, whereby an increase in growth rate of a population results in an exponential increase in that population through time (Stemberger and Gilbert, 1985). DO

concentrations would of course follow a similar trend due to the release of DO by algae through photosynthesis.

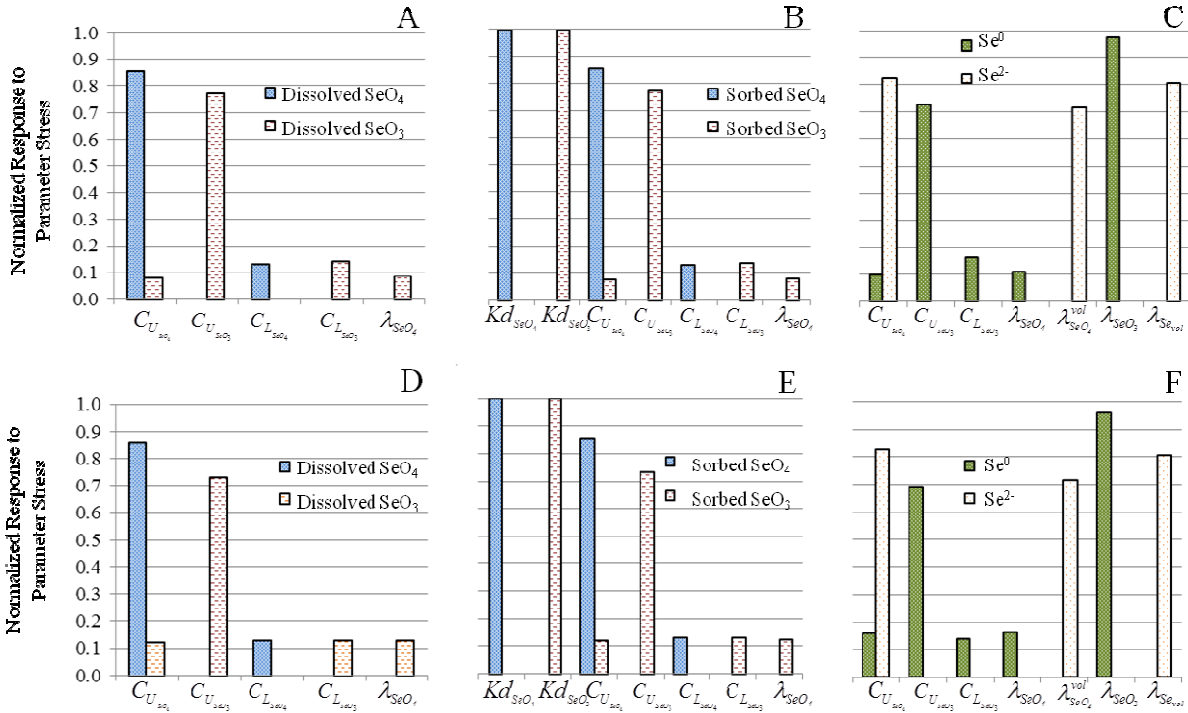


Figure 3-5. Normalized spatio-temporal averaged baseline model response to parameter stresses for in-stream (A) dissolved SeO₄ and SeO₃, (B) sorbed SeO₄ and SeO₃, and (C) Se⁰ and Se²⁻. Corresponding results for the low-NO₃ baseline model simulation are shown in (D), (E), and (F).

Results for Se species are displayed in Figure 3-5 which shows that dissolved SeO₄ was governed by specified upstream concentration of SeO₄ ($C_{U_{SeO_4}}$) and groundwater inflow SeO₄ concentration ($C_{L_{SeO_4}}$) (Figure 3-5A); dissolved SeO₃ was governed by $C_{U_{SeO_4}}$, $C_{U_{SeO_3}}$, $C_{L_{SeO_3}}$, and the rate constant for the net chemical reduction of SeO₄ to SeO₃ (λ_{SeO_4}) (Figure 3-5A); sorbed SeO₄ was governed by $K_{d_{SeO_4}}$, $C_{U_{SeO_4}}$, $C_{L_{SeO_4}}$ (Figure 3-5B); sorbed SeO₃ was governed by $K_{d_{SeO_3}}$, $C_{U_{SeO_4}}$, $C_{U_{SeO_3}}$, $C_{L_{SeO_3}}$, and λ_{SeO_4} (Figure 3-5B); Se⁰ was governed by $C_{U_{SeO_4}}$, $C_{U_{SeO_3}}$, $C_{L_{SeO_3}}$, λ_{SeO_4} , and the rate constant for the net chemical reduction of SeO₃ to Se⁰ (λ_{SeO_3}) (Figure 3-5C); and Se²⁻ was governed by $C_{U_{SeO_4}}$, the rate constant for the volatilization of SeO₄ ($\lambda_{SeO_4}^{vol}$), and the rate

constant for the conversion of volatile Se to Se^{2-} ($\lambda_{\text{Se}^{2-}}$) (Figure 3-5C). Dissolved SeO_4 and SeO_3 both showed the greatest normalized response to their respective upstream inflow concentrations ($C_{U_{\text{SeO}_4}}$ and $C_{U_{\text{SeO}_3}}$) with responses of 0.85 and 0.78, respectively. Sorbed SeO_4 and SeO_3 both showed a normalized response of 1.0 to stresses in their respective water-sediment partition coefficients ($K_{d_{\text{SeO}_4}}$ and $K_{d_{\text{SeO}_3}}$). Se^0 showed a normalized response of 0.98 to the chemical reduction of SeO_3 to Se^0 (λ_{Se^0}).

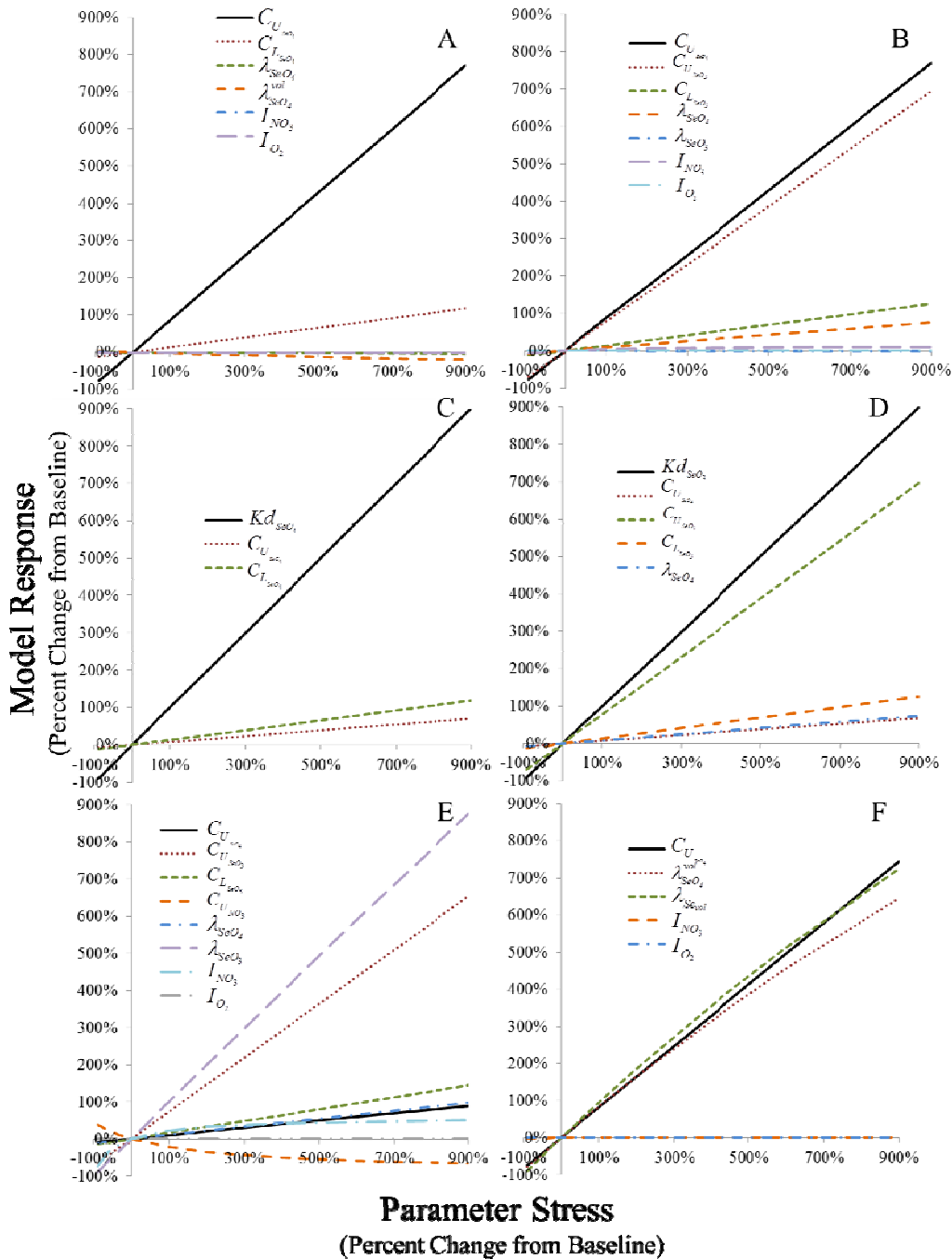


Figure 3-6. Sensitivity trends and ranking of influential parameters for in-stream (A) dissolved SeO_4 , (B) dissolved SeO_3 , (C) sorbed SeO_4 , (D) sorbed SeO_3 , (E) Se^0 , and (F) Se^{2-} . Model responses are calculated using spatio-temporal averaged model output.

As seen in the parameter-model response relationships for Se shown in Figure 3-6, C_{U,SeO_4} is the most influential parameter with respect to both dissolved SeO_4 and SeO_3 (Figure 3-6A and 3-6B). Due to the net chemical reducing conditions present in the system, reduced Se species

were affected by changes in the concentrations of Se species of higher oxidation states, but the opposite was not true. Although λ_{SeO_4} influenced dissolved SeO_3 and not dissolved SeO_4 as determined in the first part of the SA, the sensitivity of the model to this parameter was explored for both dissolved SeO_3 and SeO_4 to ensure that an increasing λ_{SeO_4} resulted in a decrease in dissolved SeO_4 . Results showed that λ_{SeO_4} had a stronger influence and displayed a positive relationship with dissolved SeO_3 , and was less influential and displayed a negative relationship with dissolved SeO_4 , reflecting the expected decrease in concentration of SeO_4 and increase in concentration of SeO_3 when increasing the rate at which SeO_4 is reduced to SeO_3 (Figure 3-6A and 3-6B).

Sorbed SeO_3 and SeO_4 were most sensitive to $K_{d_{SeO_3}}$ and $K_{d_{SeO_4}}$, respectively (Figure 3-6C and 3-6D). Percent changes in both $K_{d_{SeO_3}}$ and $K_{d_{SeO_4}}$ from baseline values showed a linear and approximately 1:1 relationship to percent change in concentration from baseline values. Sorbed SeO_4 was also sensitive to $C_{U_{SeO_4}}$ and $C_{L_{SeO_4}}$, while sorbed SeO_3 was also sensitive to $C_{U_{SeO_4}}$, $C_{U_{SeO_3}}$, $C_{L_{SeO_3}}$, and λ_{SeO_4} . That $K_{d_{SeO_3}}$ and $K_{d_{SeO_4}}$ are the most influential parameters with respect to sorbed Se is expected since water-sediment partition coefficients directly affect Se sediment concentrations while in-stream parameters are indirectly influential. Outside of $K_{d_{SeO_3}}$ and $K_{d_{SeO_4}}$, sorbed SeO_3 and SeO_4 were sensitive to the same parameters as dissolved SeO_3 and SeO_4 (Figure 3-5), highlighting the relationship between in-stream Se concentrations and sediment concentrations of the same Se species.

The concentration of Se^0 was most sensitive to λ_{SeO_3} , with a 1:1 relationship between percent change in concentration from baseline values and percent parameter stress from the

baseline (Figure 3-6E). The value of λ_{SeO_4} also was influential on Se^0 concentration but to a lesser degree than λ_{SeO_3} , likely due to the more direct relationship between SeO_3 and Se^0 as compared to the relatively indirect relationship between SeO_4 and Se^0 (Figure 1-1). As was the case for all Se species examined as part of the SA, Se^0 was affected by stresses to the concentrations of Se species of higher oxidation states. Se^{2-} was sensitive to parameters affecting SeO_4 and volatile Se species ($C_{U_{SeO_4}}$, $\lambda_{SeO_4}^{vol}$, and $\lambda_{Se_{vol}}$) (Figure 3-6F). As is shown in Figure 3-5, Se^{2-} concentrations are dictated by volatile Se species, which in turn are dictated by SeO_4 and SeO_3 concentrations. Se^{2-} is not sensitive to parameters affecting SeO_3 concentrations, likely due to the low inflow SeO_3 concentrations in the system as compared to SeO_4 .

3.2.1.2 Low NO_3 Baseline Simulations

SA results for model simulations with a lowered upstream-end inflow NO_3 concentration are shown in Figure 3-5D through 3-5F. More chemical reduction of Se is predicted to take place in the system, made apparent by the increased SeO_3 concentrations as compared to the original baseline when stressing $C_{U_{SeO_4}}$ and λ_{SeO_4} in the low NO_3 baseline by the same amount as the original baseline. The difference in normalized response of predicted dissolved SeO_3 to stressing $C_{U_{SeO_4}}$ and λ_{SeO_4} between the original baseline and the low nitrate baseline was an increase of 0.04 for both parameters (Figure 3-5A and 3-5D). Stressing $C_{U_{SeO_4}}$ and λ_{SeO_4} in the low NO_3 baseline by the same amount as in the original baseline simulation also resulted in a normalized increase in the concentrations of sorbed SeO_3 , with an increase in normalized model response of 0.04 for both parameters (Figure 3-5B and 3-5E). The effect of NO_3 concentrations on Se^0 can be seen in Figures 3-5C and 3-5F, where decreased NO_3 concentrations correspond to a normalized increase

in Se^0 concentrations by 0.06 and 0.05, respectively, when stressing $C_{U_{\text{SeO}_4}}$ and λ_{SeO_4} . The relationship between NO_3 and various Se species concentrations is dictated by the inhibition term of NO_3 for Se reduction (I_{NO_3} , see Equation 14), as the presence of high concentrations of NO_3 in aquatic environments inhibits the chemical reduction of Se. Although I_{NO_3} was not identified as a governing parameter in the initial SA test, its impacts on Se in the water column were examined in the second part of the SA (Figure 3-5A, 3-5B, 3-5E, and 3-5F) to ensure that changes in I_{NO_3} were having the expected impacts on in-stream Se concentrations. As is shown in Figure 3-6B and 3-6E, I_{NO_3} has the strongest impact on dissolved SeO_3 and Se^0 , products of chemical reduction of SeO_4 and SeO_3 , respectively.

The prediction of dissolved SeO_4 generally was unaffected by a decrease in baseline NO_3 concentrations, likely due to the high inflow concentrations of SeO_4 . Although changes in dissolved SeO_3 between the original baseline and the low- NO_3 baseline are a result of an increase in chemical reduction of dissolved SeO_4 to dissolved SeO_3 (Figure 3-5), these changes are more noticeable for SeO_3 than for SeO_4 since inflow SeO_3 concentrations are much lower than are inflow SeO_4 concentrations.

3.2.2 OTIS-QUAL2E-Se Unsteady Flow Model Calibration

Although specified concentrations of solutes at the upstream end of the river reach often were the parameters to which predicted concentrations were most sensitive, these concentrations were not targeted for model calibration since they were based on observed data. Consequently, of the 17 most influential parameters identified in the SA, only seven were candidates for adjustment during the unsteady-flow model calibration (λ_{SeO_4} , λ_{SeO_3} , $K_{d_{\text{SeO}_4}}$, $K_{d_{\text{SeO}_3}}$, $\lambda_{\text{SeO}_4}^{\text{vol}}$, λ_{Se^0} , and

$\lambda_{Alg_{max}}$). However, after running the baseline OTIS-QUAL2E-Se model, predicted DO performed well compared to observed values, and therefore $\lambda_{Alg_{max}}$ was not modified. Additionally, to further simplify the calibration process, only λ_{SeO_4} was targeted for SeO_4 and SeO_3 calibration since increasing that parameter would have the desired effect of decreasing SeO_4 concentrations and increasing SeO_3 concentrations (Figure 3-6). This eliminated the need to adjust λ_{SeO_3} and $\lambda_{SeO_4}^{vol}$ during calibration for dissolved Se species. The value of $\lambda_{Se_{vol}}$ was not adjusted during the calibration since volatile Se species and Se^{2-} concentrations were not of primary concern. The unsteady flow model was used for model calibration as it provides represents a more realistic representation of natural stream systems.

A statistical analysis was not performed on river flows predicted by the model. However, Figure 3-7 shows that the flows predicted by MODFLOW-SFR and used by the OTIS-QUAL2E-Se model very closely mimic observed flows at both the ARK12 and ARK 95 gages.

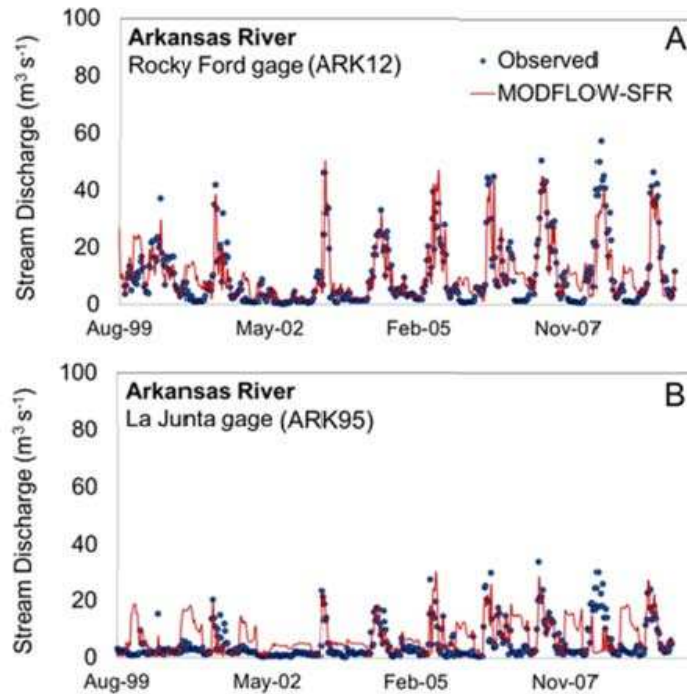


Figure 3-7. Observed and MODFLOW-SFR predicted flow rates in the Arkansas River at locations (A) ARK12 at Rocky Ford and (B) ARK95 at La Junta.

Figure 3-8 shows simulated versus observed in-stream concentrations for dissolved SeO_4 , dissolved SeO_3 , NO_3 , and DO for locations sampled over 2006-2009 in the Arkansas River (ARK 95 and ARK 164) and in the tributaries (Patterson Hollow and Crooked Arroyo 2). Figure 3-8 includes the statistics for these four observation locations and Table 3-9 shows overall statistics for the Arkansas River and tributaries.

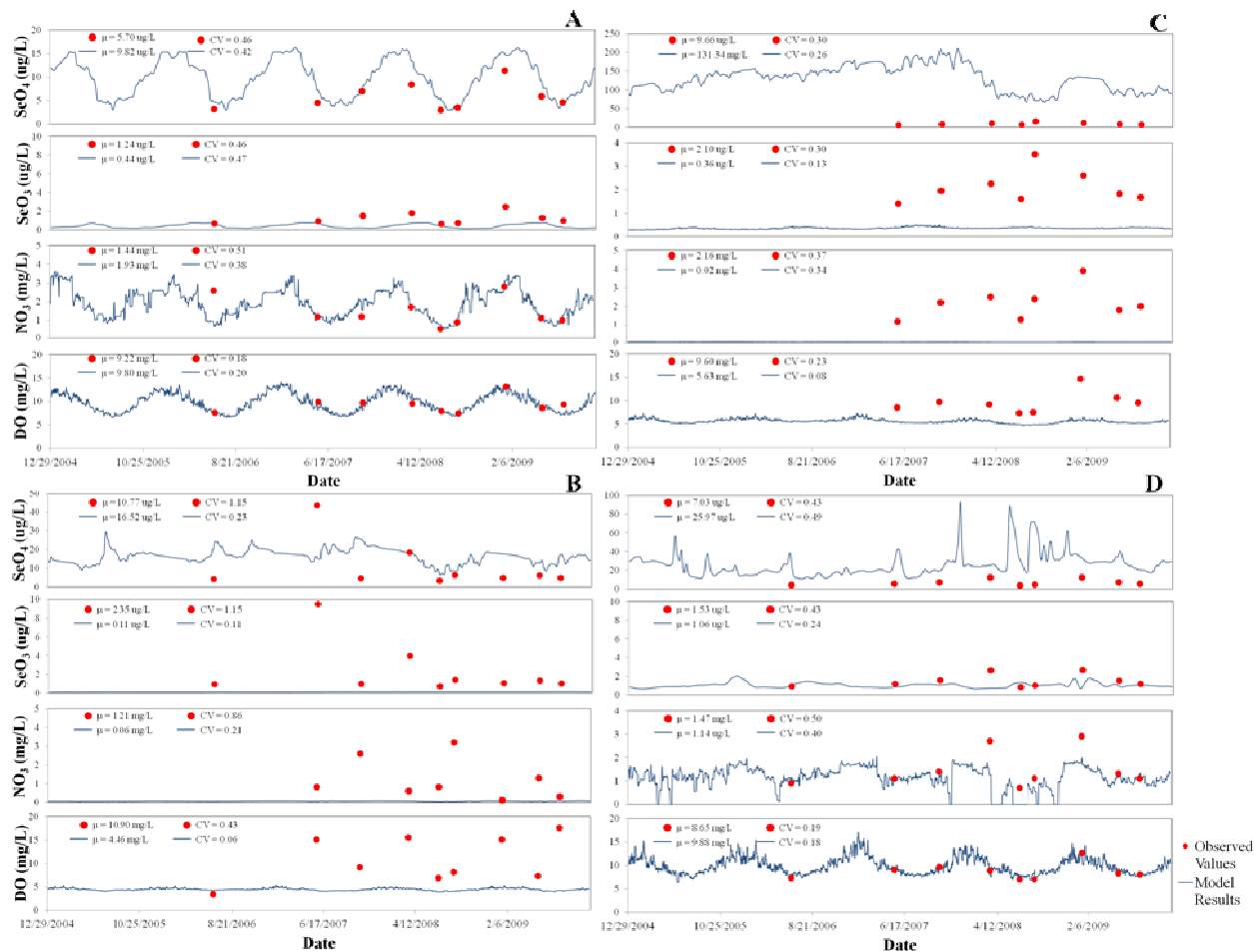


Figure 3-8. Observed and simulated dissolved SeO_4 , dissolved SeO_3 , NO_3 , and DO for (A) ARK 164, (B) Patterson Hollow, (C) Crooked Arroyo 2, and (D) ARK 95.

Table 3-9. Observed and model-predicted mean and coefficient of variation (CV) of constituent concentrations for samples gathered at all Arkansas River and tributary observation locations.

	River				Tributaries			
	μ		CV		μ		CV	
	Observed	Predicted	Observed	Predicted	Observed	Predicted	Observed	Predicted
DO (mg/L)	9.05	10.01	0.19	0.23	10.10	6.63	0.37	0.27
NO_3 (mg/L)	1.39	1.45	0.51	0.45	1.80	0.33	0.61	1.64
SeO_4 (ug/L)	6.34	13.70	0.45	0.63	10.26	46.17	0.89	1.14
SeO_3 (ug/L)	1.38	0.81	0.45	0.38	2.24	0.14	0.89	1.00

Generally, model predictions better matched field observations in the Arkansas River than in the tributaries. In summary, the mean difference between observed and predicted values at river locations was 7.36 $\mu\text{g/L}$ for dissolved SeO_4 , 0.57 $\mu\text{g/L}$ for dissolved SeO_3 , 0.06 mg/L for

NO₃, and 0.96 mg/L for DO, with associated differences in the coefficient of variation between observed and predicted values of 0.18 for dissolved SeO₄, 0.07 for dissolved SeO₃, 0.06 for NO₃, and 0.4 for DO. In comparison, the tributaries showed a mean difference between observed and predicted values of 35.91 µg/L for dissolved SeO₄, 2.10 µg/L for dissolved SeO₃, 1.47 mg/L for NO₃, and 3.47 mg/L for DO, with associated differences in the coefficient of variation between observed and predicted values of 0.25 for dissolved SeO₄, 0.11 for dissolved SeO₃, 1.03 for NO₃, and 0.1 for DO. As shown in Figure 3-8, predicted SeO₄ concentrations generally increased from upstream to downstream in the Arkansas River, likely due primarily to the over-prediction of SeO₄ concentrations in the tributaries draining into the river. The general over prediction of SeO₄ and under prediction of SeO₃ suggests that chemical reduction rate of SeO₄ to SeO₃ was too low in the baseline model. Over prediction of SeO₄ could also be linked to riparian zone chemical reduction rate that was initially set too low. Another potential source of the discrepancy between observed and predicted values, particularly for the under prediction of NO₃ in the tributaries, was the fact that the unsteady OTIS-QUAL2E-Se model did not include a mechanism whereby surface flows could see an increase in constituent concentrations as a result of mobilizing constituents while flowing over a field. Despite these observations, it should also be noted that the model results are being compared to only nine observations, and these discrepancies might be improved if more observational data was available for comparison. These potential sources of discrepancy were explored in detail in later phases of model development and calibration (see Section 3.2.4).

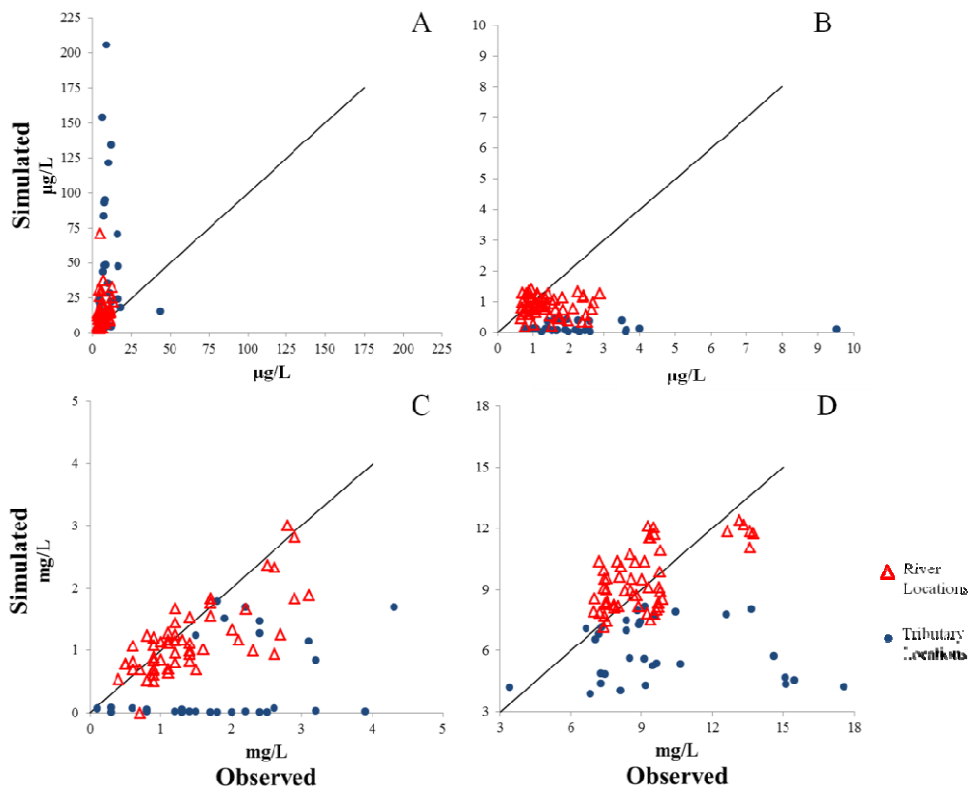


Figure 3-9. Simulated versus observed values for (A) dissolved SeO_4 , (B) dissolved SeO_3 , (C) NO_3 , and (D) DO at locations in the Arkansas River and tributaries.

As seen in Figure 3-9, the model fails to capture the fate and transport behavior of the solutes in the tributaries, even though chemical reaction parameters were modified in an attempt to yield more accurate results. Since a major source of water to the tributaries is groundwater inflow, the inaccurately-predicted solute concentrations suggests the need for a more accurate coupling between the RT3D groundwater inputs and OTIS-QUAL2E-Se surface water inputs. Rather than a loose linkage between the two models, with RT3D simulation results provided to OTIS-QUAL2E-Se, a tighter daily coupling likely is required, with aquifer and groundwater chemical reaction rates modified in RT3D to provide more accurate in-stream tributary concentrations.

For Se speciation in bed sediments, values of $K_{d_{\text{SeO}_3}}$, $K_{d_{\text{SeO}_4}}$, and λ_{SeO_3} were modified. The final values of $K_{d_{\text{SeO}_3}}$ and $K_{d_{\text{SeO}_4}}$ were 40 L/kg and 8.0 L/kg, respectively, in the Arkansas River

and 1200 L/kg and 2 L/kg, respectively, in the tributaries, within the range of 10 - 10000 L/kg and 0.04 - 1000 L/kg, respectively, reported in the literature (Allison and Allison, 2005). A total of 21 data sets collected over 2013 – 2014 in the Arkansas River resulted in calibrated $K_{d_{SeO_3}}$ values over the range of 0.5 – 17.1 L/kg and a $K_{d_{SeO_4}}$ range of 2.2 – 12.4 L/kg, while 16 data sets collected over the same period in the tributaries resulted in a calibrated $K_{d_{SeO_3}}$ range of 4.9 – 70.7 L/kg and a $K_{d_{SeO_4}}$ range of 4.4 – 35.5 L/kg. When analyzing the same dataset for total Se partition coefficients, results indicated a calibrated range of $K_{d_{Se}}$ in the Arkansas River of 14.9 – 142.7 L/kg and 39.4 – 290.4 L/kg in the tributaries. These values are in line with Presser and Luoma (2010) who reported values for $K_{d_{Se}}$ typically ranging between 100 – 300 L/kg for streams and rivers but varying by as much as two orders of magnitude. A value of 1.5 day⁻¹ for λ_{SeO_4} yielded model results for SeO₃ and SeO₄ that most closely matched observed values. The final value of λ_{SeO_3} was 1.0 day⁻¹, within the reported range of approximately 0.08 day⁻¹ to 1.4 day⁻¹ (Chow et al., 2004; Guo et al., 1999).

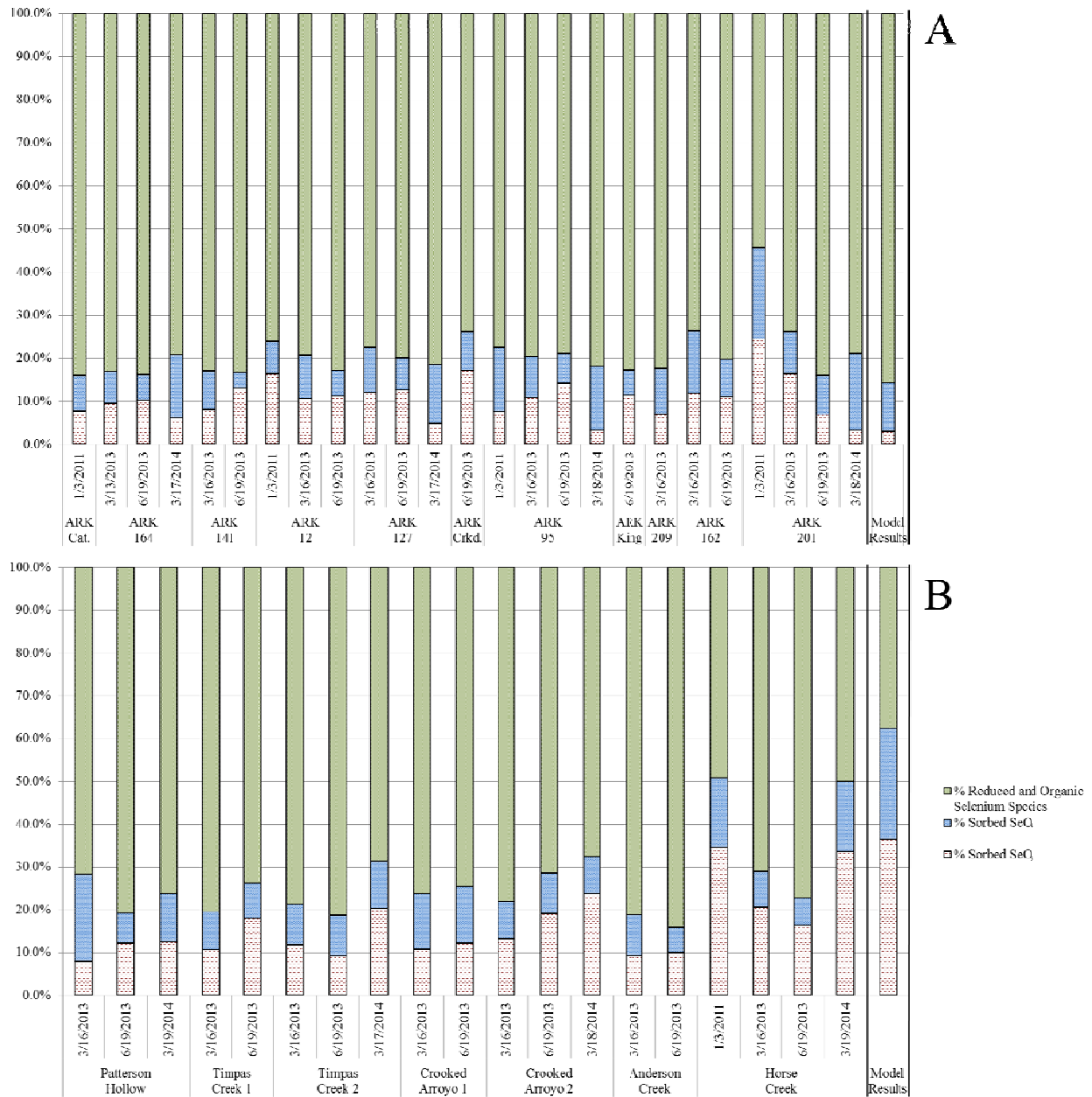


Figure 3-10. Observed and simulated spatio-temporal averaged Se partitioning in sediment for (A) the Arkansas River and (B) its tributaries.

Both field results and final model predictions are presented in Figure 3-10, with field results shown for the date of each sampling event at each sampled stream cross-section. Results are reported as the portion of reduced and organic Se, sorbed SeO₄, and sorbed SeO₃ that makes up the total Se mass in the stream bed sediment. Results from Arkansas River sites are shown in Figure 3-10A, and results from tributary sites are shown in Figure 3-10B. The average portions

predicted by the model are shown in the last column. The OTIS-QUAL2E-Se model predicts average Se concentrations in the Arkansas River sediment of approximately 85% reduced and organic Se, 12% sorbed SeO_4 , and 3% sorbed SeO_3 . These values compare well with the range of observed values in the river. In comparison, as shown in Figure 3-10B, predicted Se concentrations in tributary sediment are approximately 38% reduced and organic Se, 25% sorbed SeO_4 , and 37% sorbed SeO_3 . Although sorbed SeO_4 is within the range of observed values, OTIS-QUAL2E-Se generally is under-predicting reduced and organic Se partitioning and over-predicting sorbed SeO_3 partitioning. The likely source of this discrepancy is the SeO_3 water-sediment partition coefficient which, when calibrated, would shift the Se partitioning in sediment away from reduced and organic Se and toward sorbed SeO_3 .

3.2.3 OTIS-QUAL2E-Se General Observations

It was found that the most influential in-stream parameters governing Se fate and transport were the reaction rates that determine the net chemical reduction of Se species of various valence states. Although Se speciation in sediment was also sensitive to in-stream reduction rate parameters, the most influential parameters governing total Se mass in sediment were those most impactful to sorbed SeO_4 and sorbed SeO_3 , being the SeO_4 and SeO_3 water-sediment partition coefficients. Additionally, although NO_3 concentrations were not sensitive as defined by Equations (15) or (16), changes in NO_3 concentrations had the anticipated outcomes when examining model parameters under a low- NO_3 simulation.

3.2.4 RT3D-OTIS Testing and Calibration

As discussed in Section 2.3.2.1, the general approach to calibrate the RT3D-OTIS model was to first calibrate the model with respect to DO and NO_3 concentrations due to their impact on

Se speciation. Additionally, due to specific environmental concerns associated with SeO_4 concentration, SeO_4 was the primary form of Se that drove calibration efforts. Although SeO_4 , NO_3 , and DO concentrations were primary targets for calibration, and calibration occurred in a specific order, to simplify the presentation of results the calibrations of each chemical species are presented as parallel efforts. Due to the impact of later inflow concentrations on surface-water concentrations, as was made apparent during the SA, parameters impacting lateral groundwater concentrations were targeted first during calibration. These parameters included the heterotrophic reduction rate of SeO_4 and NO_3 in the riparian zones along the Arkansas River and tributaries. Unable to sufficiently increase NO_3 concentrations through the adjustment of these parameters, tailwater multiplication factors were added to the model. No further calibration of the OTIS-QUAL2E-Se parameters (described in Section 3.2.2) occurred. See Section 2.3.2.1 for additional details regarding the calibration approach of the RT3D-OTIS model.

As was the case with the OTIS-QUAL2E-Se model, concentrations of DO simulated by the RT3D-OTIS model using default parameter values very closely matched observed values. This was true throughout the various steps of the calibration process described later. As such, beyond checking that further calibration efforts did not impact DO concentrations unexpectedly, DO concentrations were not a focus of the RT3D-OTIS calibration effort.

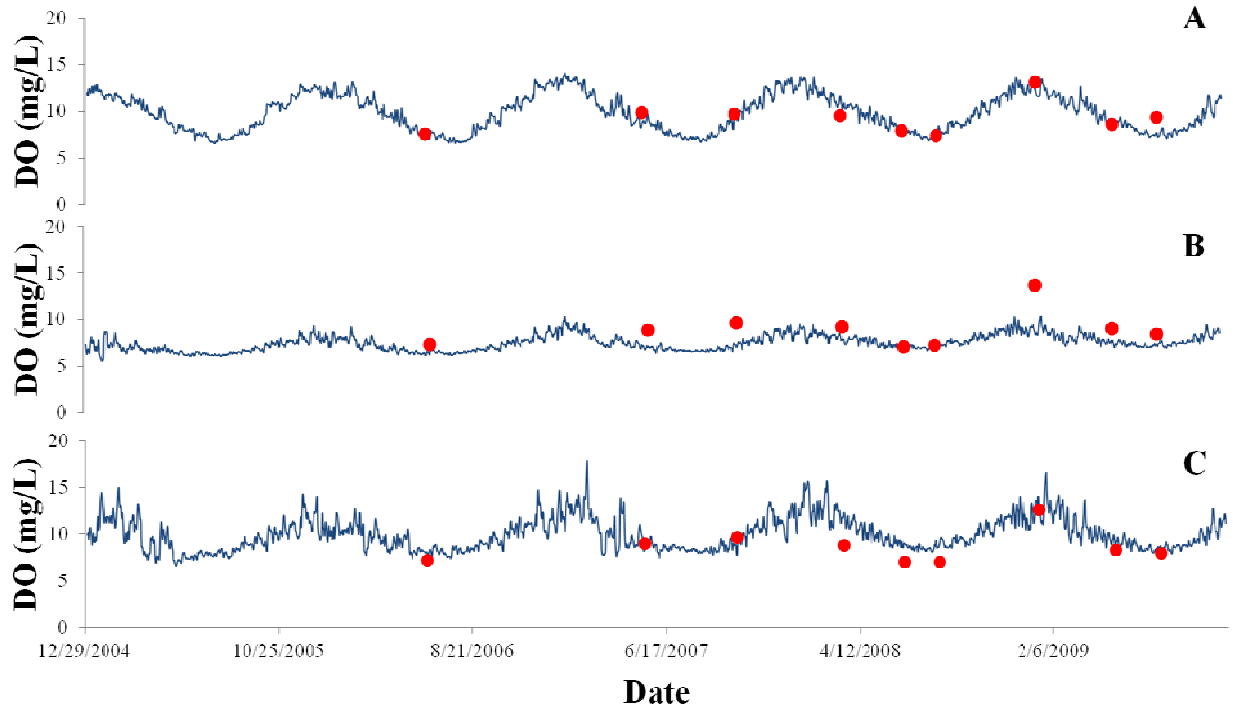


Figure 3-11. RT3D-OTIS simulated and observed DO concentrations using default RT3D-OTIS parameters at observation locations (A) ARK164, (B) Timpas2, and (C) ARK95.

It was expected that the coupled RT3D-OTIS model would simulate in-stream concentrations of SeO_4 and NO_3 more accurately due to its more realistic representation of the highly interconnected aquifer-surface water system that exists in the LARV. However, initial simulations using default parameter values resulted in a general over prediction of in-stream Se concentrations and an under prediction of in-stream NO_3 concentrations.

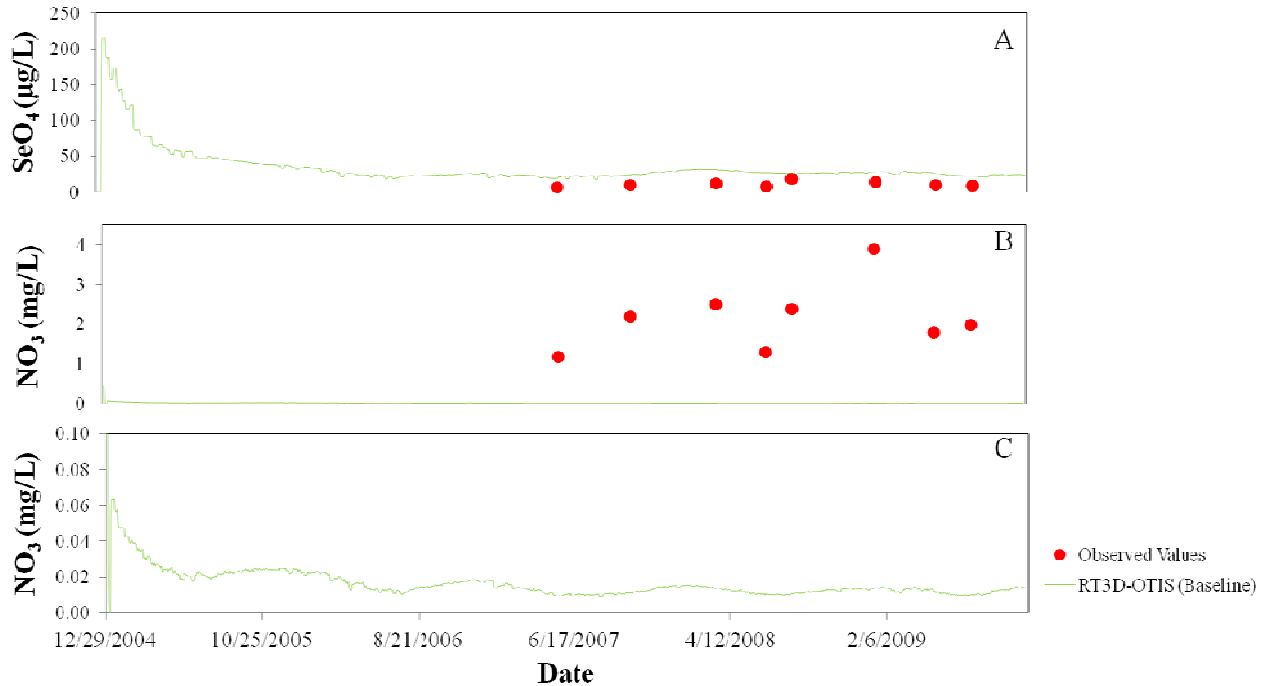


Figure 3-12. Baseline RT3D-OTIS simulated and observed values at observation location Crooked 2 for (A) SeO_4 and (B) and (C) NO_3 .

As shown in Figure 3-12A, initial predicted concentrations of SeO_4 reach approximately 220 $\mu\text{g/L}$ at the sampling location Crooked Arroyo 2, well above values ever observed at that location. Although these extremely high concentrations are lowered and converge on an average concentration of approximately 40 $\mu\text{g/L}$ after about two years into the simulation, the simulated concentrations are still well above observed concentrations of SeO_4 at this location. Figure 3-12B illustrates a similar disconnect between simulated and observed concentrations, in this case for NO_3 . Where observed values at observation location Crooked Arroyo 2 range between approximately 1-3 mg/L , simulated concentrations were two orders of magnitude lower than observed values.

The first step in the RT3D-OTIS calibration process was to incorporate into the RT3D-OTIS model the parameter values that were obtained from the OTIS-QUAL2E-Se calibration effort. Tailwater multiplication factors were also added to the model at this point. With a combination of default parameter values and those obtained from the OTIS-QUAL2E-Se

calibration, it was expected that an improvement would be seen when comparing simulated in-stream concentrations to observed concentrations.

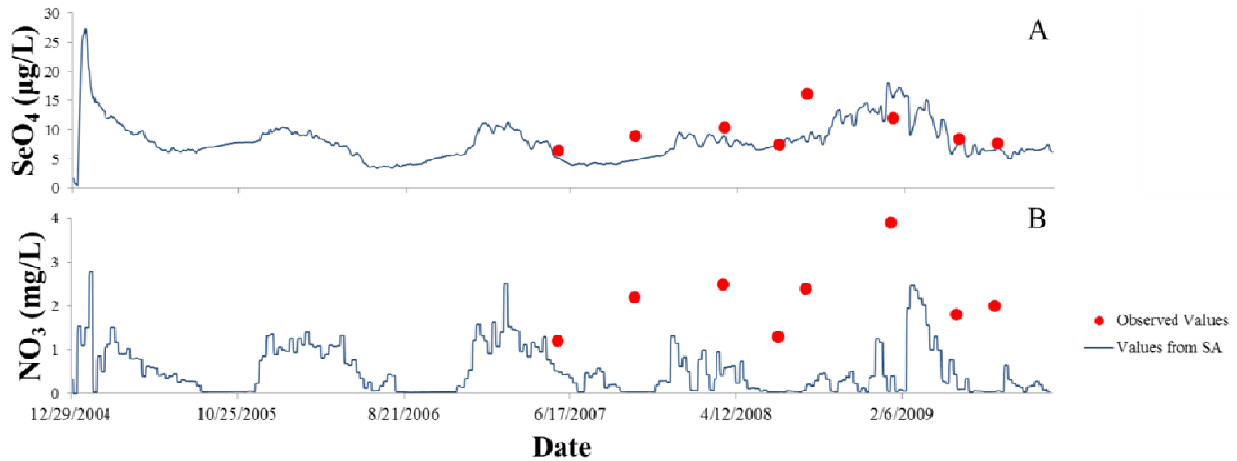


Figure 3-13. RT3D-OTIS simulated and observed concentrations using parameter values from the OTIS-QUAL2E-Se model at observation location Crooked Arroyo 2 for (A) SeO_4 and (B) NO_3 .

As is made apparent when comparing Figures 3-12A and 3-12B with Figures 3-13A and 3-13B, the RT3D-OTIS model (including tailwater multiplication factors) performed much better using parameter values obtained from the OTIS-QUAL2E-Se model and calibration as compared to using only default parameter values. However, although an improvement at observation location Crooked Arroyo 2 was apparent, the model was still generally over predicting SeO_4 concentrations and under-predicting NO_3 concentrations on a system level. With the OTIS-QUAL2E-Se model parameters having already been perturbed and sufficiently calibrated as discussed in Section 3.2.2, further calibration efforts were directed toward model parameters governing the RT3D groundwater component of the coupled RT3D-OTIS model, with lateral groundwater and surface water inflow concentrations being targeted. Due the potential of riparian zones to chemically reduce high valence forms of SeO_4 and NO_3 as discussed in Section 2.3.2.1, $\lambda_{\text{SeO}_4_{RH}}$ and $\lambda_{\text{NO}_3_{RH}}$ were adjusted in an effort to decrease in-stream SeO_4 concentrations and to increase in-stream NO_3 concentrations. Simulated in-stream SeO_4 concentrations were

driven down by increasing λ_{SeO_4RH} , since such a change increases the modeled rate at which SeO_4 is converted to SeO_3 in groundwater as it moves through the riparian zone before entering surface water as lateral groundwater flow. As expected, the opposite effect was obtained by decreasing λ_{NO_3RH} .

Perturbations of λ_{NO_3RH} values had little noticeable effect on in-stream NO_3 concentrations, likely for reasons discussed in later sections. However, with numerous previous studies reporting the reducing effects of riparian zones on NO_3 , λ_{NO_3RH} was increased from its default value of 0.02 day^{-1} to 0.04 day^{-1} for riparian zone cells. Despite the minimal effect of λ_{NO_3RH} on NO_3 concentrations, increasing λ_{SeO_4RH} had a marked impact on in-stream SeO_4 concentrations likely due to the elevated concentrations of SeO_4 entering the stream from lateral groundwater flow. This impact was even more evident in tributary SeO_4 concentrations, as groundwater flows passing through riparian buffers make up a much greater percentage of total tributary flows compared to total River flows. After multiple iterations of altering the λ_{SeO_4RH} parameter value, an increase of λ_{SeO_4RH} to 0.10 day^{-1} from its baseline value of 0.02 day^{-1} was determined to yield the best simulation results on a system-wide basis. This value falls within the $0.08\text{-}1.4 \text{ day}^{-1}$ range of values for λ_{SeO_4RH} reported in the studies of Guo et al. (1994) and Chow et al. (2004). Since λ_{SeO_4RH} was the only parameter required to be altered in order to drive SeO_4 concentrations sufficiently closer to observed values, no other RT3D parameters were altered for in-stream SeO_4 calibration.

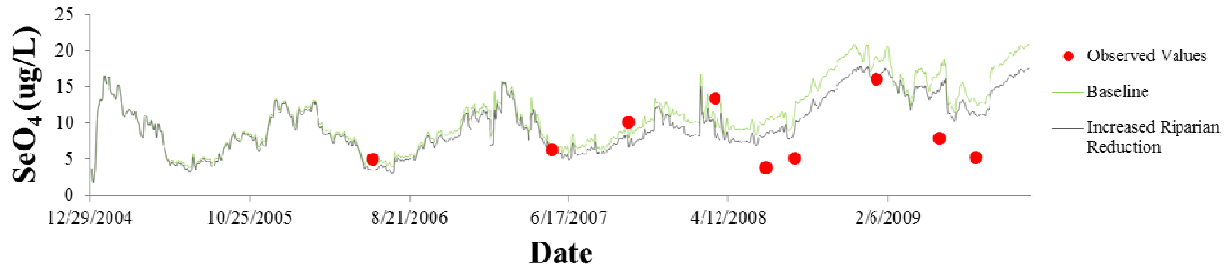


Figure 3-14. RT3D-OTIS baseline simulated values of SeO₄, simulated values of SeO₄ with increased λ_{SeO_4RH} , and observed values of SeO₄ at observation location ARK 127.

With predicted in-stream NO₃ concentrations determined to be largely insensitive to λ_{NO_3RH} , the TW_{NO_3} parameter was targeted for calibration. In an effort to increase simulated in-stream NO₃ concentrations, TW_{NO_3} was incrementally increased from its baseline value of 1 until the maximum reported value of 8 was achieved, meaning that the irrigation tailwater runoff entering surface water as overland flow had NO₃ concentrations eight times higher than concentrations applied to the fields in irrigation water. This is supported by the reported ability of surface irrigation water to mobilize and transport nitrogen fertilizer when traveling over fertilized fields. Concentrations of NO₃ in irrigation tailwater have been reported as being 3.3-8.0 times those of the irrigation water being applied to fields (Ciotti, 2005; MacKenzie and Viets, 1974).

3.2.5 RT3D-OTIS General Observations

The calibration approach taken in this study yielded simulated concentrations that were more representative of observed values as compared to concentrations simulated using default RT3D-OTIS parameter values. DO concentrations were well-predicted by using default model parameters, and were not substantially altered by measures taken to calibrate SeO₄ and NO₃. By altering riparian reduction rates and tailwater multiplication factors for SeO₄ and NO₃, respectively, as well as using in-stream OTIS-QUAL2E-Se model parameters from the SA and

calibration effort described in Sections 3.2.1 and 3.2.2, model parameters affecting in-stream NO_3 and SeO_4 concentrations were calibrated such that simulated NO_3 and SeO_4 concentrations matched observed concentrations to a level deemed sufficient to justify using the RT3D-OTIS model for estimating changes in in-stream concentrations that would result from land and water BMP adoption, described in Section 3.2.6 following.

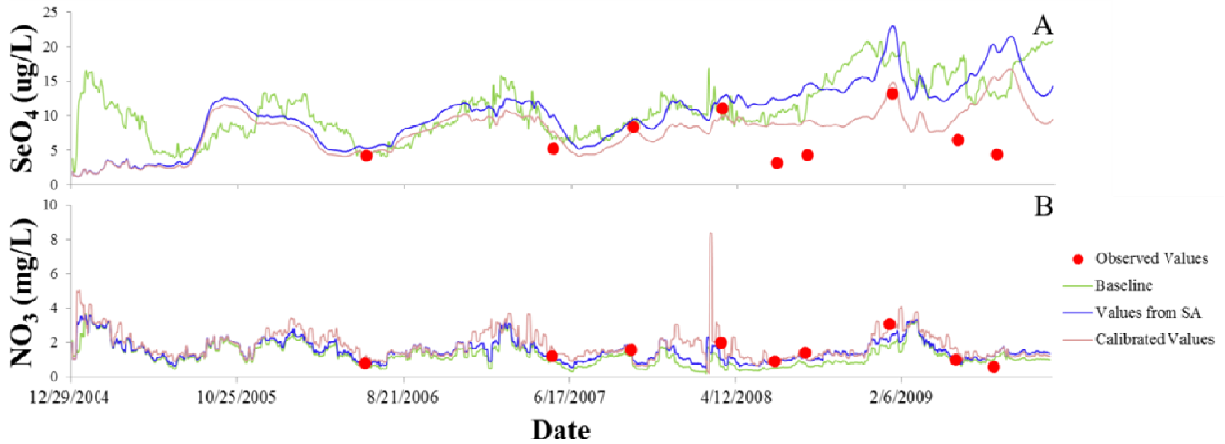


Figure 3-15. RT3D-OTIS baseline simulations, simulations using SA parameter values, and simulations using calibrated parameter values at observation location ARK 127 for (A) SeO_4 and (B) NO_3 .

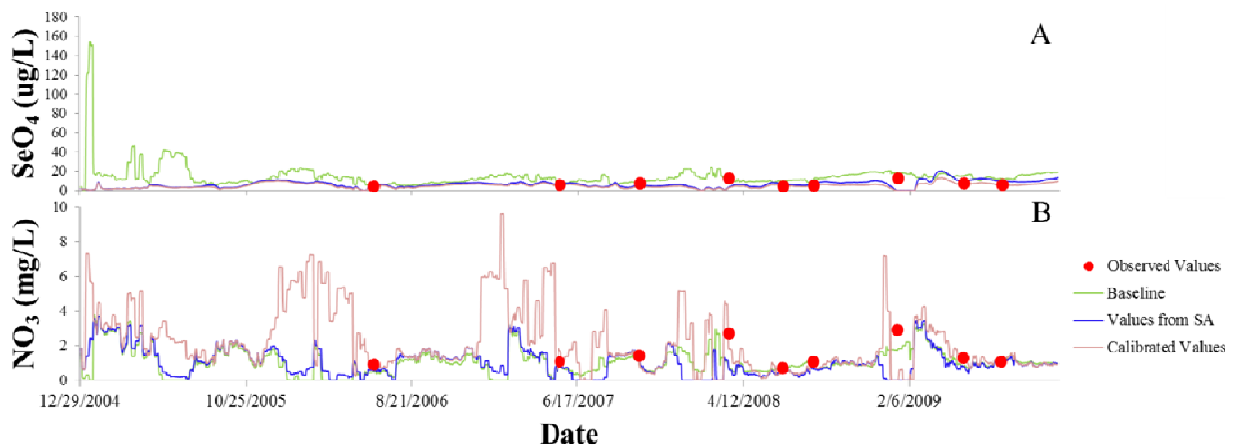


Figure 3-16. RT3D-OTIS baseline simulations, simulations using SA parameter values, and simulations using calibrated parameter values at observation location ARK 95 for (A) SeO_4 and (B) NO_3 .

Figures 3-15A and 3-15B and 3-16A and 3-16B illustrate the changes in simulated SeO_4 and NO_3 concentrations through the three main steps of the calibration process. It is clear that the evolution of the RT3D-OTIS model from the default version to the fully-calibrated model

yielded more accurate results at each step of the calibration process. The evolution of the RT3D-OTIS model is quantified in Tables 3-10 and 3-11 below.

Table 3-10. Spatio-temporally averaged observed and simulated concentrations of SeO₄, SeO₃, NO₃, and DO for the Arkansas River.

	SeO ₄ (µg/L)	SeO ₃ (µg/L)	NO ₃ (mg/L)	DO (mg/L)
Observed (Avg.)	6.34	1.38	1.40	9.05
Baseline Parameter Values (Avg.)	15.28	1.89	1.20	8.82
Difference from Observed	141%	37%	-15%	-2%
MAE	2.47			
SA Parameter Values (Avg.)	10.95	1.08	1.22	8.82
Difference from Observed	73%	-22%	-13%	-2%
MAE	1.33			
Calibrated Parameter Values (Avg.)	9.29	1.57	1.46	8.82
Difference from Observed	47%	13%	4%	-2%
MAE	0.86			

Table 3-11. Spatio-temporally averaged observed and simulated concentrations of SeO₄, SeO₃, NO₃, and DO for the tributaries of the Arkansas River.

	SeO ₄ (ug/L)	SeO ₃ (ug/L)	NO ₃ (mg/L)	DO (mg/L)
Observed (Avg.)	10.20	2.22	1.83	9.75
Baseline Parameter Values (Avg.)	177.02	0.96	0.40	6.10
Difference from Observed	1635%	-57%	-78%	-37%
MAE	43.29			
SA Parameter Values (Avg.)	10.25	1.07	0.48	5.91
Difference from Observed	0%	-52%	-74%	-39%
MAE	1.60			
Calibrated Parameter Values (Avg.)	8.36	1.03	1.00	5.91
Difference from Observed	-18%	-54%	-45%	-39%
MAE	1.93			

As shown in Table 3-10, simulated SeO₄ concentrations in the Arkansas River were lowered from a 141% over-prediction, compared to observed values, to a 47% over-prediction, while simulated NO₃ concentrations were increased from a 15% under-prediction to a 4% over-prediction. Table 3-11 shows that simulated SeO₄ concentrations in the tributaries were reduced from a 1,635% over-prediction to an 18% under-prediction, while NO₃ concentrations were increased from a 78% under-prediction to a 45% under-prediction. When examining Tables 3-10 and 3-11 together, it is clear that the calibrated RT3D-OTIS model more closely predicts

observed concentrations in the Arkansas River as compared to the tributaries. Additionally, as is shown by Tables 3-10 and 3-11, further efforts to drive either simulated Arkansas River or tributary concentrations to a 0% difference from observed values would result in the untargeted surface water type (i.e. Arkansas River or tributaries) to be driven further from observed values. Given this inverse relationship, and with priority given to more accurately predicting Arkansas River concentrations compared to tributary concentrations, it was determined that RT3D-OTIS model was sufficiently calibrated.

3.2.6 Best Management Practice Analysis Using RT3D-OTIS

With a calibrated RT3D-OTIS model in hand, attention was then turned to using the model to simulate the impacts of implementing reduced fertilization (RF), reduced irrigation (RI), land fallowing (LF), and canal sealing (CS) BMPs. These BMPs were specifically examined by comparing BMP simulations to baseline model output after reducing fertilization by 10% (RF10), 20% (RF20), and 30% (RF30), reducing irrigation applications by 10% (RI10), 20% (RI20), and 30% (RI30), fallowing cultivated fields by 5% (LF5), 15% (LF15), and 25% (LF25), and sealing canals such that canal conductance was reduced by 20% (CS20), 40% (CS40), and 80% (CS80).

3.2.6.1 Reduced Fertilization BMPs

As expected, the RF BMP resulted in reductions in SeO_4 , SeO_3 , and NO_3 concentrations.

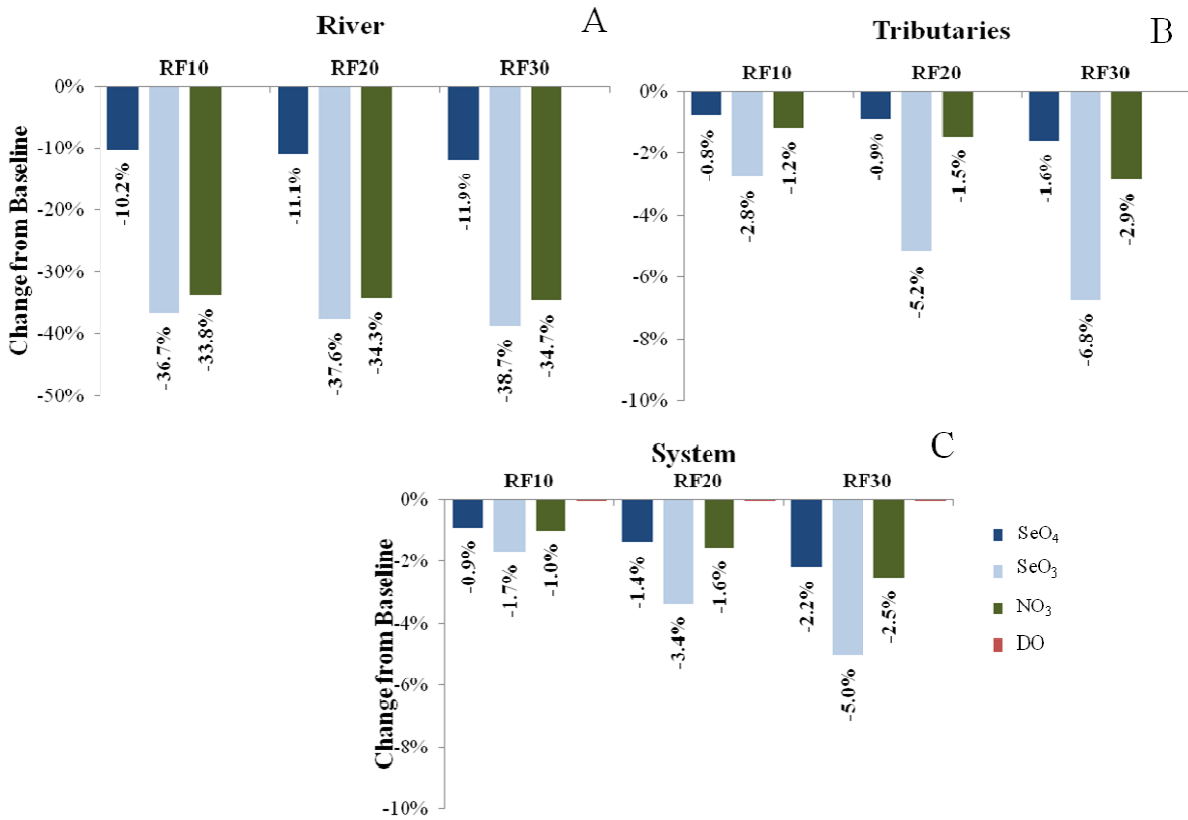


Figure 3-17. Percent change from the spatio-temporal averaged baseline SeO_4 , SeO_3 , NO_3 , and DO concentrations simulated by RT3D-OTIS under the reduced fertilizer BMPs in the (A) Arkansas River, (B) tributaries, and (C) entire stream system.

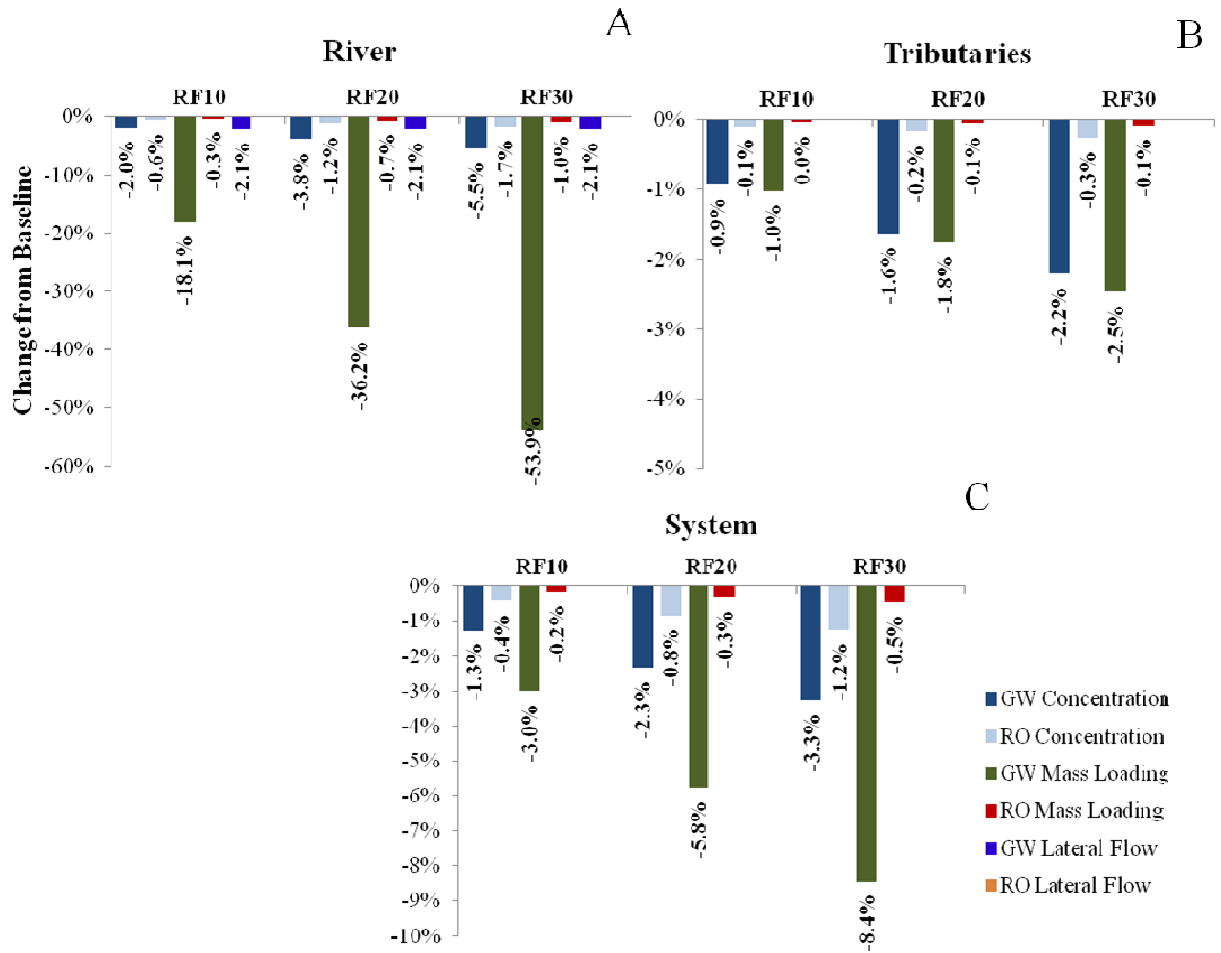


Figure 3-18. Percent change from the spatio-temporal averaged baseline SeO_4 groundwater (GW) concentration, runoff (RO) concentration, GW mass loading, RO mass loading, GW lateral flow, and RO lateral flow simulated by RT3D-OTIS under the RF BMPs along the (A) Arkansas River, (B) tributaries, and (C) entire stream system.

As RF was increased in intensity, an expected decrease in in-stream concentrations resulted. Interestingly, as is shown in Figure 3-17, the effects of RF are more pronounced in the Arkansas River, as compared to the tributaries, with a 30% lowering of fertilizer application resulting in an 11.9% reduction in average SeO_4 concentration and a 34.7% reduction in average NO_3 concentration in the Arkansas River, compared to a 1.6% reduction in average SeO_4 concentration and a 2.9% reduction in average NO_3 concentration in the tributaries. These results can be explained when examining Figure 3-18, which illustrates that the predicted impacts to groundwater concentrations adjacent to the Arkansas River, concentrations of runoff entering the

Arkansas River, and associated mass loading to the Arkansas River were greater than those for the tributaries.

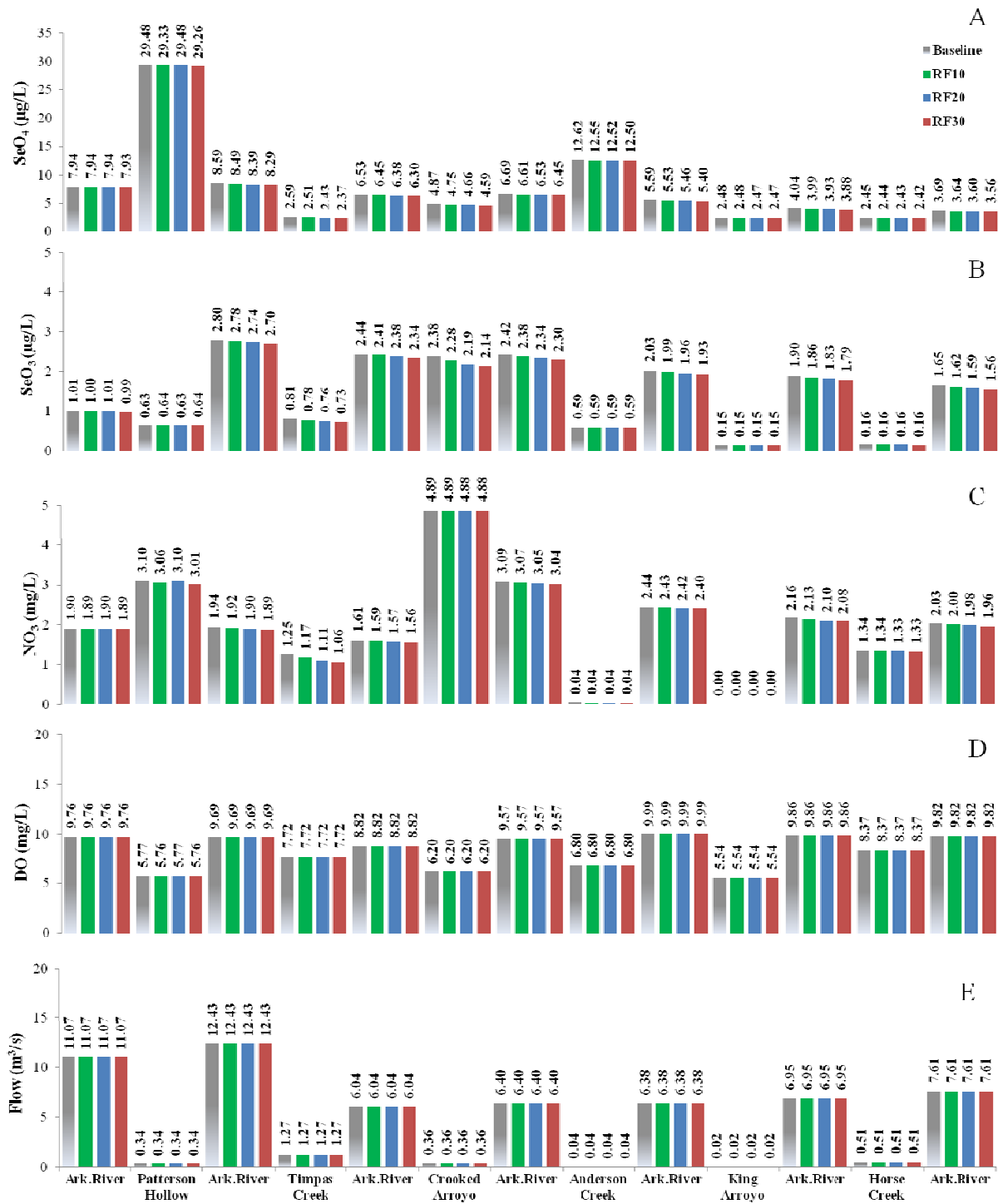


Figure 3-19. Temporally averaged (A) SeO₄ concentration, (B) SeO₃ concentration, (C) NO₃ concentration, (D) DO concentration, and (E) flow rate simulated by RT3D-OTIS at each observation location for the baseline and for the RF BMPs.

Figure 3-19 illustrates decreases in SeO_4 , SeO_3 , and NO_3 concentrations from the simulated baseline concentrations at all observation locations in the study region. Concentrations generally are higher in the tributaries as compared to the Arkansas River. Because of this, similar decreases in SeO_4 concentrations are more pronounced in the Arkansas River than the tributaries, as shown in Figures 3-17A and 3-17B. Time series plots of SeO_4 , SeO_3 , NO_3 , and DO concentrations; flow; groundwater SeO_4 mass loading; runoff SeO_4 mass loading; groundwater return flow; runoff return flow; groundwater and runoff concentrations of SeO_4 for the baseline, RF10, RF20, and RF30 scenarios are provided in Appendix A.

3.2.6.2 Reduced Irrigation BMPs

Compared to the RF results, the results of the model simulations of the RI scenarios are more complex as they involve changes in groundwater and surface water return flows.

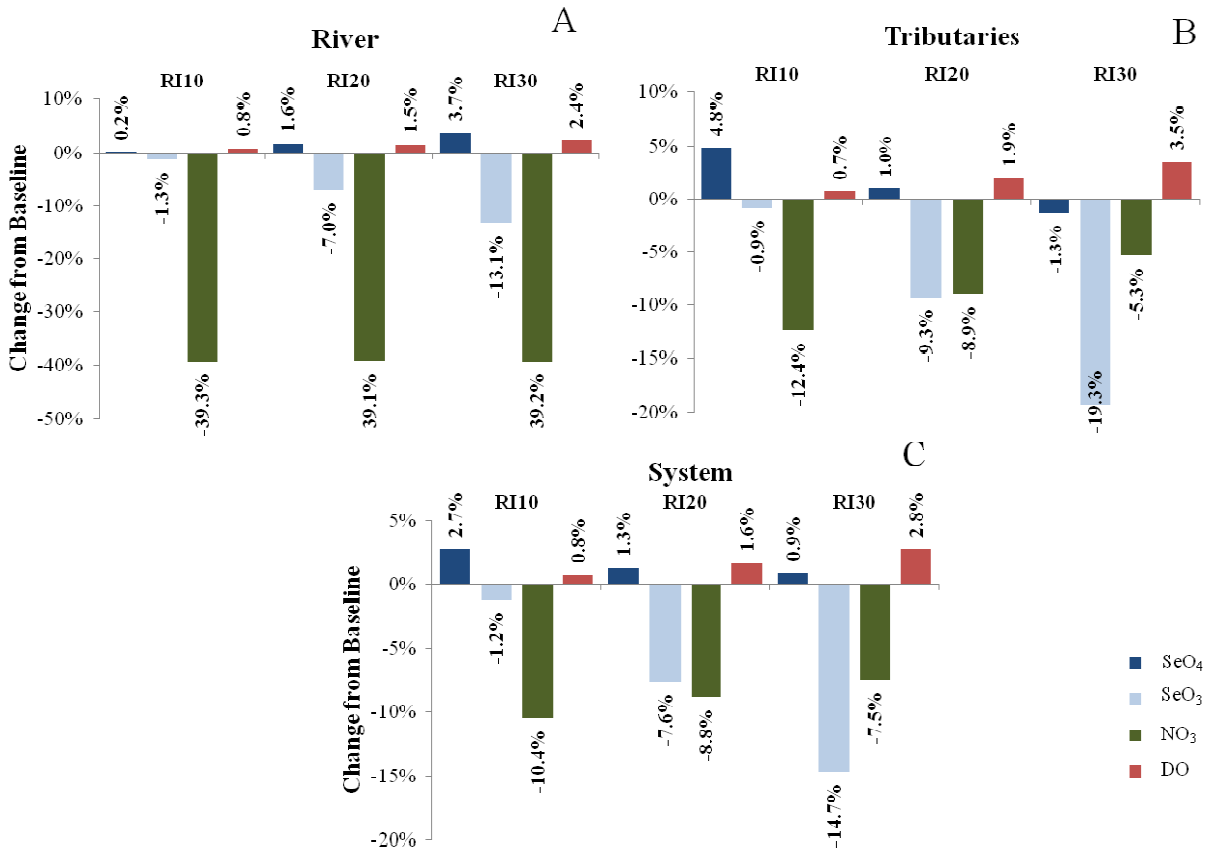


Figure 3-20. Percent change from the spatio-temporal averaged baseline SeO₄, SeO₃, NO₃, and DO concentrations simulated by RT3D-OTIS under the reduced irrigation BMPs in the (A) Arkansas River, (B) tributaries, and (C) entire stream system.

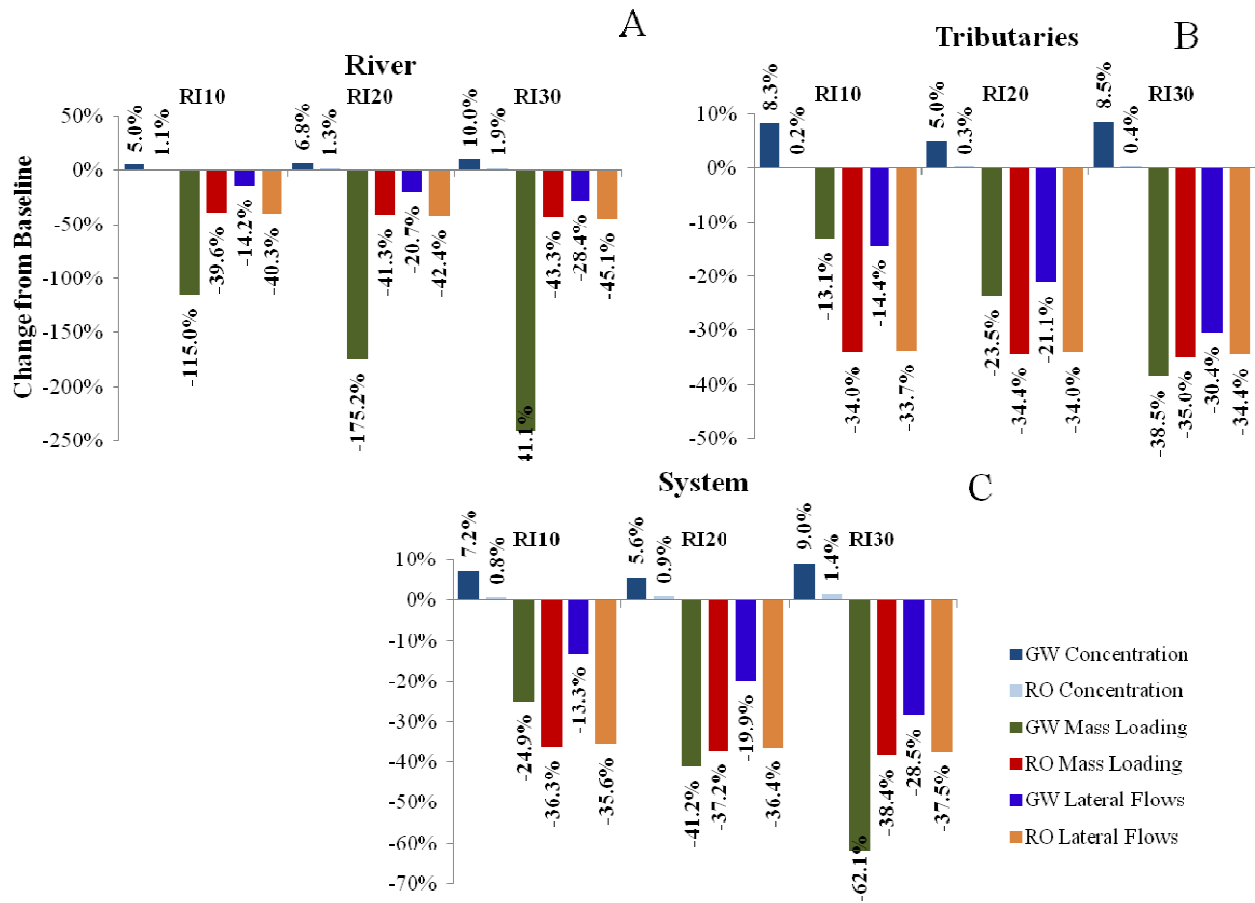


Figure 3-21. Percent change from the spatio-temporal averaged baseline SeO_4 groundwater (GW) concentration, runoff (RO) concentration, GW mass loading, RO mass loading, GW lateral flow, and RO lateral flow simulated by RT3D-OTIS under the RI BMPs along the (A) tributaries, (B) Arkansas River, and (C) entire stream system.

As shown in Figure 3-20A, reducing the irrigation water applied to fields resulted in simulated increases in SeO_4 concentrations in the Arkansas River. This might be due to a concentrating effect in adjacent groundwater caused by less water percolating from the surface. This is supported by Figure 3-21A, which shows that simulated groundwater SeO_4 concentrations increase when applied irrigation water was reduced. Similarly, Figures 3-20B and 3-21B also indicate a possible concentrating effect of reduced irrigation on SeO_4 concentrations in groundwater along the tributaries. However, unlike along the Arkansas River where increasing the magnitude of the reduced irrigation resulted in further increases in in-stream SeO_4 concentrations, an opposite effect was simulated along the tributaries. As shown in Figure 3-21B,

groundwater concentrations of SeO_4 adjacent to the tributaries increase with increased reductions in irrigation, while Figure 3-21B also shows that runoff SeO_4 mass loading decreased with larger decreases in irrigation water. Since in-stream SeO_4 concentrations in the tributaries followed the trend of runoff mass loading and not the trend of groundwater mass loading, an unexpectedly significant influence of surface runoff on tributary in-stream SeO_4 concentrations can be implied. This is supported by the time series plots included in Appendix A, which clearly show that groundwater return flows outweigh runoff return flows along the Arkansas River, while runoff return flows far outweigh groundwater return flows along the tributaries. It should be noted that although increases in in-stream SeO_4 concentration associated with the reduced irrigation BMP can be explained through a concentrating effect in adjacent groundwater, this result is generally unexpected. As such, a possibility exists that deficiencies in the model and/or parameter values are the source of this result. Therefore, further investigation into the model code and parameter values are required in order to validate this result.

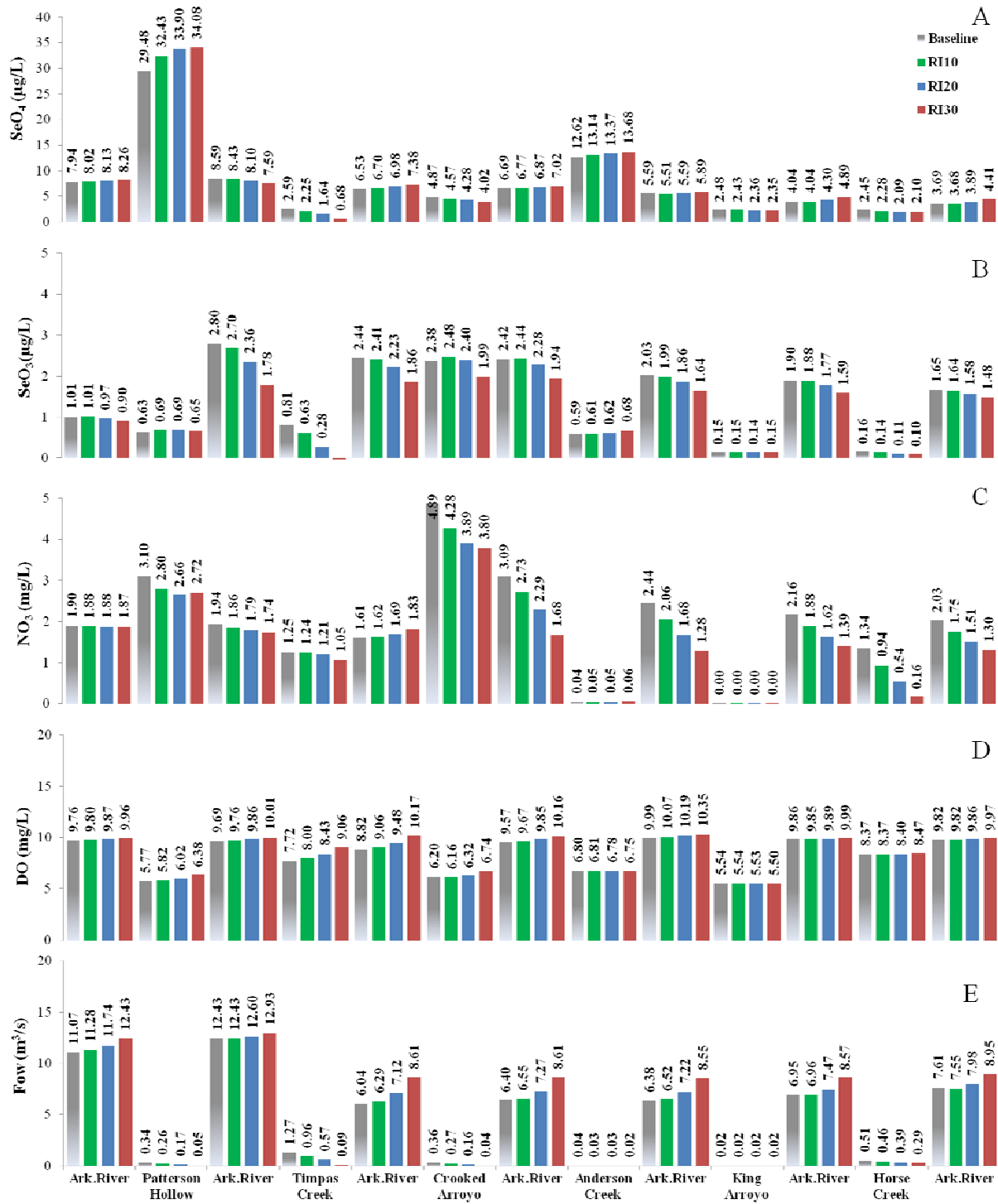


Figure 3-22. Temporally averaged (A) SeO_4 concentration, (B) SeO_3 concentration, (C) NO_3 concentration, (D) DO concentration, and (E) flow rate simulated by RT3D-OTIS at each observation location for the baseline and RI BMP scenarios.

Figure 3-22 provides additional insight into the spatial trends of in-stream constituents throughout the study region for the various RI scenarios. As discussed above, it is likely that in locations where simulated SeO_4 and NO_3 concentrations decrease as irrigation applications are further reduced are more influenced by changes in surface water return flows than by changes in groundwater return flows. The opposite is likely true for locations where SeO_4 and NO_3 are increasing as irrigation applications are reduced.

Figure 3-22A shows that in the Arkansas River, predicted SeO_4 concentrations are higher than the baseline for each of the RI BMPs. Additionally, SeO_4 concentrations increase with the magnitude of reduced irrigation. Although the tributaries show a decreasing trend and a reduction of in-stream SeO_4 concentration with the RI30 BMP, as shown in Figure 3-22B, the negative effect of reduced irrigation on concentrating SeO_4 in groundwater return flows appears to result in overall increases in SeO_4 concentration in the Arkansas River.

3.2.6.3 Land Fallowing BMPs

Land fallowing is a unique BMP in that it is a combination of the RF and RI BMPs, as fallowed land receives neither nitrogen fertilizer nor irrigation water. However, as is shown by Figure 3-23, modeled LF scenarios yielded model results more similar to the RI than to the RF BMPs, suggesting that changes to water management practices are more impactful than changes to fertilization practices. Percent changes from the baseline for simulated SeO_4 , SeO_3 , and DO concentrations were very similar both in magnitude and in trend to the RI BMPs. This implies that with respect to SeO_4 , SeO_3 , and DO concentrations, fallowing 5% of cultivated fields is approximately as impactful as reducing irrigation applications by 10%, fallowing 15% of cultivated fields is approximately as impactful as reducing irrigation by 20%, and fallowing 25%

of cultivated fields is approximately as impactful as reducing irrigation by 30%. Although there was a reduction in average predicted NO₃ concentration in the streams, it was not as pronounced as the NO₃ reduction simulated in the RI BMP model results, particularly in the Arkansas River. LF5, LF15, and LF25 scenarios resulted in predicted NO₃ reductions of 8.8%, 8.4%, and 9.2%, respectively, while RI10, RI20, and RI30 scenarios resulted in NO₃ reductions of 39.3%, 39.1%, and 39.2%, respectively. As with the RI results, the NO₃ concentrations in the River predicted under the LF BMP suggests a possible error in the model and/or parameter values as it would be expected to see a higher reduction in NO₃ concentrations as compared to the RI BMP since the LF BMP includes both reduced irrigation and reduced fertilization.

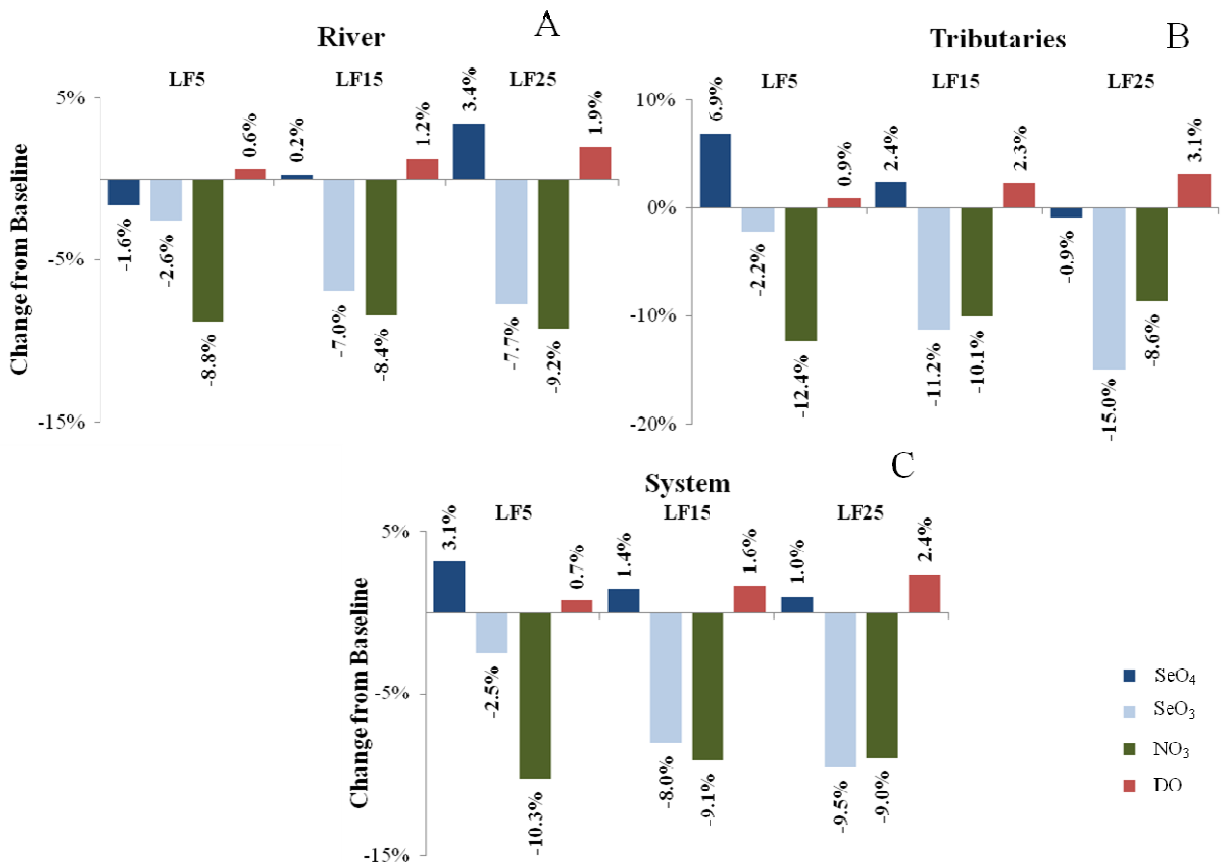


Figure 3-23. Percent change from the spatio-temporal averaged baseline SeO₄, SeO₃, NO₃, and DO concentrations simulated by RT3D-OTIS under the land following BMPs in the (A) Arkansas River, (B) tributaries, and (C) entire stream system.

In examining predicted SeO_4 in surface runoff and groundwater return flows, the LF BMPs showed percent changes from the baseline and trends that were similar to those of the RI BMPs, as shown in Figure 3-24.

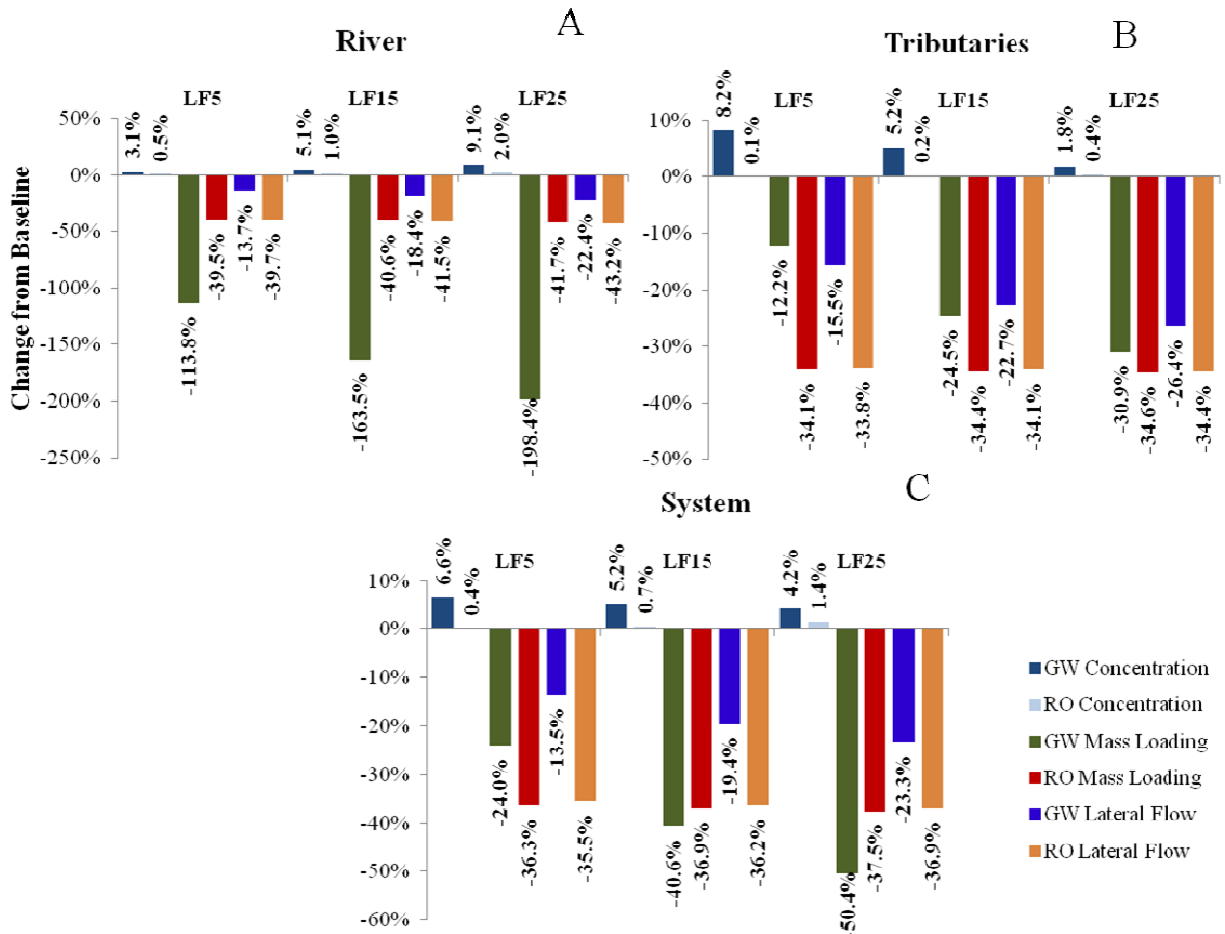


Figure 3-24. Percent change from the spatio-temporal averaged baseline SeO_4 groundwater (GW) concentration, runoff (RO) concentration, GW mass loading, RO mass loading, GW lateral flow, and RO lateral flow simulated by RT3D-OTIS under the LF BMPs along the (A) Arkansas River, (B) tributaries, and (C) the entire stream system.

Although the LF results closely resemble the RI results on a system-averaged basis, differences between the two are apparent when examining model results at each observation location, particularly in the tributaries. For example, as shown in Figure 3-25, Patterson Hollow shows simulated SeO_4 concentrations that are higher than the baseline and increasing with the degree of the RI BMPs, while simulated SeO_4 concentrations are higher than the baseline but decreasing as the degree of the LF BMP increases. It is unclear why these trends are opposite, as

3.2.6.4 Canal Sealing BMPs

On a system-wide basis, canal sealing was the worst performing BMP, with both an increase in predicted SeO_4 concentrations and an increasing trend. Additionally, although predicted NO_3 concentrations were lower than the baseline for all three CS scenarios, they too displayed an increasing trend as the degree of the CS BMP was increased. Like the other water management BMPs, the CS BMP appears to be concentrating SeO_4 in groundwater, resulting in increased in-stream SeO_4 concentrations. Although increases in in-stream SeO_4 concentration associated with the canal sealing BMP can be explained through a concentrating effect in adjacent groundwater, this result is generally unexpected. As such, a possibility exists that deficiencies in the model and/or parameter values are the source of this result. Therefore, further investigation into the model code and parameter values are required in order to validate this result.

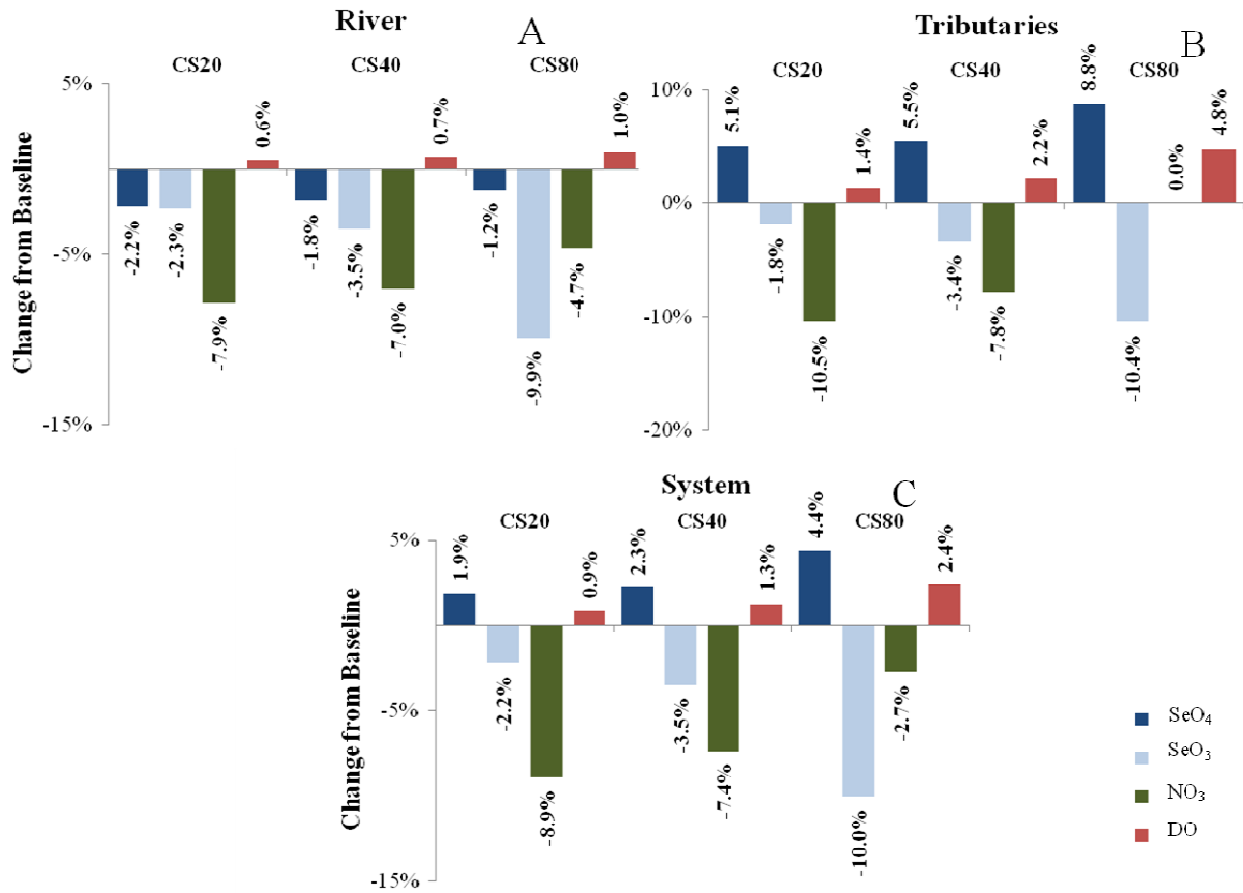


Figure 3-26. Percent change from the spatio-temporal averaged baseline SeO₄, SeO₃, NO₃, and DO concentrations simulated by RT3D-OTIS under the canal sealing BMPs in the (A) Arkansas River, (B) tributaries, and (C) the entire stream system.

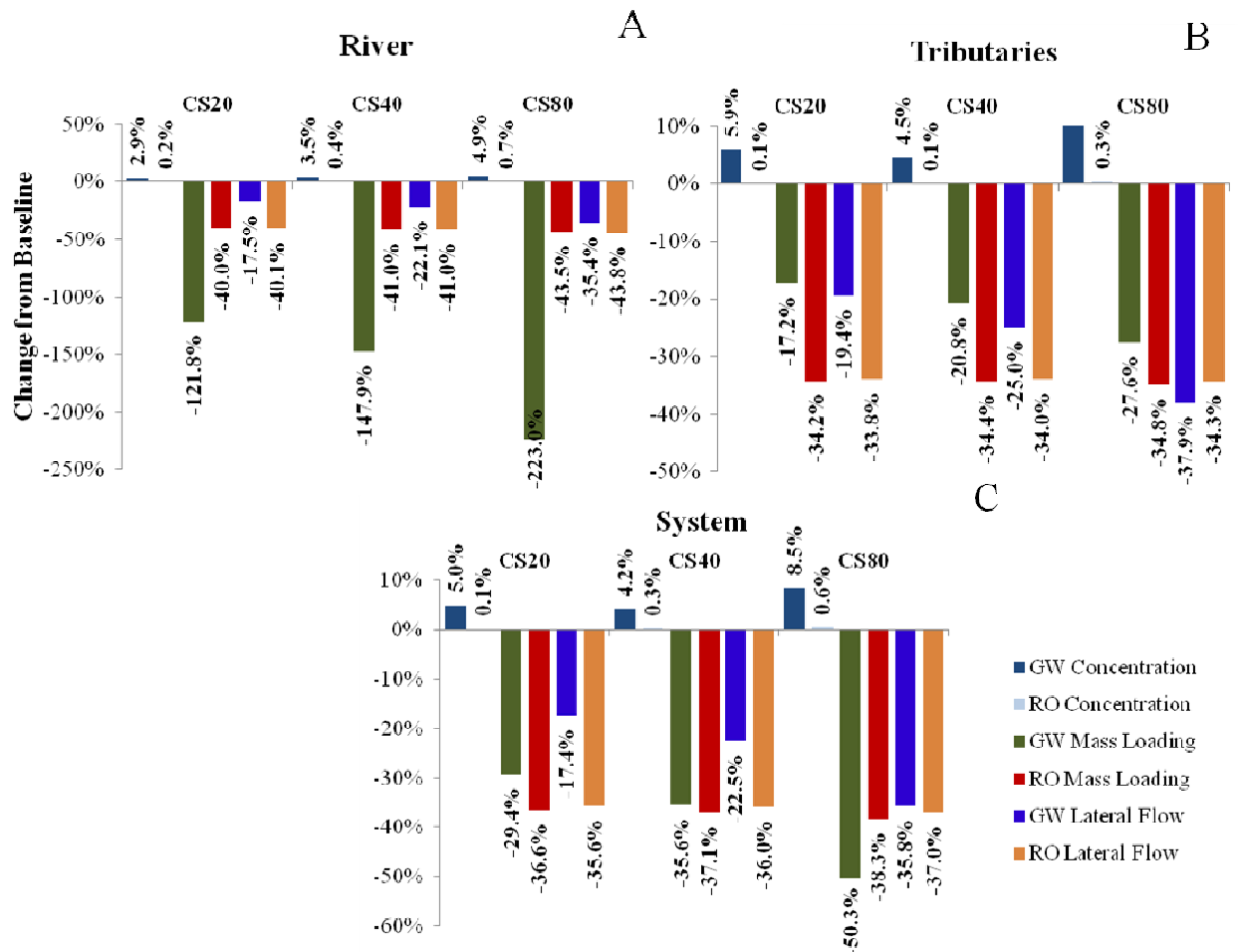


Figure 3-27. Percent change from the spatio-temporal averaged baseline SeO_4 groundwater (GW) concentration, runoff (RO) concentration, GW mass loading, RO mass loading, GW lateral flow, and RO lateral flow simulated by RT3D-OTIS under the CS BMPs along the (A) Arkansas River, (B) tributaries, and (C) entire stream system.

When examining individual observation locations, the CS BMPs closely resemble the RI BMPs with respect to predicted SeO_4 concentrations and trends. This is expected, as the sealing of canals reduces seepage influx to groundwater just as reduced irrigation reduces percolation influx to groundwater. Additionally, unlike the LF BMPs, the CS BMPs do not involve changes to fertilization practices. As such, a closer resemblance to the RI BMPs, as compared to either the RF or LF BMPs, is expected.

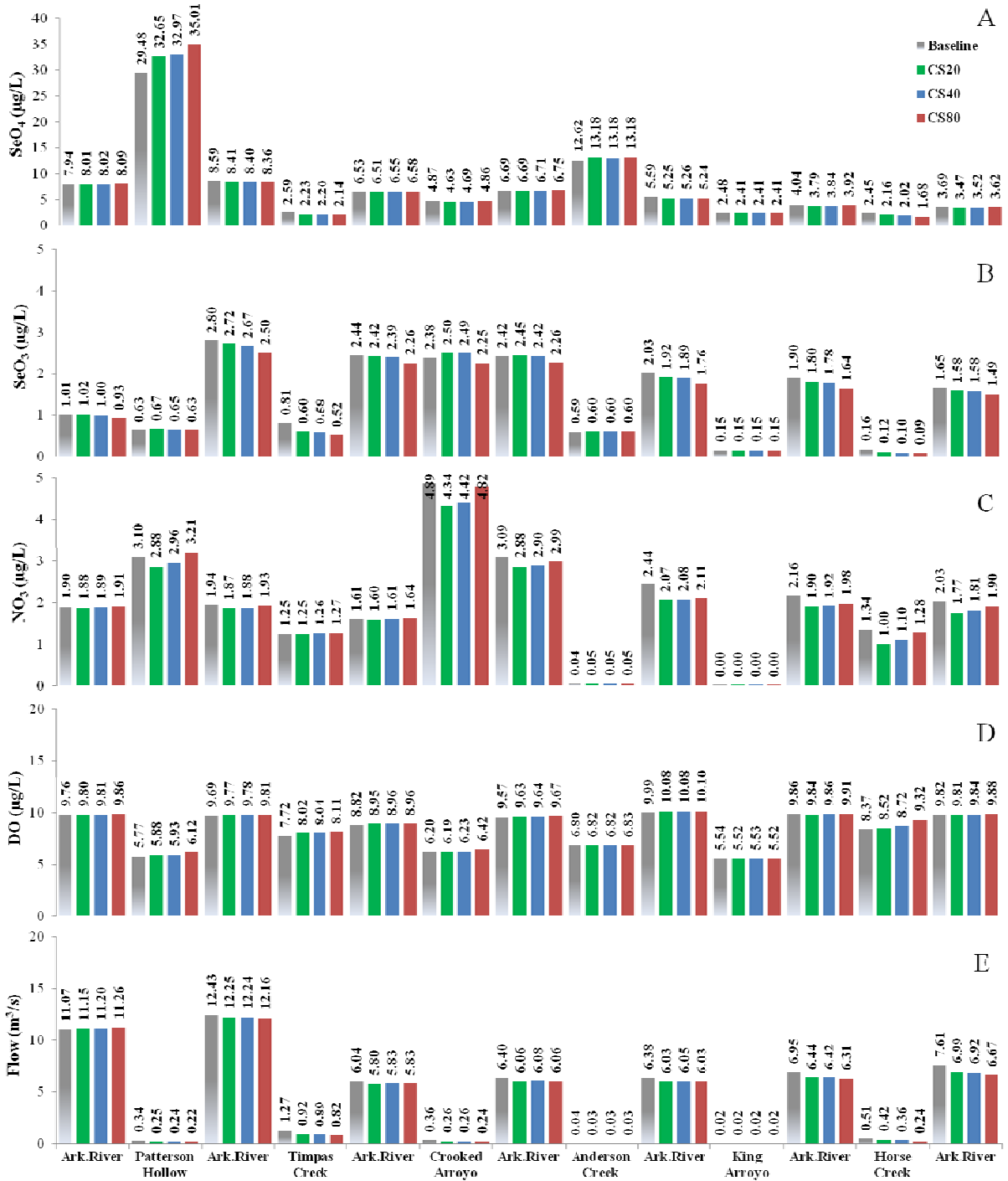


Figure 3-28. Temporally averaged (A) SeO₄ concentration, (B) SeO₃ concentration, (C) NO₃ concentration, (D) DO concentration, and (E) flow rate simulated by RT3D-OTIS at each observation location for the baseline and CS BMP scenarios.

3.2.6.5 BMP General Observations

The RF BMP was the only BMP that yielded consistent predicted decreases in in-stream Se and NO₃ concentrations, as well as larger decreases in in-stream concentrations as the magnitude of the RF BMP was increased. The RI BMP displayed increases from the baseline condition, likely due to the concentration of SeO₄ in groundwater adjacent to the Arkansas River and tributaries. This concentrating effect in adjacent groundwater is shown in Figures 3-21, 3-24, and 3-27, whereby SeO₄ concentrations in adjacent groundwater are higher than those of the baseline condition. Although this is a plausible explanation, it is an unexpected result that warrants validation through further examination of the model code and/or parameter values. Interestingly, the trends were opposite for the RI BMP when examining the Arkansas River and tributaries, highlighting the unexpected influence of surface runoff concentrations from irrigation tailwater on in-stream concentrations in the tributaries. Groundwater concentrations were more influential on Arkansas River concentrations, however. The LF BMPs displayed characteristics of both the RF and the RI BMPs, and as such did not result in increases in in-stream concentrations that were as high as those for the RI BMPs. The trends of the LF BMPs matched those of the RI BMPs, where although the LF scenarios resulted in increased predicted SeO₄ concentrations as compared to the baseline, concentrations decreased on a system-averaged basis as the degree of the LF BMPs increased. The CS BMPs performed the worst on a system-averaged basis out of the four BMPs examined. However, this was driven by tributary concentrations, as when examining only the Arkansas River, the CS BMPs performed second to the RF BMPs in terms of reductions in in-stream SeO₄, SeO₃, and NO₃ concentration. Generally, the impact of each BMP was highly spatially variable, both in terms of each observation location and in terms of Arkansas River versus tributary concentrations. As such, the efficacy of each

BMP depends on perspective, namely if the changes in in-stream concentrations are being examined on a system-averaged basis, an Arkansas River versus tributary basis, or at each individual observation location. As discussed throughout Section 3.2.6, although most of the unexpected increases in in-stream SeO_4 concentration can be explained through a concentrating effect in adjacent groundwater, further investigation into the model and/or parameter values is required to validate these results. A summary of results is provided in Table 3-12.

Table 3-12. Changes in SeO_4 concentration associated with each BMP examined.

	RF10	RF20	RF30	RI10	RI20	RI30	LF5	LF15	LF25	CS20	CS40	CS80
River	-10.20%	-11.10%	-11.90%	0.20%	1.60%	3.70%	-1.60%	0.20%	3.40%	-2.20%	-1.80%	-1.20%
Tributaries	-0.80%	-0.90%	-1.60%	4.80%	1.00%	-1.30%	6.90%	2.40%	-0.90%	5.10%	5.50%	8.80%
System	-0.90%	-1.40%	-2.20%	2.70%	1.30%	0.90%	3.10%	1.40%	1.00%	1.90%	2.30%	4.40%

3.3 Multi-Criteria Decision Analysis

The results of the MCDA AHP survey are presented in three main sections, the first being an analysis of the main criteria (i.e. cost, ease of implementation, economic benefits, and environmental benefits). Next the sub-criteria are examined, which provide additional insight into the ranking of the main criteria. The five BMPs considered in this study are then analyzed with respect to each of the main criteria. Last, an overall rank of the BMPs is provided. At each step of the analysis, survey results are broken down into groups based on population characteristics including age of farmer, type of irrigation used, and acres farmed. A detailed examination of the reasoning behind the responses of each group is not provided, as the sociological and psychological analyses that would be required to provide such an evaluation is outside the scope of this study.

3.3.1 Main Criteria for BMP Decision Making

The ranking of the main criteria for BMP decision making, in regard to importance, is shown in Figure 3-29. The grouping categories shown in Figure 3-29 were determined in an effort to provide insight into the preferences of various age groups, irrigation types, and farm sizes. Although no specific discussion regarding the preferences of each group, the reasons behind them, or their implications is made here, such discussions will likely be a part of future work. Economic benefits ranked the highest among the four main criteria for all groups, with a score as high as 0.50 for those who use flood irrigation (the sum of all relative importance scores sums to one). The lowest relative importance score for economic benefits was 0.37, which was the score of those surveyed who farm between 40 and 640 acres. Ranked second was cost, with relative scores ranging between 0.21 for those who use flood irrigation and 0.32 for both those who use sprinkler or drip irrigation and for those who farm between 40 and 640 acres. Ranked third was ease of implementation, with relative scores ranging narrowly between 0.17 and 0.21. The lowest rank was environmental benefits, with an average relative importance score of 0.14. When examining these results, it is worth noting that there was no overlap between main criteria for any of the groups surveyed, suggesting that the relative importance scores of the main criteria were consistent among all groups surveyed. The first and second ranking main criteria highlight the expected result that stakeholders seem to care more about their own economic status than about how easy a BMP is to implement and the effects it might have on the environment. All groups surveyed cared least about environmental considerations out of the four main criteria examined. The statistical significance of the results was assessed through examining the margin of error (MOE) associated with a sample size of 25 in relation to the estimated 199 farmers between Manzanola, Rocky Ford, La Junta, and Las Animas (United States Census Bureau /

American Community Survey, 2014). Using this sample and population size and a confidence interval of 95%, the margin of error associated with these results was calculated to be 13% using Equation (23) (Triola, 2006).

$$MOE = z * \sqrt{\frac{p(1-p)}{n}} \tag{23}$$

where *MOE* is the margin of error, *z* is the z-value associated with the 95% confidence interval (CI) (1.96), *p* is the fraction of the population sampled, and *n* is the sample size. Since population data regarding the specific groups shown in Figures 3-29 through 3-32 were not available, the MOE is only reported for the sample average. It was assumed that those sampled were representative of the farming community of Manzanola, Rocky Ford, La Junta, and Las Animas as a whole.

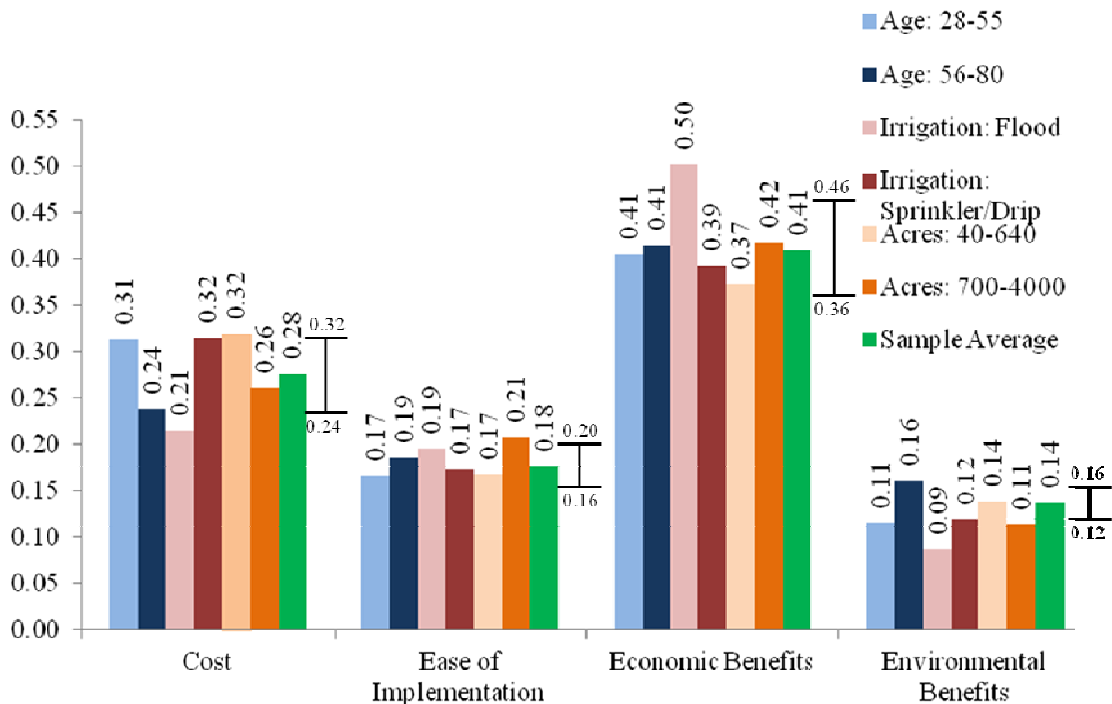


Figure 3-29. Relative importance scores and MOE by surveyed stakeholders of the main criteria for BMP decision making, with higher scores being more preferred.

As shown in Figure 3-29, the 95% CI MOE suggests that chance that Economic Benefits are the most important criteria, Cost is the second most important criteria, and either Ease of

Implementation or Environmental Benefits are the third and fourth most important criteria amongst the collective group of farmers between . The uncertainty in the 95% CI MOE with respect to Ease of Implementation and Environmental Benefits arises from the overlap in their margins of error, thus their rank cannot be stated with 95% certainty.

3.3.2 Sub-Criteria for BMP Decision Making

Providing additional insight into the main criteria results are the results of the sub-criteria analysis shown in Figure 3-30.

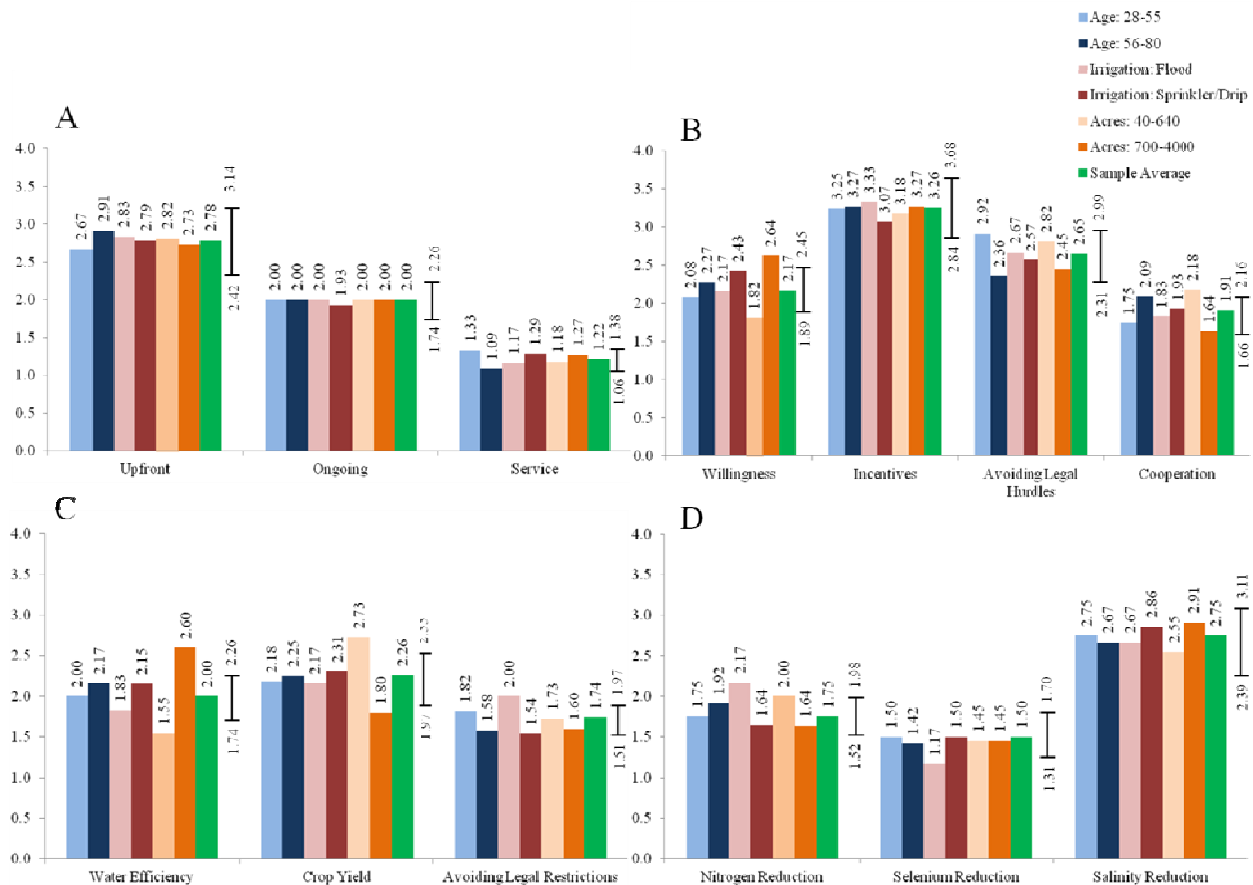


Figure 3-30. Average sub-criteria scores by surveyed stakeholders for (A) cost, (B) ease of implementation, (C) economic benefits, and (D) environmental benefits, with higher scores being more preferred.

As discussed in Section 3.3.1, economic benefits ranked the highest among all groups surveyed. Figure 3-30C suggests that the strongest motivator behind that main criteria rank is

crop yield, with the highest average score of 2.26. Water efficiency and avoiding legal restrictions ranked second and third on an overall average basis, respectively. However, of the four main criteria, the sub-criteria related to economic benefits displayed the most overlap between sub-criteria, suggesting that the three sub-criteria vary in importance between groups. None of the sub-criteria associated with economic benefits were statistically significant for the sample average using a 95% CI.

Cost was the second ranked main criteria. As shown in Figure 3-30A, upfront costs were consistently ranked the most important among all types of costs, with an average score of 2.78. Ongoing costs were ranked second, and service costs third. The high rank of upfront cost and the low variability between groups suggests that for BMPs to be successfully implemented, costs to stakeholders would have to be taken into careful consideration. All of the sub-criteria associated with economic benefits were statistically significant for the sample average using a 95% CI. Reinforcing this result is Figure 3-30B, which shows that incentives are the most important component of ease of implementation on an average basis with an average score of 3.26. Incentives also showed the least variability among the ease of implementation sub-criteria. Ranked second was avoiding legal hurdles with a score of 2.65, third was willingness with a score of 2.17, and last was cooperation. Despite these overall scores, the sample average MOE suggests that incentives could be ranked first or second, avoiding legal hurdles could be ranked first, second, or third, willingness could be ranked second, third, or fourth, and cooperation could be ranked third or fourth.

Figure 3-30D overwhelmingly suggests that salinity reduction is the primary environmental concern of stakeholders in the LARV, with an average rank of 2.75 and a maximum rank of 2.91 among those who farm between 700 and 4,000 acres. Reduction in Se

ranked last as a sub-criterion, with an average score of 1.50, while N reduction has an average score of 1.75. Figure 3-30D also shows that salinity reduction being ranked first is statistically significant, while either nitrogen reduction or Se reduction could be ranked second and third.

In general, Figures 3-30A, B, C, and D suggest that primarily upfront and ongoing costs to stakeholders have to be addressed as incentives for successful BMP implementation.

Additionally, it was shown the crop yield was the most important motivator behind the highest rank of the economic benefits main criteria, although this result was not statistically significant.

Results also exhibit the strong importance of salinity reduction, which is an environmental issue both visible to farmers and generally known to reduce crop yield. Not surprisingly, Se reduction ranked last among stakeholders, as the environmental impacts of Se are not as visible or as directly consequential to stakeholders as salinity. Nitrogen reduction also ranked significantly lower than salinity reduction. This result suggests that significant investments in stakeholder education and awareness of the Se problem in LARV are required. It can also be implied from these results that BMPs are far more likely to be adopted by stakeholders if their ability to reduce salt concentrations is emphasized.

3.3.3 BMP Ranks

The final ranks of the BMPs derived from the survey are shown in Figure 3-31.

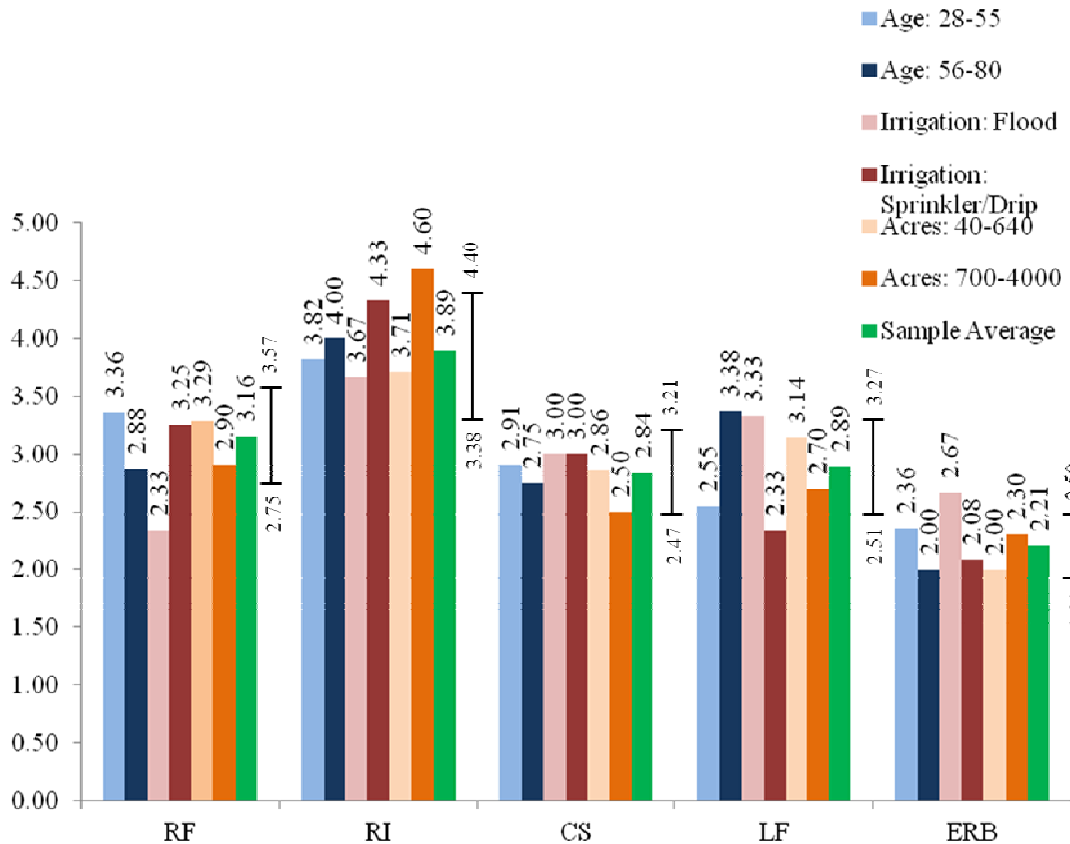


Figure 3-31. Average overall rank of BMPs by surveyed stakeholders, with higher scores being more preferred.

Average rankings show that reduced irrigation is the most preferred BMP among surveyed stakeholders in the LARV with an average rank of 3.89, reduced fertilization ranked second with an average rank of 3.16, land following ranked third with an average rank of 2.89, canal sealing ranked third with an average rank of 2.84, and enhanced riparian buffer ranked 2.21 with an average rank of 2.21. Additionally, there was no overlap for any groups between reduced irrigation and any other BMP, suggesting the reduced irrigation was consistently the most preferred. Reduced fertilization, canal sealing, and land following all showed considerable overlap, suggesting a relative indifference between those three BMPs when examining all groups. Enhanced riparian buffer was clearly ranked last out of the five BMPs.

Despite these results, Figure 3-31 also shows that there was no rank that was statistically significant. Based on the 95% CI and associated MOE, reduced irrigation could be ranked first or second, reduced fertilization could be ranked first, second, third or fourth, land fallowing could be ranked second, third, or fourth, canal sealing could be ranked second, third, fourth, or fifth, and enhanced riparian buffer could be ranked either fourth or fifth. It is worth noting that only the reduced irrigation and reduced fertilization BMPs could be ranked first, while neither the canal sealing, land fallowing, nor enhanced riparian buffer BMPs could be ranked first using the 95% CI.

Figure 3-32 serves to bridge the gap between these final BMP ranking and the results of the main criteria and sub-criteria.

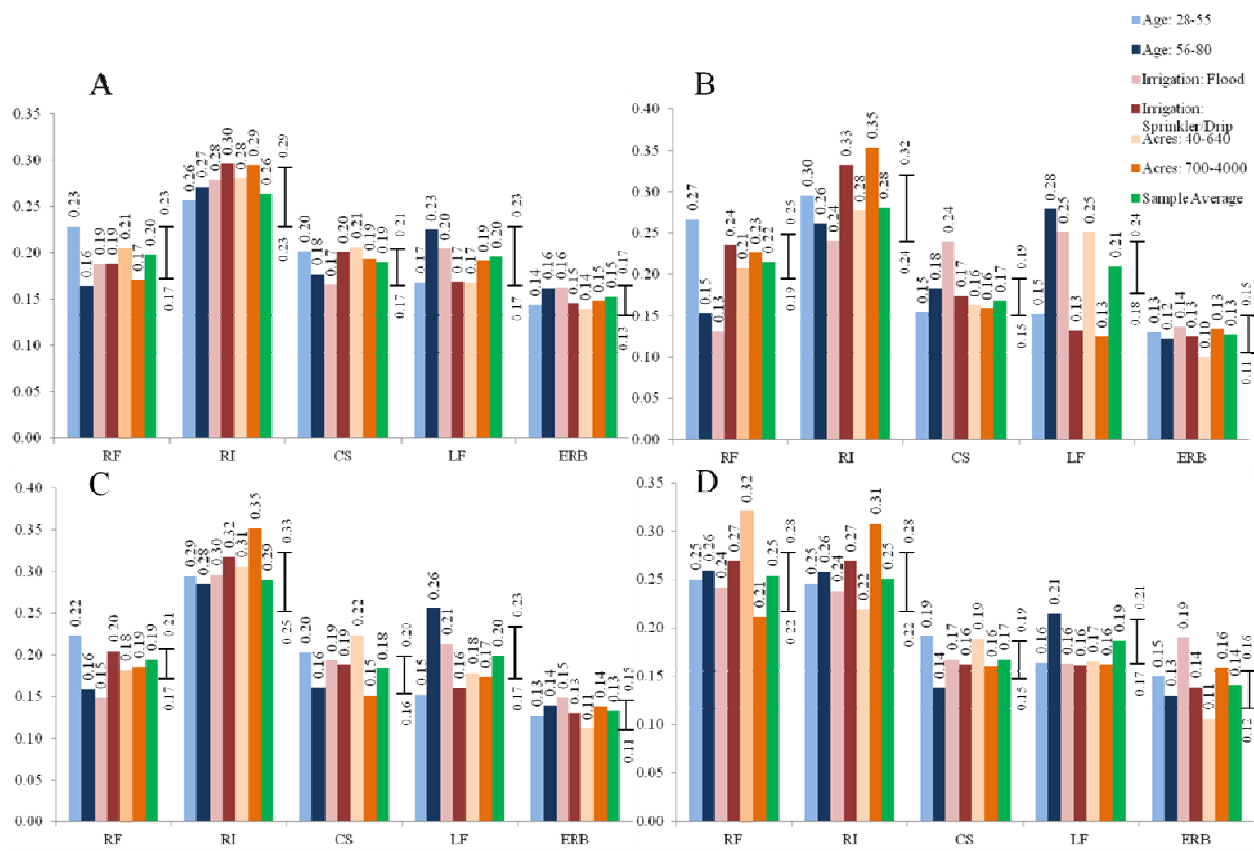


Figure 3-32. Relative importance of BMPs by surveyed stakeholders with respect to (A) cost, (B) ease of implementation, (C) economic benefits, and (D) environmental benefits, with higher scores being more preferred.

As mentioned, reduced irrigation was consistently the most preferred BMP. As shown in Figure 3-32C, reduced irrigation scored consistently the highest among all groups with respect to economic benefits, which was the highest ranking main criteria. The same is true when examining Figure 3-32A, with reduced irrigation having the highest relative importance score with respect to cost, which was the second highest ranking main criteria. With reduced irrigation ranking highest with respect to both of the highest ranking main criteria, significant weight was given to reduced irrigation resulting in it being ranked overall the most preferred BMP. Reduced irrigation also ranked highest with respect to ease of implementation, although it did not outrank other BMPs to the extent that it did with respect to economic benefits and cost.

The mixed results of surveyed stakeholders' perceptions of reduced fertilization, canal sealing, and land fallowing can also be explained when examining Figure 3-32A, B, and C, which show very mixed relative importance scores with respect to each of the three highest ranking main criteria. Although it seems that surveyed stakeholders perceive that reduced irrigation and reduced fertilization are the most effective with respect to environmental benefits, as shown in Figure 3-32D, the environmental benefits main criteria carried almost no weight as compared to the other three. As such, the dominance of reduced fertilization over canal sealing and land fallowing displayed in Figure 3-32D was drowned out by the mixed results of the more dominant main criteria shown in Figures 3-32A, B, and C. The enhanced riparian buffer ranked the lowest among all BMPs with respect to each of the main criteria. As such, it received the lowest overall rank.

Despite the conclusions outlined above, Figure 3-32 also shows that there was only one rank that was statistically significant, being that reduced irrigation was ranked first with respect to economic benefits as shown in Figure 3-32 C. In Figures 3-32 A, B, and D, reduced

fertilization and reduced irrigation could be ranked either first or second. Additionally, there is a 95% chance that neither the canal sealing nor enhanced riparian buffer BMPs would be ranked first out of the five BMPs considered.

3.3.4 General Observations

From the survey results, economic benefits are most important to stakeholders in the LARV within the given MOE. Cost is the second most important main criteria within the given MOE. Unlike economic benefits and cost, there is overlap in the MOE associated with ease of implementation and environmental benefits, so it is not possible to determine the relative importance of these criteria with respect to each other. The average relative importance scores amongst the 25 surveys conducted are depicted in Figure 3-33.

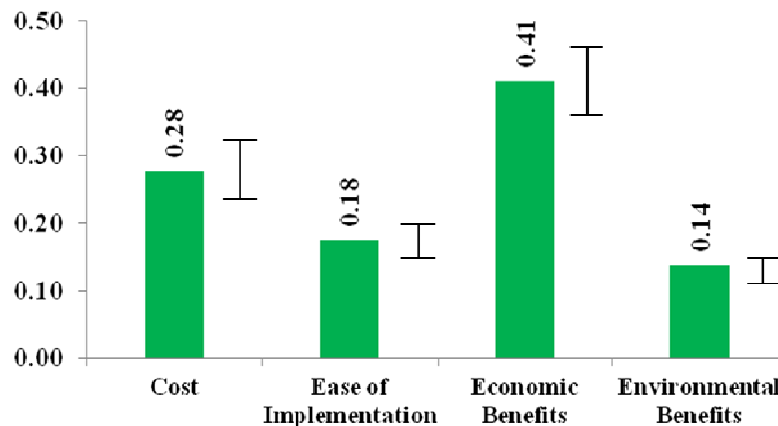


Figure 3-33. Average main criteria relative importance scores with error bars associated with a 95% confidence interval.

When examining the sub-criteria, the most important consideration appears to be crop yield, although this cannot be stated with a 95% CI as all three of the economic considerations sub-criteria show overlap in their MOE. The most important cost considerations are upfront costs. With respect to the ease of implementation main criteria, incentives rank the highest of the sub-criteria, suggesting that stakeholders will require incentives to offset any economic burdens

associated with implementing a particular BMP. The results of the environmental benefits main criteria also fit into the overall context of the importance of economic considerations with salinity reduction far outweighing both N reduction and Se reduction. High salinity is well known to reduce crop yield, which was the highest ranking sub-criteria of the highest ranking main criteria. Average ranks of sub-criteria are shown in Figure 3-34.

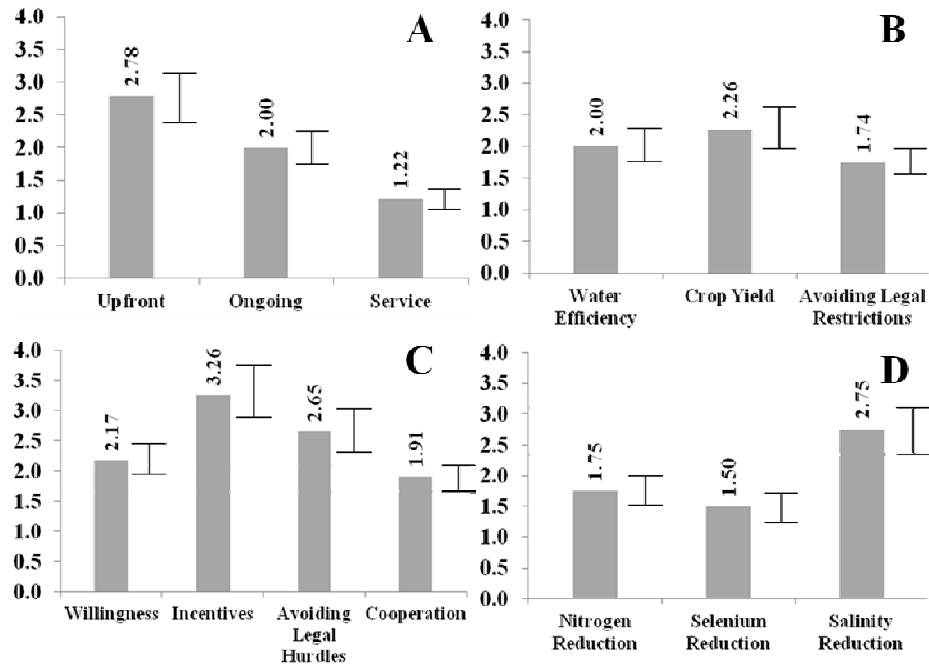


Figure 3-34. Average sub-criteria ranks with error bars associated with a 95% confidence interval.

It appears that reduced irrigation was the most preferred BMP among stakeholders, but based on the MOE, reduced fertilization could also be ranked first. There was significant overlap in the MOE for the reduced fertilization, canal sealing, and land fallowing BMPs, making it difficult to discern individual ranks for these BMPs. The enhanced riparian buffer BMP appears to be the least preferred among stakeholders in the LARV, although there is slight overlap between its MOE and that of canal sealing. The enhanced riparian buffer BMP also ranked the lowest with respect to each of the main criteria. The average final ranks of the BMPs are shown in Figure

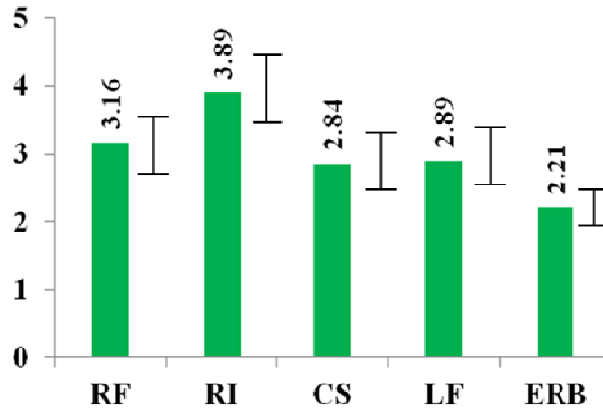


Figure 3-35. Average BMP ranks with error bars associated with a 95% confidence interval.

Adding value to use of the AHP MCDA method is the traceability that it provides with respect to the final ranks of alternatives. Figure 3-36 illustrates an example of how the final ranking of the reduced irrigation and enhanced riparian buffer BMPs can be traced through each phase of the AHP.

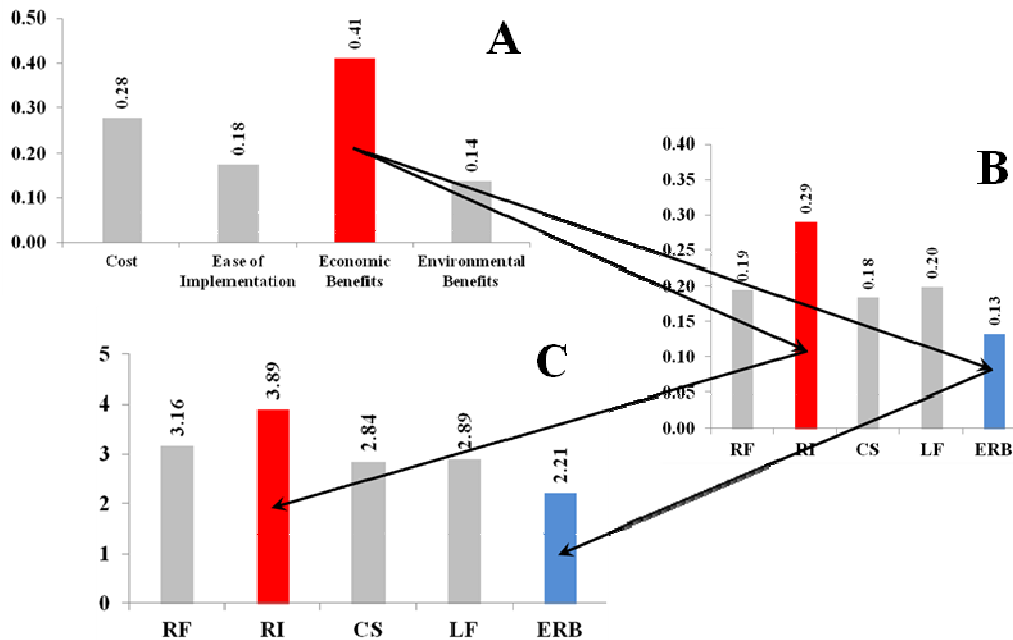


Figure 3-36. Example of traceability for the reduced irrigation and enhanced riparian buffer BMPs showing (A) relative importance of main criteria, (B) average BMP ranks with respect to economic benefits, and (C) the average overall BMP ranks.

As shown in Figure 3-36 A, economic benefits was the most important main criterion to stakeholders. Figure 3-36 B shows that reduced irrigation was the most preferred BMP with respect to economic benefits while enhanced riparian buffer was the least preferred. The fact that reduced irrigation was the most preferred and enhanced riparian buffer was the least preferred BMP, respectively, in regard to the main criteria that carried the most weight, resulted in reduced irrigation being ranked higher on average than enhanced riparian buffer.

CHAPTER 4: Conclusion

In high concentrations, Se can pose a number of environmental risks including birth and developmental defects in aquatic fauna. Criteria established both on a state and federal level have set guidelines for in-stream Se concentrations which should not be exceeded due to these environmental risk factors. One of the most significant challenges in reducing in-stream Se concentrations is that Se occurs naturally in alluvial formations across much of the Western United States. In areas with high levels of irrigated agricultural activity, the naturally occurring process of mobilizing Se from the alluvium is accelerated, particularly in the presence of increased groundwater flux resulting from excess irrigation and elevated levels of NO_3 from fertilizer. As a result of these processes, surface waters in the LARV regularly exceed Colorado's aquatic life standard and all segments of the Lower Arkansas River are designated as "water quality limited" with respect to the Clean Water Act.

Because of high levels of Se in the LARV and the associated environmental risks, this study examined land and water BMPs aimed at reducing in-stream Se concentrations. The first step was to characterize the various forms of Se as they exist in surface water in a representative upstream study region (USR) of the LARV located near Rocky Ford, Colorado. A number of sampling events took place between 2006 and 2014. From these events, a number of conclusions regarding the speciation of Se in the LARV could be drawn. It was determined that dissolved SeO_4 was the dominant form of Se in the water column, accounting for approximately 80% of the total Se mass. This fraction is in line with other sampling studies conducted in the region. It also was observed that Se concentrations are consistently higher in the tributaries than in the main stem of the Arkansas River. The same was generally true for NO_3 and DO concentrations, being higher in the tributaries than in the River. Due to the inhibiting effects of NO_3 and DO on

the chemical reduction of SeO_4 and SeO_3 , these data suggested that the higher concentrations of Se in the tributaries were more likely to remain in more toxic, high valence forms.

A number of water quality constituents and parameters were measured during each sampling event, including ORP and pH. With an abundance of water quality data, it was possible to perform a statistical analysis to identify correlations between various forms of Se as well as between various forms of Se and other water quality constituents and parameters. This statistical analysis identified a number of statistically significant correlations between ORP and precipitated and organic Se, pH and sorbed SeO_4 and SeO_3 , and total dissolved Se and NO_3 , for example. All statistically significant correlations could be explained through known Se chemical processes. Sampling efforts in the LARV also included samples collected and analyzed for algae concentrations. Water samples were analyzed for suspended algae while sediment samples were analyzed for algae located within the top 10 – 20 mm of channel bed sediment. Algae sampling has scarcely ever been undertaken in the LARV, and there are few studies in the literature that involve sampling for algae in stream sediment at any other site.

With Se characterized through sampling, the focus shifted to the development of a model to predict changes in in-stream concentrations due to BMP implementation. Knowing that this would require a model calibration, a sensitivity analysis was performed on the steady state OTIS-QUAL2E-Se model to identify model parameters best suited for calibration. With sensitive parameters identified, the unsteady OTIS-QUAL2E-Se was used for calibration as it more closely reflected the hydrologic and chemical conditions in the LARV. Ultimately four parameters were used to sufficiently calibrate the model to observed data collected over the simulation period. However, there a disconnect was made apparent between simulated surface water and groundwater conditions as evidenced by the nature of predicted concentrations in the

tributaries, which are more hydraulically connected to the surrounding aquifer on a per unit volume basis than is the Arkansas River. As such, the need for a dynamic linkage between the OTIS-QUAL2E-Se surface water model and the RT3D groundwater model was demonstrated.

The initial run of the combined RT3D-OTIS model using default parameter values generally over predicted SeO_4 concentrations and under predicted NO_3 concentrations. Although incorporating parameter values from calibration of the OTIS-QUAL2E-Se model yielded improved results, it also was necessary to calibrate RT3D parameters. The combined RT3D-OTIS model ultimately was calibrated through the adjustment of in-stream chemical reduction rates of SeO_4 and SeO_3 , SeO_4 and SeO_3 sediment partition coefficients, riparian zone reduction rates of SeO_4 and NO_3 , and a NO_3 tailwater multiplication factor.

With a calibrated RT3D-OTIS model, it then was possible to use the model to examine the BMPs considered as part of this study. Reduced fertilization showed the most promising results, with reductions in SeO_4 and NO_3 in the River and tributaries. The results of the other three BMPs generally indicated increases in SeO_4 concentrations, likely attributed mostly to a simulated concentrating effect of SeO_4 in the groundwater adjacent to the Arkansas River and tributaries. Additionally, the SeO_4 concentrations often increased with an increase in the degree of RI, LF, and CS implementation. However, although the increases in in-stream SeO_4 concentrations can be explained through the simulated concentrating effect of SeO_4 in adjacent groundwater, the results of the water management BMPs showing an increase in in-stream SeO_4 concentration is generally unexpected. As such, to verify the results of the water management BMPs, possible deficiencies in the model and/or parameter values have to be ruled out as a possible explanation through future work. One interesting conclusion that could be drawn from the results of the water management BMPs was that the tributaries appear to be more impacted

by changes to surface runoff concentrations than the Arkansas River, as tributary flow rates are driven more by surface runoff than by lateral groundwater flows. The opposite is true for the Arkansas River, which appears to be affected more by changes in lateral groundwater flows than by surface runoff.

The final step in the assessment of the BMPs examined as part of this study was the AHP MCDA survey. Results from the survey of 25 stakeholders in the LARV highlighted the expected result that the primary concern of stakeholders in the LARV are economic in nature, with economic benefits and cost being ranked first and second, respectively, in terms of the most important main criteria. These results propagated through other portions of the survey results. Reduced irrigation was ranked first in preference amongst all other BMPs, with reduced fertilization ranked second. The reasons for these ranks were clear, as both of these BMPs were perceived by stakeholders to be the most beneficial from an economic standpoint. Stakeholders ranked environmental concerns last out of the four main criteria, and Se contamination was ranked last out of the three associated sub-criteria. Salinity was ranked first of the environmental concern sub-criteria, likely due to the well-known impacts of salinity on crop yield and therefore on the income of the stakeholder. The enhancing riparian buffer zone BMP was ranked last out of the five considered BMPs. The results of this survey suggested that if a particular BMP is to be implemented, its positive impacts on the economic well-being of stakeholders must be emphasized over environmental benefits, and that stakeholders are likely to require incentives to implement a BMP.

With RT3D-OTIS model results predicting changes in in-stream concentrations in the LARV associated with the BMPs, and AHP survey results providing insight into the socio-economic feasibility of those BMPs, it was possible to examine the BMPs from both

perspectives to determine which was likely the best option for the LARV. It could be reasonably inferred from the results here that reduced fertilization is the single best BMP examined, as it was the second most preferred according the AHP survey and it was the only BMP to show consistent reductions in in-stream SeO_4 and NO_3 concentrations. Also, canal sealing is likely the worst alternative based on the results of presented here, as it resulted in the highest overall increases in SeO_4 concentrations and it was among the lower ranked BMPs according to the AHP survey. However, despite the conclusions inferred by these results, the margins of error associated with the AHP survey results in combination with the potential for deficiencies in the model and/or parameter values allows for the possibility that other BMPs are most suitable for implementation. Given the questionable reliability of the model results as discussed in Section 3.2.6 in conjunction with the margins of error discussed in Section 3.3, further work is needed to determine a hierarchy of BMP environmental efficacy and socio-economic feasibility.

In summary, this study helped quantify the nature and extent of Se in a representative region in the LARV and to establish this region as environmentally threatened and worthy of future research ancillary to Se remediation. This study initiated a coupled surface water-groundwater modeling effort that is currently being carried on to model the environmental effectiveness of various BMPs. This study was also the first to incorporate MCDA, particularly the AHP, into a sampling and modeling study in the region to help rank BMPs not based solely on modeled-predicted remedial effectiveness but also on socio-economic feasibility. Future work should include modeling various combinations of BMPs, as various combinations of BMPs with varying magnitudes are more likely to be implemented in the LARV than a single BMP. Although enhanced riparian buffers was included in the AHP survey, it was not modeled as part of this study as it was unclear how to model progressive enhancements to riparian buffers that

would occur over the simulation period. Future modeling work should examine enhanced riparian buffers. The model also should be further amended under the assumption that these BMPs are likely to be implemented not just in the USR, but in agricultural regions upstream of the USR that affect Arkansas River concentrations entering at the upstream end of the river system. Further work is also needed in testing the computational processes and parameter values of the RT3D-OTIS model.

APPENDIX A: Supplementary Information

Table A-1. Baseline and stressed parameter values used in the OTIS-QUAL2E-Se SA.

Model Parameter	Symbol	Units	Baseline Value	Stressed Value
Upstream concentration of SeO ₄	$C_{U_{SeO_4}}$	µg/L	12	120
Upstream concentration of SeO ₃	$C_{U_{SeO_3}}$	µg/L	0.5	5
SeO ₄ concentration of lateral flow	$C_{L_{SeO_4}}$	µg/L	10	100
SeO ₃ concentration of lateral flow	$C_{L_{SeO_3}}$	µg/L	0.5	5
Rate constant for SeO ₄ sorption to sediment	$\lambda_{SorbSeO_4}$	sec ⁻¹	0.000056	0.00056
Mass accessible sediment per unit volume of water for SeO ₄ sorption	$\rho_{SorbSeO_4}$	g/m ³	4000	40000
SeO ₄ partition coefficient in sediment	Kd_{SeO_4}	L/kg	1.43x10 ⁷	1.43x10 ⁸
Rate constant for SeO ₃ sorption to sediment	$\lambda_{SorbSeO_3}$	sec ⁻¹	0.000056	0.00056
Mass accessible sediment per unit volume of water for SeO ₃ sorption	$\rho_{SorbSeO_3}$	g/m ³	4000	40000
SeO ₃ partition coefficient in sediment	Kd_{SeO_3}	L/kg	1.43x10 ⁷	1.43x10 ⁸
Rate constant for the chemical reduction of SeO ₄ to SeO ₃	λ_{SeO_4}	day ⁻¹	0.2	2
Rate constant for the volatilization of SeO ₄ to species such as dimethylselenide	$\lambda_{SeO_4}^{vol}$	day ⁻¹	0.05	0.5
Rate constant for the chemical reduction of SeO ₃ to Se ⁰	λ_{SeO_3}	day ⁻¹	0.1	1
Rate constant for the volatilization of SeO ₃	$\lambda_{SeO_3}^{vol}$	day ⁻¹	0.05	0.5
Rate constant for the assimilation of selenite to SeMet	$\lambda_{SeO_3}^{assim}$	day ⁻¹	0.005	0.05
Rate constant for the conversion of volatile Se species to Se ²⁻	$\lambda_{Se_{vol}}$	day ⁻¹	0.05	0.5
Fraction of algal biomass that can be converted to SeMet	α_{Se}^{SeMet}	mg Se / mg algal biomass	0.00005	0.0005
Algal preference factor for SeO ₄	f_{SeO_4}	-	0.8	8
Inhibition term of nitrate for selenium reduction	I_{NO_3}	mg NO ₃ / L	1.3	13
Lateral inflow rate	q_L	m ³ /day/m	0.000027515	0.00027515
Dispersion coefficient	D	m ² /day	0.5	5
Upstream concentration of algae	$C_{U_{Alg}}$	mg/L	1.5	15
Ratio of chlorophyll a to algal biomass	ai_0	µg chla / mg alg	50	500
Non-algal portion of the light extinction coefficient	k_{Alg_0}	m ⁻¹	1	10
Linear algal self-shading coefficient	k_{Alg_1}	m ⁻¹ (ug chla / L) ⁻¹	0.03	0.3
Non-linear algal self-shading coefficient	k_{Alg_2}	m ⁻¹ (ug chla / L) ²	0.054	0.54
Maximum specific algal growth rate	$\lambda_{Alg_{max}}$	day ⁻¹	2	20
Local algal respiration rate	$\lambda_{Alg_{resp}}$	day ⁻¹	0.5	5
Solar radiation fraction that is photosynthetically active	fr_{phos}	-	0.3	3
Local algal settling rate	σ_{Alg}	m / day	1	10
Half-saturation coefficient for light	K_{light}	MJ / (m ² day)	3.2	32
DO concentration of Lateral Flow	$C_{L_{DO}}$	mg/L	7	70

Table A-2. Water quality data collected from locations in the Arkansas River and its tributaries from 2006-2010.

Sample Location	Sample Date	DO (mg/L)	NO ₃ (mg/L)	Total Se (µg/L)	Dissolved SeO ₄ ** (µg/L)	Dissolved SeO ₃ * (µg/L)	
ARK 164	6/13/2006	7.54	2.6	3.82	3.14	0.68	
	5/15/2007	9.87	1.2	5.47	4.49	0.98	
	10/6/2007	9.7	1.2	8.46	6.95	1.51	
	3/17/2008	9.55	1.7	10.20	8.37	1.83	
	6/21/2008	7.86	0.5	3.63	2.98	0.65	
	8/14/2008	7.41	0.9	4.28	3.51	0.77	
	1/15/2009	13.15	2.8	13.90	11.41	2.49	
	5/13/2009	8.56	1.1	7.17	5.89	1.28	
	7/21/2009	9.38	1	5.58	4.58	1.00	
	11/19/2009	12.36	2.2	11.40	9.36	2.04	
	3/12/2010	9.23	2.3	10.60	8.70	1.90	
	5/14/2010	7.18	1.3	9.22	7.57	1.65	
	ARK 167	6/13/2006	7.4	0.9	4.38	3.60	0.78
		5/15/2007	9.76	2.1	5.89	4.84	1.05
10/6/2007		9.79	1.4	9.74	8.00	1.74	
3/17/2008		9.51	1.7	11.00	9.03	1.97	
6/21/2008		8.08	0.6	3.87	3.18	0.69	
8/14/2008		7.52	1.1	5.24	4.30	0.94	
1/15/2009		13.32	2.9	13.30	10.92	2.38	
5/13/2009		8.74	1.2	8.10	6.65	1.45	
7/21/2009		7.56	1.2	7.31	6.00	1.31	
11/19/2009		12.46	2.3	11.70	9.61	2.09	
3/12/2010		9.15	NS	NS	NS	NS	
5/14/2010		7.22	1.4	9.80	8.05	1.75	
Patterson Hollow		6/20/2006	3.39	NS	5.29	4.34	0.95
		5/24/2007	15.12	0.8	53.20	43.68	9.52
	10/11/2007	9.18	2.6	5.62	4.61	1.01	
	3/20/2008	15.49	0.6	22.40	18.39	4.01	
	6/26/2008	6.87	0.8	4.26	3.50	0.76	
	8/14/2008	8.13	3.2	7.89	6.48	1.41	
	1/17/2009	15.11	0.1	6.04	4.96	1.08	
	5/14/2009	7.29	1.3	7.50	6.16	1.34	
	7/22/2009	17.56	0.3	5.90	4.84	1.06	
	ARK 141	6/13/2006	7.21	1.5	4.62	3.79	0.83
5/15/2007		9.79	2.3	5.88	4.83	1.05	
10/6/2007		9.74	1.4	9.43	7.74	1.69	
3/17/2008		9.27	1.7	11.80	9.69	2.11	
6/21/2008		7.99	0.4	3.76	3.09	0.67	
8/14/2008		7.53	0.9	5.01	4.11	0.90	
1/15/2009		13.74	2.5	14.20	11.66	2.54	
5/13/2009		8.53	0.9	7.57	6.22	1.35	
7/21/2009		8.12	0.9	6.40	5.25	1.15	
11/19/2009		11.22	2.4	12.60	10.34	2.26	
3/12/2010		13.01	2.1	11.40	9.36	2.04	
5/14/2010		7.75	0.6	6.88	5.65	1.23	
ARK 12		6/13/2006	7.44	1.4	4.47	3.67	0.80
		5/15/2007	9.3	0.8	6.16	5.06	1.10
	10/6/2007	9.55	1.2	9.02	7.41	1.61	
	3/17/2008	9.39	2.2	12.50	10.26	2.24	
	6/21/2008	7.87	0.5	3.80	3.12	0.68	
	8/14/2008	7.56	0.7	4.48	3.68	0.80	
	1/15/2009	13.61	2.6	13.50	11.08	2.42	
	5/13/2009	8.66	0.9	7.46	6.12	1.34	
	7/21/2009	9.24	0.6	5.14	4.22	0.92	
	11/19/2009	11.95	2.3	11.00	9.03	1.97	
	3/12/2010	12.86	2.3	11.20	9.20	2.00	
	5/14/2010	7.42	0.9	NS	NS	NS	

Timpas Creek 2	6/20/2006	7.34	3.2	9.29	7.63	1.66	
	5/24/2007	8.85	1.5	8.55	7.02	1.53	
	10/11/2007	9.61	2.4	13.80	11.33	2.47	
	3/20/2008	9.16	3.1	14.60	11.99	2.61	
	6/26/2008	7.07	1.9	8.54	7.01	1.53	
	8/14/2008	7.21	1.8	9.32	7.65	1.67	
	1/17/2009	13.68	4.3	20.30	16.67	3.63	
	5/14/2009	8.96	2.4	12.20	10.02	2.18	
	7/22/2009	8.38	2.2	10.60	8.70	1.90	
	11/20/2009	11.28	4.4	21.40	17.57	3.83	
	3/20/2010	11.63	2.4	11.90	9.77	2.13	
	5/16/2010	7.02	2.9	13.00	10.67	2.33	
	ARK 127	6/13/2006	7.4	0.8	5.01	4.11	0.90
		5/15/2007	9.12	1.2	6.30	5.17	1.13
10/6/2007		9.62	1.6	10.10	8.29	1.81	
3/17/2008		9.31	2	13.40	11.00	2.40	
6/21/2008		7.45	0.9	3.84	3.15	0.69	
8/14/2008		7.48	1.4	5.18	4.25	0.93	
1/15/2009		13.61	3.1	16.10	13.22	2.88	
5/13/2009		8.58	1	7.86	6.45	1.41	
7/21/2009		8.79	0.6	5.31	4.36	0.95	
11/19/2009		11.33	3	15.60	12.81	2.79	
3/12/2010		12.3	2.2	11.00	9.03	1.97	
5/14/2010		6.97	1.3	8.62	7.08	1.54	
Crooked Arroyo 2		5/24/2007	8.53	1.2	7.84	6.44	1.40
		10/11/2007	9.65	2.2	10.90	8.95	1.95
	3/20/2008	9.14	2.5	12.60	10.34	2.26	
	6/26/2008	7.29	1.3	8.98	7.37	1.61	
	8/14/2008	7.46	2.4	19.60	16.09	3.51	
	1/17/2009	14.63	3.9	14.60	11.99	2.61	
	5/14/2009	10.65	1.8	10.20	8.37	1.83	
	7/22/2009	9.48	2	9.37	7.69	1.68	
	11/20/2009	12.56	3.1	13.40	11.00	2.40	
	3/20/2010	11.92	1.9	11.00	9.03	1.97	
	5/16/2010	7.36	2.5	9.97	8.19	1.78	
	Anderson Creek	3/20/2008	10.47	0.1	20.20	16.58	3.62
		6/26/2008	6.68	1.5	6.94	5.70	1.24
		8/14/2008	8.39	1.4	12.90	10.59	2.31
5/14/2009		12.6	0.3	11.10	9.11	1.99	
7/22/2009		8.92	1.7	14.70	12.07	2.63	
11/20/2009		15.06	1.4	14.90	12.23	2.67	
3/19/2010		12.01	1	9.32	7.65	1.67	
5/16/2010		8.06	0.6	12.80	10.51	2.29	
ARK 95		6/13/2006	7.25	0.9	5.24	4.30	0.94
		5/15/2007	9.03	1.1	6.72	5.52	1.20
		10/6/2007	9.7	1.4	8.86	7.27	1.59
		3/17/2008	8.87	2.7	14.90	12.23	2.67
		6/21/2008	7.01	0.7	4.88	4.01	0.87
		8/14/2008	7.03	1.1	5.85	4.80	1.05
	1/15/2009	12.62	2.9	15.10	12.40	2.70	

5/13/2009	8.31	1.3	8.64	7.09	1.55
7/21/2009	8.01	1.1	6.88	5.65	1.23
11/19/2009	11.39	2.8	13.90	11.41	2.49
3/12/2010	11.36	2.5	12.40	10.18	2.22
5/14/2010	7.55	7.2	8.46	6.95	1.51

*Dissolved SeO₄ was estimated as approximately 82% of total selenium, which was directly measured (based on average fractions observed in data collected from 2011-2014 (see Table A-3)). ** Dissolved SeO₃ was estimated above as approximately 18% of total dissolved selenium, and was measured directly from 2011-2014 (see Table A-3).

Table A-3. Sediment and associated water quality selenium data collected from locations in the Arkansas River and its tributaries from 2011-2014.

Sample Location	Sample Date	Selenium in the Water Column			Selenium in Sediment		
		Total Se (µg/L)	Dissolved SeO ₃ (µg/L)	Dissolved SeO ₄ * (µg/L)	Sorbed SeO ₃ (µg/g)	Sorbed SeO ₄ ** (µg/g)	Precipitated and Organic Se*** (µg/g)
ARK Cat.	1/3/2011	NS	NS	NS	0.01	0.01	0.13
ARK 164	3/13/2013	13.80	1.69	12.11	0.09	0.09	0.77
	6/19/2013	6.64	2.05	4.59	0.08	0.05	0.63
	3/17/2014	13.00	1.36	11.64	0.01	0.03	0.16
Patterson Hollow	3/16/2013	19.00	1.26	17.74	0.10	0.22	0.86
	6/19/2013	11.70	2.36	9.34	0.17	0.10	1.20
	3/19/2014	21.10	0.90	20.21	0.10	0.09	0.63
ARK 141	3/16/2013	13.10	1.59	11.51	0.07	0.08	0.68
	6/19/2013	6.59	1.97	4.62	0.10	0.04	0.65
ARK 12	1/3/2011	NS	NS	NS	0.03	0.02	0.15
	3/16/2013	12.60	1.70	10.90	0.05	0.06	0.41
	6/19/2013	6.59	2.15	4.44	0.04	0.03	0.35
Timpas Creek 1	3/16/2013	20.70	1.23	19.47	0.18	0.14	1.02
	6/19/2013	9.89	1.99	7.90	0.33	0.15	1.39
Timpas Creek 2	3/16/2013	20.70	1.60	19.10	0.17	0.13	1.14
	6/19/2013	10.50	2.07	8.43	0.18	0.14	1.18
	3/17/2014	18.50	1.55	16.95	0.34	0.18	1.13
ARK 127	3/16/2013	12.80	0.85	11.96	0.07	0.06	0.41
	6/19/2013	7.14	1.88	5.26	0.08	0.07	0.60
	3/17/2014	13.40	1.25	12.15	0.01	0.03	0.18
Crooked Arroyo 1	3/16/2013	6.04	< 0.8	5.24	0.19	0.21	1.29
	6/19/2013	7.38	2.14	5.24	0.12	0.13	0.77
Crooked Arroyo 2	3/16/2013	8.27	< 0.8	7.47	0.20	0.13	1.18
	6/19/2013	7.07	2.00	5.07	0.40	0.19	1.46
	3/18/2014	19.20	1.14	18.06	0.62	0.23	1.76
ARK Crkd./And.	6/19/2013	6.85	2.48	4.37	0.12	0.06	0.45
Anderson Creek	3/16/2013	NS	NS	NS	0.13	0.17	1.35
	6/19/2013	NS	NS	NS	0.34	0.20	2.85
ARK 95	1/3/2011	NS	NS	NS	0.01	0.02	0.12
	3/16/2013	13.30	1.44	11.86	0.08	0.08	0.60
	6/19/2013	6.76	2.35	4.41	0.05	0.03	0.30
	3/18/2014	14.10	1.21	12.89	0.01	0.03	0.17
ARK King	6/19/2013	6.48	1.62	4.86	0.10	0.07	0.76
	8/21/2013	12.20	2.35	9.85	0.11	0.13	NA
ARK 162	3/16/2013	9.99	1.52	8.47	0.08	0.12	0.71
	6/19/2013	7.84	1.40	6.44	0.06	0.06	0.55
	8/21/2013	11.50	4.11	7.39	0.05	0.09	NA
ARK 209	3/16/2013	9.76	1.37	8.39	0.04	0.07	0.63
Horse Creek	1/3/2011	NS	NS	NS	0.35	0.16	0.49
	3/16/2013	11.40	2.25	9.15	0.49	0.18	1.77
	6/19/2013	8.17	3.37	4.80	0.28	0.10	1.41
	8/21/2013	11.20	2.66	8.54	0.03	0.08	NA
	3/19/2014	11.10	1.75	9.35	0.79	0.39	1.17

ARK 201	1/3/2011	<i>NS</i>	<i>NS</i>	<i>NS</i>	0.04	0.03	0.08
	3/16/2013	12.70	0.97	11.73	0.10	0.07	0.49
	6/19/2013	8.75	2.03	6.72	0.04	0.07	0.67
	8/21/2013	11.30	< 0.8	10.50	0.05	0.09	<i>NA</i>
	3/18/2014	13.60	< 0.8	12.80	0.01	0.05	0.22

*Dissolved SeO_4 was estimated as the difference between total dissolved selenium and SeO_3 . **Sorbed SeO_4 was estimated as the difference between total recoverable selenium and SeO_3 from the decanted 0.1 M K_2HPO_4 solution. ***Precipitated and organic selenium was estimated using the difference between the total selenium present in the sediment and the total recoverable selenium from the decanted 0.1 M K_2HPO_4 solution.

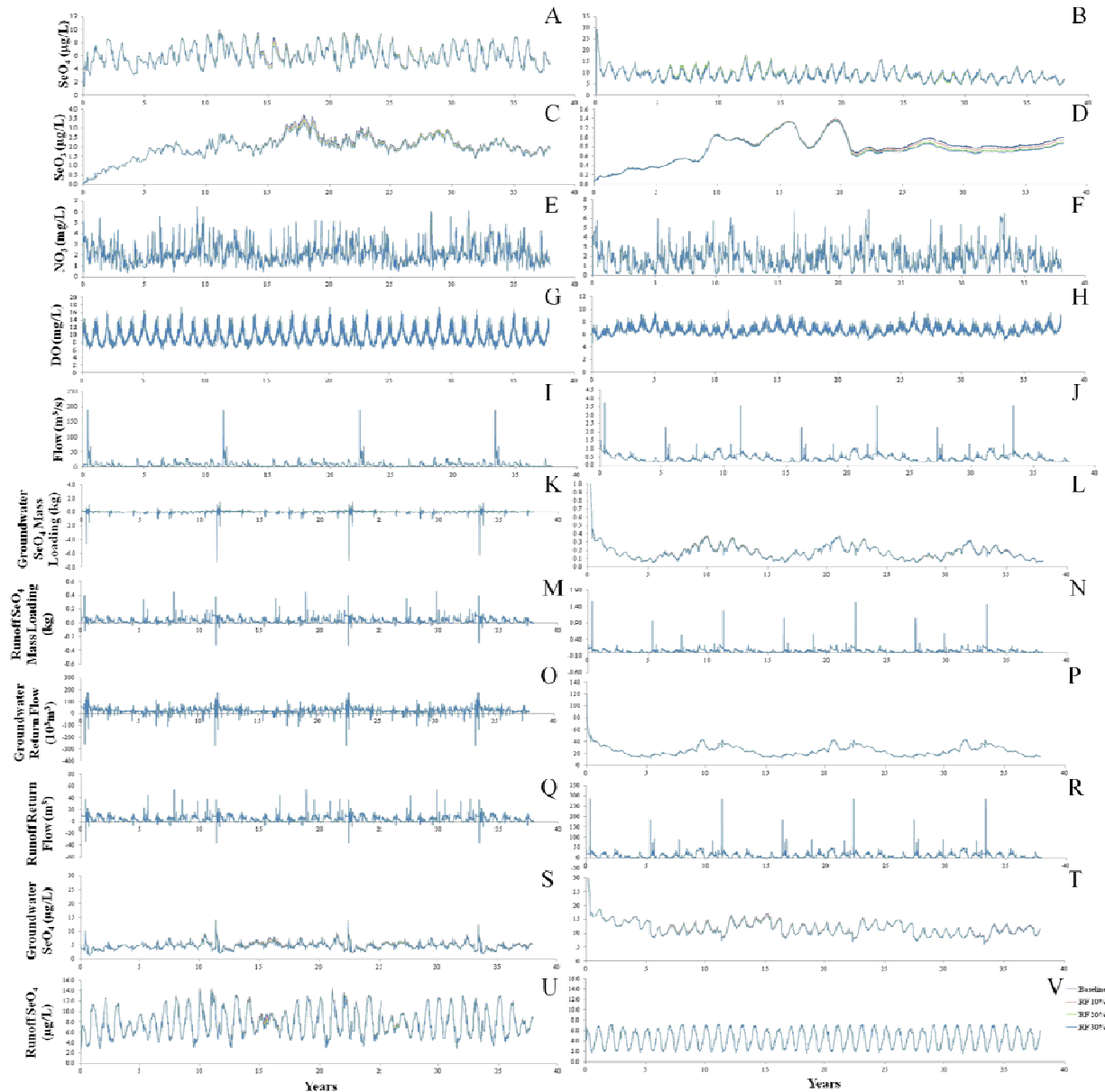


Figure A-1. Reduced fertilizer time series plots showing Baseline, RF10, RF20, and RF30 model output of dissolved SeO_4 in the (A) River and (B) tributaries, dissolved SeO_3 in the (C) River and (D) tributaries, NO_3 in the (E) River and (F) tributaries, DO in the (G) River and (H) tributaries, discharge in the (I) River and (J) tributaries, SeO_4 mass loading from groundwater along the (K) River and (L) tributaries, SeO_4 mass loading from surface runoff along the (M) River and (N) tributaries, return flow from groundwater along the (O) River and (P) tributaries, return flow from surface runoff along the (Q) River and (R) tributaries, SeO_4 concentration in groundwater return flow along the (S) River and (T) tributaries, and SeO_4 concentration in surface runoff return flow along the (U) River and (V) tributaries.

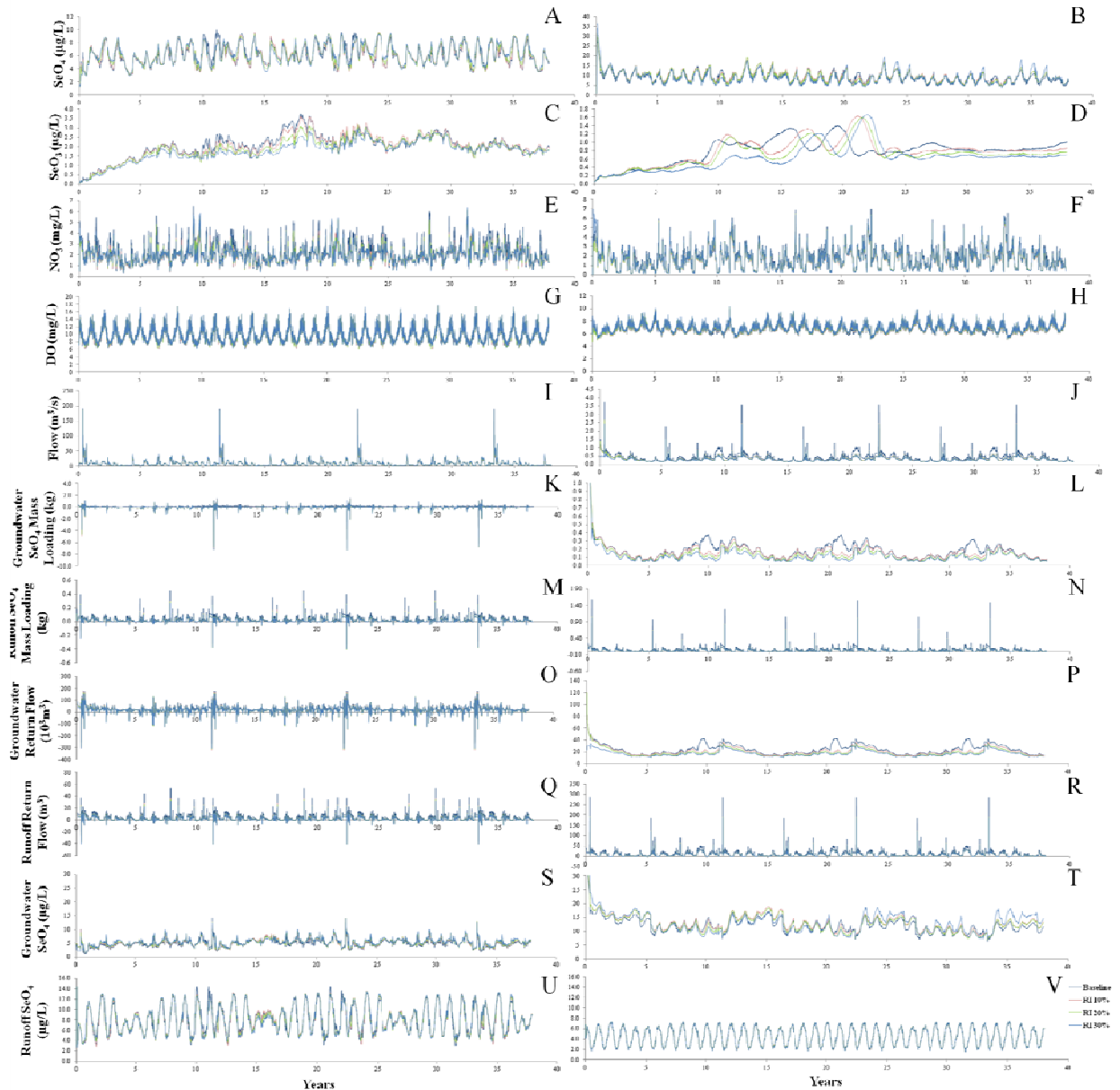


Figure A-2. Reduced irrigation time series plots showing Baseline, RI10, RI20, and RI30 model output of dissolved SeO_4 in the (A) River and (B) tributaries, dissolved SeO_3 in the (C) River and (D) tributaries, NO_3 in the (E) River and (F) tributaries, DO in the (G) River and (H) tributaries, discharge in the (I) River and (J) tributaries, SeO_4 mass loading from groundwater along the (K) River and (L) tributaries, SeO_4 mass loading from surface runoff along the (M) River and (N) tributaries, return flow from groundwater along the (O) River and (P) tributaries, return flow from surface runoff along the (Q) River and (R) tributaries, SeO_4 concentration in groundwater return flow along the (S) River and (T) tributaries, and SeO_4 concentration in surface runoff return flow along the (U) River and (V) tributaries.

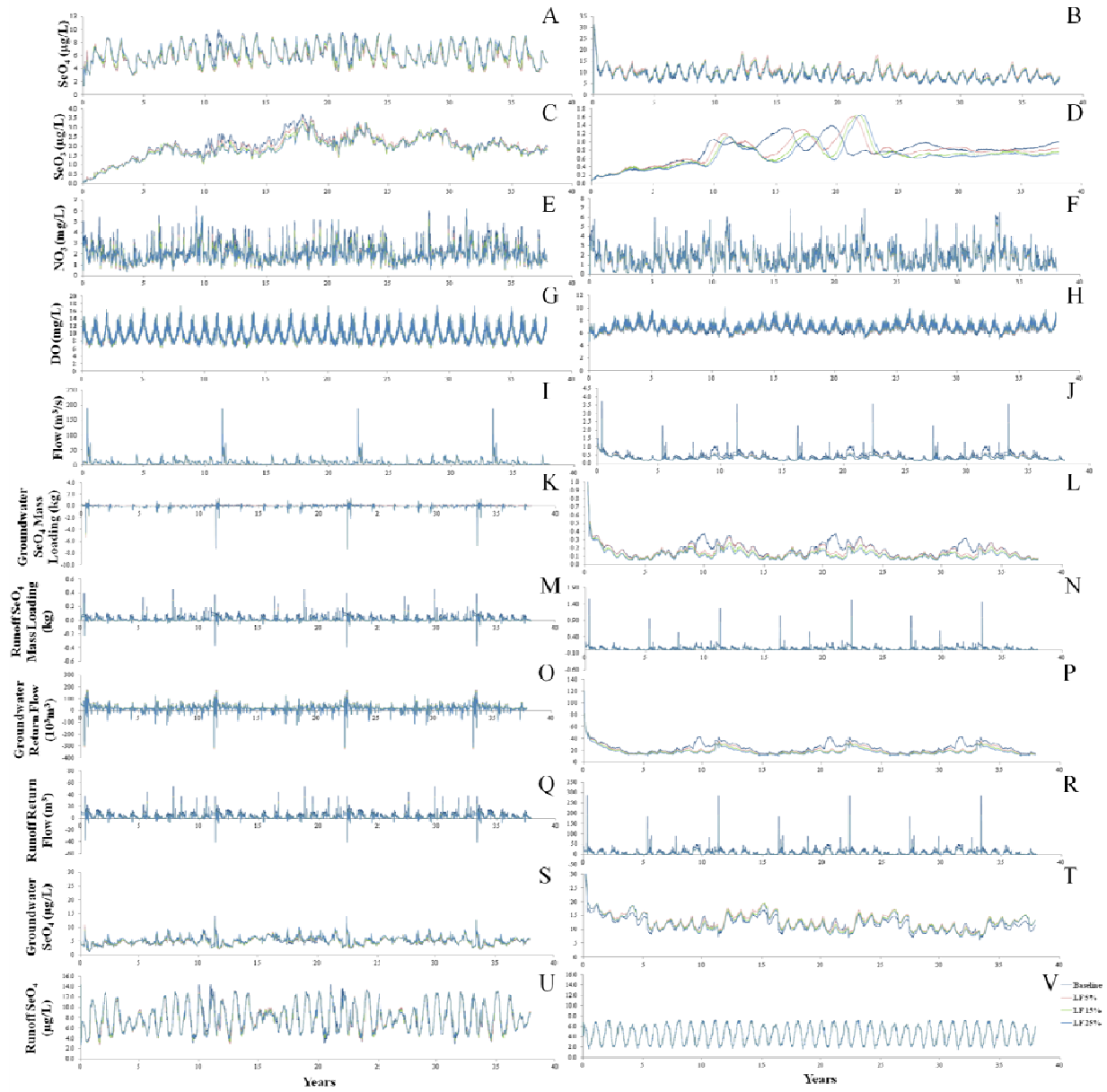


Figure A-3. Land following time series plots showing Baseline, LF5, LF15, and LF25 model output of dissolved SeO_4 in the (A) River and (B) tributaries, dissolved SeO_3 in the (C) River and (D) tributaries, NO_3 in the (E) River and (F) tributaries, DO in the (G) River and (H) tributaries, discharge in the (I) River and (J) tributaries, SeO_4 mass loading from groundwater along the (K) River and (L) tributaries, SeO_4 mass loading from surface runoff along the (M) River and (N) tributaries, return flow from groundwater along the (O) River and (P) tributaries, return flow from surface runoff along the (Q) River and (R) tributaries, SeO_4 concentration in groundwater return flow along the (S) River and (T) tributaries, and SeO_4 concentration in surface runoff return flow along the (U) River and (V) tributaries.

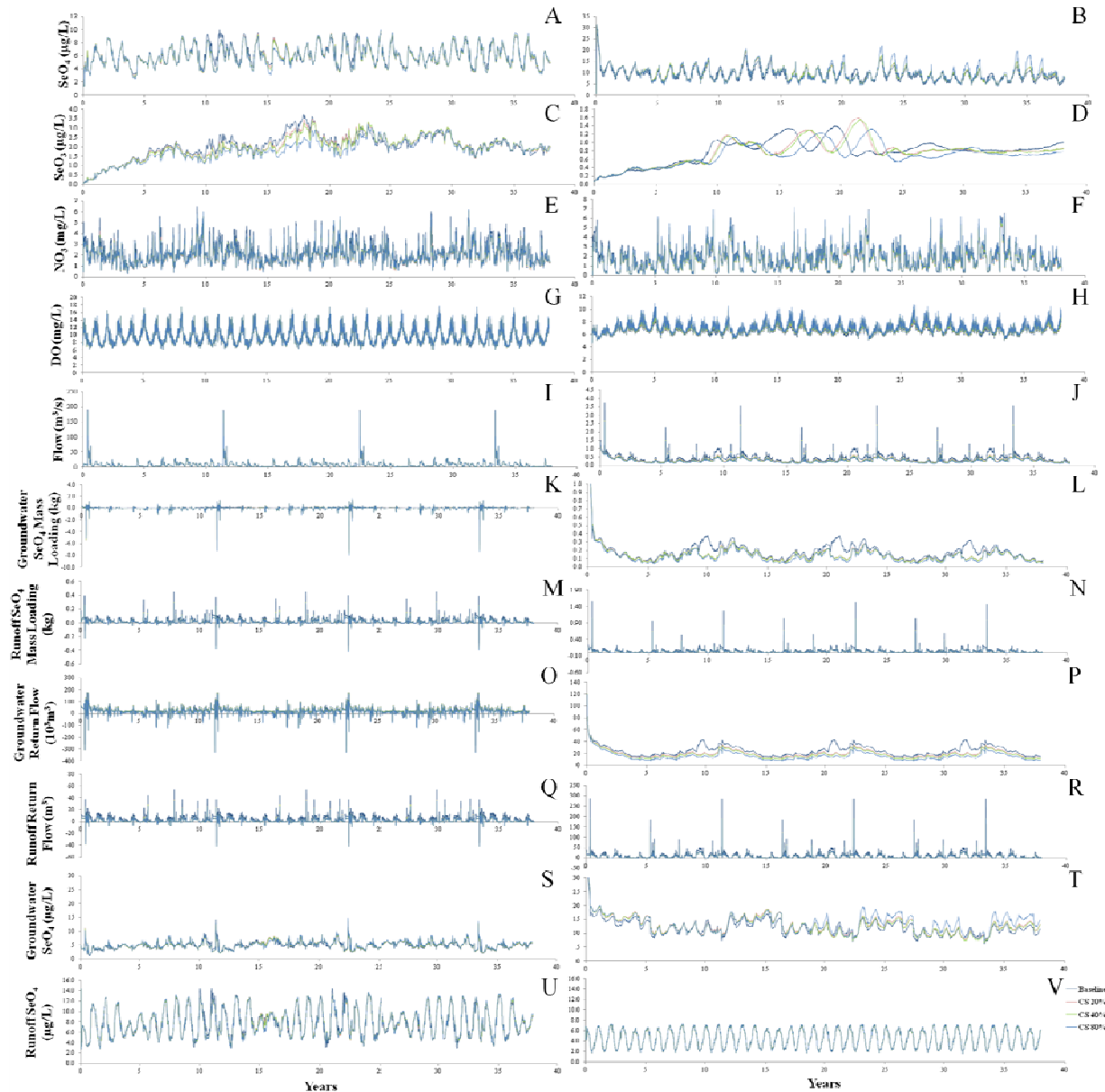


Figure A-4. Canal sealing time series plots showing Baseline, CS20, CS40, and CS80 model output of dissolved SeO_4 in the (A) River and (B) tributaries, dissolved SeO_3 in the (C) River and (D) tributaries, NO_3 in the (E) River and (F) tributaries, DO in the (G) River and (H) tributaries, discharge in the (I) River and (J) tributaries, SeO_4 mass loading from groundwater along the (K) River and (L) tributaries, SeO_4 mass loading from surface runoff along the (M) River and (N) tributaries, return flow from groundwater along the (O) River and (P) tributaries, return flow from surface runoff along the (Q) River and (R) tributaries, SeO_4 concentration in groundwater return flow along the (S) River and (T) tributaries, and SeO_4 concentration in surface runoff return flow along the (U) River and (V) tributaries.

REFERENCES

- Addiscott, T.M. and Mirza, N.A. (1998). Modelling contaminant transport at catchment or regional scale. *Journal of Agriculture, Ecosystems and Environment* 67, 211-221.
- Ahlich, S. and Hossner, L.R. (1987). Selenate and selenite mobility in overburden by saturated flow. *Journal of Environmental Quality* 16, 95-98.
- Ahrens, H. and Kantelhardt, J. (2007). Integrating ecological and economic aspects in land use concepts for agricultural landscapes. *German Journal of Agricultural Economics* 56(3), 166-174.
- Alemi, M.H., Goldhamer, D.A., and Nielsen, D.R. (1991). Modeling Selenium Transport in Steady-State, Unsaturated Soil Columns. *Journal of Environmental Quality* 20, 89-95.
- Allison, J.D. and Allison, T.L. (2005). Partition coefficients for metals in surface water, soil, and waste (EPA Publication No. 600/R-05/074). Athens, GA: National Exposure Research Laboratory.
- Almasri, M.N. and Kaluarachchi, J.J. (2007). Modeling nitrate contamination of groundwater in agricultural watersheds. *Journal of Hydrology* 343, 211-229.
- Almasri, M.N. and Kaluarachchi, J.J. (2005). Multi-criteria decision analysis for the optimal management of nitrate contamination of aquifers. *Journal of Environmental Management* (74), 365-381.
- Alphonse, C.B. (1997). Application of the Analytic Hierarchy Process in Agriculture in Developing Countries. *Agricultural Systems* 53, 97-112.
- Arar, E.J. and Collins, G.B. (1997). In Vitro Determination of Chlorophyll *a* and Pheophytin *a* in Marine and Freshwater Algae by Fluorescence (USEPA Method 445.0). National Exposure Research Laboratory, Office of Research and Development, USEPA.
- Azzellino, A., Salvetti, R., Vismara, R., and Bonomo, L. (2006). Combined use of the EPA-QUAL2E simulation model and factor analysis to assess the source apportionment of point and non point loads of nutrients to surface waters. *Journal of The Science of the Total Environment* 371, 214-222.
- Bailey, R.T., Hunter, W.J., and Gates, T.K. (2012). The influence of nitrate on selenium in irrigated agricultural groundwater systems. *Journal of Environmental Quality*.
- Bailey, R.T., Morway, E.D., Niswonger, R.G., and Gates, T.K. (2013). Modelign variably saturated multispecies reactive groundwater solute transport with MODFLOW-UZF and RT3D. *Journal of Groundwater* 51, 752-761.
- Bailey, R.T. and Ahmadi, M. (2014). Spatial and temporal variability of in-stream water quality parameter influence on dissolved oxygen and nitrate within a regional stream network. *Journal of Ecological Modelling* 277, 87-96.
- Bailey, R.T., Gates, T.K., and Ahmadi, M. (2014). Simulating reactive transport of selenium coupled with nitrogen in a regional-scale irrigated groundwater system. *Journal of Hydrology* 515, 29-46.

- Bailey, R.T., Romero, E.C., and Gates, T.K. (2015). Assessing best management practices for remediation of selenium loading in groundwater to streams in an irrigated region. *Journal of Hydrology* 521, 341-359.
- Baines, S.B., Fisher, N.S., Doblin, M.A., Cutter, G.A., Cutter, L.S., and Cole, B. (2004). Light dependence of selenium uptake by phytoplankton and implications for predicting incorporation into food webs. *Journal of Limnology and Oceanography* 49, 566-578.
- Balistrieri, L.S. and Chao, T.T. (1987). Selenium adsorption by Geothite. *Soil Science Society American Journal* 51, 1145-1151.
- Barnes, H.H. Jr. (1967). Roughness characteristics of natural channels. US Department of the Interior, US Geological Survey.
- Beck, M.B. (1987). Water quality modeling: a review of the analysis of uncertainty. *Journal of Water Resources Research* 23(8), 1393-1442.
- Behzadian, M., Kazemzadeh, R.B., Albadvi, A., and Aghdasi, M. (2010). PROMETHEE: A comprehensive literature review on methodologies and applications. *European Journal of Operational Research* 200, 198-215.
- Belton, V. (1986). A comparison of the analytic hierarchy process and a simple multi-attribute value function. *European Journal of Operational Research* 26(1), 7-21.
- Bencala, K.E. (1983). Simulation of solute transport in a mountain pool-and-riffle stream with a kinetic mass transfer model for sorption. *Journal of Water Resources Research* 19(3), 732-738.
- Bennett, W.N., Brooks, A.S., and Boraas, M.E. (1986). Selenium uptake and transfer in an aquatic food chain and its effects on fathead minor larvae. *Archives of Environmental Contamination and Toxicology* 15, 513-517.
- Boender, C. G. E., De Graan, J. G., and Lootsma, F. A. (1989). Multi-criteria decision analysis with fuzzy pairwise comparisons. *Fuzzy sets and Systems* 29(2), 133-143.
- Boyer, E.W., Alexander, R.B., Parton, W.J., Li, C., Butterbach-Bahl, K., Donner, S.D., Skaggs, R.W., and Del Grosso, S.J. (2006). Modeling denitrification on terrestrial and aquatic ecosystems at regional scales. *Journal of Ecological Applications* 16(6), 2123-2142.
- Brown, L.C. and Barnwell, T.O. (1987). The enhanced stream water quality models QUAL2E and QUAL2E-UNCAS: documentation and user manual, EPA/600/3-87/007. U.S. Environmental Protection Agency, Environmental Research Laboratory, Athens, GA.
- Buchleiter, G. W., H. J. Farahani, and L. R. Ahuja. Model evaluation of groundwater contamination under center pivot irrigated corn in eastern Colorado. *Proceedings of the International Symposium on Water Quality Modeling*. Orlando, Florida. 1995.
- Campolongo, F. and Saltelli, A. (1997). Sensitivity analysis of an environmental model: an application of different analysis methods. *Journal of Reliability Engineering and System Safety* 57, 49-69.
- Canton, S.P. and Van Derveer, W.D. (1997). Selenium toxicity to aquatic life: an argument for sediment-based water quality criteria. *Journal of Environmental Toxicology and Chemistry* 16(6), 1255-1259.

- Chow, A., Tanji, K., and Gao, S. (2004). Modeling drainwater selenium removal in wetlands. *Journal of Irrigation and Drainage Engineering* 130(1), 60-69.
- Chaplot, V., Saleh, A., Jaynes, D.B., and Arnold, J. (2004). Predicting Water, Sediment and NO₃-N Loads Under Scenarios of Land-Use and Management Practices in a Flat Watershed. *Water, Air, and Soil Pollution* 154, 271-293.
- Chapman, P.M., Adams, W.J., Brooks, M.L., Delos, C.G., Luoma, S.N., Maher, W.A., Ohlendorf, H.M., Presser, T.S., and Shaw, D.P. (2010). Ecological assessment of selenium in the aquatic environment. Society of Environmental Toxicology and Chemistry (SETAC). Pensacola, FL.
- Chapra, S.C. (1997). Surface water-quality modeling. McGraw-Hill Companies, Inc.; Singapore.
- Chapra, S.C., Pelletier, G.J., and Tao, H. (2008). QUAL2K: a modeling framework for simulating river and stream water quality, version 2.11: documentation and user manual. Civil and Environmental Engineering Dept., Tufts University, Medford, MA.
- Ciotti, D.C. (2005). Water Quality of Runoff from Flood Irrigated Pasture in the Klamath Basin, Oregon. A thesis submitted to Oregon State University.
- Conan, C., Bouraoui, F., Turpin, N., de Marsily, G., and Bidoglio, G. (2003). Modeling Flow and Nitrate Fate at Catchment Scale in Brittany (France). *Journal of Environmental Quality* (32), 2026-2032.
- Conde, J.E. and Alaejos, M.S. (1997). Selenium concentrations in natural environmental waters. *Chem. Rev.* 97, 1979-2003.
- Cooke, T.D. and Bruland, K.W. (1987). Aquatic chemistry of selenium: evidence of biomethylation. *Journal of Environmental Science Technology* 21, 1214-1219.
- Cooper, B.A. (1990). Nitrate depletion in the riparian zone and stream channel of a small headwater catchment. *Hydrobiologia* 202, 13-26.
- Cox, B.A. and Whitehead, P.G. (2005). Parameter sensitivity and predictive uncertainty in a new water quality model, Q². *Journal of Environmental Engineering* 131, 147-157.
- Cutter, G.A. (1989). The Estuarine Behaviour of Selenium in San Francisco Bay. *Estuarine, Coastal and Shelf Science* 28, 13-34.
- Davies, A.L., Bryce, R., and Redpath, S.M. (2013). Use of Multicriteria Decision Analysis to Address Conservation Conflicts. *Conservation Biology* 27(5), 936-944.
- DeSteiguer, J.E., Duberstein, J., Lopes, V. (2003). The analytic hierarchy process as a means for integrated watershed management. Kenneth G. Renard First Interagency Conference on Research on the Watershed, 736-740.
- Dooley, A.E., Smeaton, D.C., Sheath, G.W., and Ledgard, S.F. (2009). Application of Multiple Criteria Decision Analysis in the New Zealand Agricultural Industry. *Journal of Multi-Criteria Decision Analysis* 16, 39-53.
- Dzombak, D.A. and Morel, F.M.M. Surface Complexation Modeling: Hydrous Ferric Oxide. John Wiley & Sons, 1990.
- Ellis, D.R. and Salt, D.E. (2003). Plants, selenium, and human health. *Current Opinion in Plant Biology* 6(3), 273-279.

- Fernandez-Martinez, A. and Charlet, L. (2009). Selenium environmental cycling and bioavailability: a structural chemist point of view. *Journal of Environmental Science and Biotechnology* 8, 81-110.
- Frind, E.O., Duynisveld, W.H., Strelbel, O., and Boettcher, J. (1990). Modeling of Multicomponent Transport with Microbial Transformation in Groundwater: The Fuhrberg Case. *Water Resources Research* 26(8), 1707-1719.
- Gao, S., Tanji, K.K., Peters, D.W., and Herbel, M.J. (2000). Water Selenium Speciation and Sediment Fractionation in a California Flow-Through Wetland System. *Journal of Environmental Quality* 29, 1275-1283.
- Gao, S., Tanji, K.K., Lin, Z.Q., Terry, N., and Peters, D.W. (2003). Selenium Removal and Mass Balance in a Constructed Flow-Through Wetland System. *Journal of Environmental Quality* 32(4), 1557-1570.
- Gates, T. K., Cody, B. M., Herting, A. W., Donnelly, J. P., Bailey, R. T., and Mueller Price, J. (2009). Assessing selenium contamination in the irrigated stream-aquifer system of the Arkansas River, Colorado. *Journal of Environmental Quality*, 38(6): 2344 – 2356.
- Gates, T. K., Steed, G. H., Niemann, J. D., and Labadie, J. W. (2016). Data for improved water management in Colorado's Arkansas River Basin: Hydrological and water quality studies. Colorado Water Institute Special Report No. 24, Colorado State University, Fort Collins, CO.
- Gerla, P.J., Sharif, M.U., and Korom, S.F. (2011). Geochemical processes controlling the spatial distribution of selenium in soil and water, west central South Dakota. *Journal of Environmental Earth Science* 62, 1551-1560.
- Guitouni, A. and Martel, J.M. Some Guidelines for Choosing an MCDA Method Appropriate to a Decision Making Context. *Faculté des sciences de l'administration de l'Université Laval, Direction de la recherche*, 1997.
- Guitouni, A. and Martel, J.M. (1998). Tentative guidelines to help choosing an appropriate MCDA method. *European Journal of Operational Research* 109, 501-521.
- Guo, L., Frankenberger, W.T. Jr., Jury, W.A. (1999). Evaluation of simultaneous reduction and transport of selenium in saturated soil columns. *Water Resources Research* 35(3), 663-669.
- Hajkovicz, S. and Collins, K. (2007). A Review of Multiple Criteria Analysis for Water Resources Planning and Management. *Water Resources Management* 21, 1553-1566.
- Hamalainen, R. P., Kettunen, E., and Ehtamo, H. (2001). Evaluating and Framework for Multi-Stakeholder Decision Support in Water Resources Management. *Group Decision and Negotiation* 10, 331-353.
- Hamby, D.M. (1994). A review of techniques for parameter sensitivity analysis of environmental models. *Journal of Environmental Monitoring and Assessment* 32, 135-154.
- Hamer, C.E., Halbert, B.E., Webster, M., and Scharer, J.M. (2012). Assessment of model adequacy and parameter identifiability for predicting contaminant transport in the Beaverlodge Lake area, Canada. *Journal of Transactions on Ecology and the Environment* 164, 1743-3541.

- Hamilton, S.J. (2004). Review of selenium toxicity in the aquatic food chain. *Journal of the Science of the Total Environment* 326, 1-31.
- Hayashi, K. (2000). Multicriteria analysis for agricultural resource management: A critical survey and future perspectives. *European Journal of Operational Research* 122, 486-500.
- Heathwaite, A.L., Griffiths, P., and Parkinson, R.J. (1998). Nitrogen and phosphorus in runoff from grassland with buffer strips following application of fertilizers and manures. *Soil Use and Management* 14(3), 142-148.
- Hefting, M.M. and de Klein, J.J.M. (1998). Nitrogen removal in buffer strips along a lowland stream in the Netherlands: a pilot study. *Environmental Pollution* 102(1), 521-526.
- Hunsaker, C. T. and Levine, D.A. (1995). Hierarchical approaches to the study of water quality in rivers. *BioScience* 45(3), 193-203.
- Ivahnenko, T., Ortiz, R.F., and Stogner, R.W Sr. (2013). Characterization of Streamflow, Water Quality, and Instantaneous Dissolved Solids, Selenium, and Uranium Loads in Selected Reaches of the Arkansas River, Southeastern Colorado, 2009-2010. US Department of the Interior, US Geological Survey.
- Jacobs, T.C. and Gilliam, J.W. (1985). Riparian Losses of Nitrate from Agricultural Drainage Waters. *Journal of Environmental Quality* 14, 472-478.
- Kiker, G.A., Bridges, T.S., Varghese, A., Seager, T.P., and Linkov, I. (2005). Application of Multicriteria Decision Analysis in Environmental Decision Making. *Integrated Environmental Assessment and Management* 1(2), 95-108.
- Koontz, T.M. and Thomas, C.W. (2006). What Do We Know and Need to Know about the Environmental Outcomes of Collaborative Management? *Articles on Collaborative Management*, 111-121.
- Koontz, L., Hoag, D., and DeLong, D. (2012). Disparate Stakeholder Management: The Case of Elk and Bison Feeding in Southern Greater Yellowstone. *Society and Natural Resources* 0, 1-17.
- Lackey, G., Neupauer, R. M., and Pitlick, J. (2015). Effects of Streambed Conductance on Stream Depletion. *Water* (7) 271-287.
- Ledoux, E., Gomez, E., Monget, J.M., Viavattene, C., Viennot, P., Benoit, M., Mignolet, C., Schott, C., and Mary, B. (2007). Agriculture and groundwater nitrate contamination in the Seine basin. The STICS-MODCOU modeling chain. *Science of the Total Environment* 375(1-3), 33-47.
- Lee, M., Park, G., Park, M., Park, J., Lee, J., and Kim, S. (2010). Evaluation of non-point source pollution reduction by applying best management practices using a SWAT model and QuickBird high resolution satellite imagery. *Journal of Environmental Sciences* 22(6), 826-833.
- Lemly, A.D. (1999). Selenium transport and bioaccumulation in aquatic ecosystems: a proposal for water quality criteria based on hydrological units. *Journal of Ecotoxicology and Environmental Safety* 42, 150-156.

- Lin, Z.Q. and Norman, T. (2003). Selenium removal by constructed wetlands: quantitative importance of biological volatilization in the treatment of selenium-laden agricultural drainage water. *Environmental Science & Technology* 37(3), 606-615.
- Losi, M.E. and Frankenberger, W.T. Jr. (1998). Microbial oxidation and solubilization of precipitated elemental selenium in soil. *Journal of Environmental Quality* 27, 836-843.
- Ma, L., Nielsen, D. C., Ahuja, L. R., Malone, R. W., Saseendran, S. A., Rojas, K. W., and Benjamin, J. G. (2003). Evaluation of RZWQM under varying irrigation levels in eastern Colorado. *Transactions of the ASAE* 46(1), 39-49.
- Macharis, C., Springael, J., DeBrucker, K., and Verbeke, A. (2004). PROMETHEE and AHP: The design of operational synergies in multicriteria analysis. Strengthening PROMETHEE with ideas of AHP. *European Journal of Operational Research* 153, 307-317.
- MacKenzie, A.J. and Viets, F.G. (1974). Nutrients and Other Chemicals in Agricultural Drainage Waters. *Drainage for Agriculture*, 489-508.
- Martin, J.L. and Wool, T.A. (2002). A dynamic one-dimensional model of hydrodynamics and water quality (EPD-RIV1), version 1.0. Model documentation and user manual. Georgia Environmental Protection Division, Atlanta, GA.
- Masscheleyn, P.H., Delaune, R.D., and Patrick, W.H.Jr. (1989). Transformations of selenium as affected by sediment oxidation-reduction potential and pH. *Journal of Environmental Science and Technology* 24, 91-96.
- Masscheleyn, P.H. and Patrick, W.H. Jr. (1993). Biogeochemical processes affecting selenium cycling in wetlands. *Journal of Environmental Toxicology and Chemistry* 12, 2235-2243.
- McKnight, D.M., Hornberger, G.M., Bencala, K.E., and Boyer, E.W. (2002). In-stream sorption of fulvic acid in an acidic stream: a stream-scale transport experiment. *Journal of Water Resources Research* 38(1), 6-1 – 6-12.
- Miller, W.W., Guitlens, J.C., and Mahannah, C.N. (1977). Quality of Irrigation Water and Surface Return Flows from Selected Agricultural Land in Nevada During the 1974 Irrigation Season. *Journal of Environmental Quality* 6(2), 193-200.
- Miller, L.D., Watts, K.R., Ortiz, R.F., and Ivahnenko, T. (2010) Occurrence and Distribution of Dissolved Solids, Selenium, and Uranium in Groundwater and Surface Water in the Arkansas River Basin from the Headwaters to Coolidge, Kansas, 1970-2009. US Department of the Interior, US Geological Survey.
- Molenat, J. and Gascuel-Oudou, C. (2002). Modelling flow and nitrate transport in groundwater for the prediction of water travel times and of consequences of land use evolution on water quality. *Hydrological Processes* 16(2), 479-492.
- Moran, D., McVittie, A., Allcroft, D.J., and Elston, D.A. (2007). Quantifying public preferences for agri-environmental policy in Scotland: A comparison of methods. *Ecological Economics* 63, 42-53.
- Morari, F., Lugato, E., and Borin, M. (2004). An integrated non-point source model-GIS system for selecting criteria of best management practices in the Po Valley, North Italy. *Journal of Agriculture, Ecosystems and Environment* 102, 247-262.

- Morway, E.D., Gates, T.K., and Niswonger, R.G. (2013). Appraising options to reduce shallow groundwater tables and enhance flow conditions over regional scales in an irrigated alluvial aquifer system. *Journal of Hydrology* 495, 216-237.
- Myers, T. (2013). Remediation scenarios for selenium contamination, Blackfoot watershed, southeast Idaho, USA. *Hydrogeology Journal* 21, 655-671.
- Nolan, B.T. and Clark, M.L. (1997). Selenium in irrigated agricultural areas of the western United States. *Journal of Environmental Quality* 26, 849-857.
- Oram, L.L., Strawn, D.G., Marcus, M.A., Fakra, S.C., and Moller, G. (2008). Macro- and Microscales Investigation of Selenium in Blackfoot River, Idaho Sediments. *Environmental Science and Technology* 42(18), 6830-6836.
- Oremland, R.S., Hollibaugh, J.T., Maest, A.S., Presser, T.S., Miller, L.G., and Culbertson, C.W. (1989). Selenate reduction to elemental selenium by anaerobic bacteria in sediments and culture: biogeochemical significance of a novel, sulfate-independent respiration. *Applied and Environmental Microbiology* 55(9), 2333-2343.
- Oremland, R. S., Steinberg, N. A., Maest, A. S., Miller, L. G., and Hollibaugh, J. T. (1990), Measurement of in situ rates of selenate removal by dissimilatory bacterial reduction in sediments. *Environ. Sci. Technol.* 24:1157-1164.
- Peterjohn, W.T. and Correll, D.L. (1984). Nutrient Dynamics in an Agricultural Watershed: Observations on the Role of a Riparian Forest. *Ecology* 65(5), 1466-1475.
- Presser, T.S. and Luoma, S.N. (2010). A methodology for ecosystem-scale modeling of selenium. *Integrated Environmental Assessment and Management* 6(4), 685-710.
- Presser, T.S., Sylvester, M.A., and Low, W.H. (1994). Bioaccumulation of selenium from natural geologic sources in western states and its potential consequences. *Journal of Environmental Management* 18(3), 423-436.
- Prudic, D. E., Konikow, L.F, and Banta, E.R. (2004). A new Streamflow-Routing (SFR1) Package to simulate stream-aquifer interaction with MODFLOW-2000. US Department of the Interior, US Geological Survey.
- Rehmel, M. (2007). Application of Acoustic Doppler Velocimeters for Streamflow Measurements. *Journal of Hydraulic Engineering* 133(12), 1433-1438.
- Rezaei-Moghaddam, K. and Karami, E. (2008). A multiple criteria evaluation of sustainable agricultural development models using AHP. *Environmental Development and Sustainability* 10(4), 407-426.
- Riedel, G.F., Sanders, J.G., and Gilmour, C.C. (1996). Uptake, transformation, and impact of selenium in freshwater phytoplankton and bacterioplankton communities. *Journal of Aquatic Microbial Ecology* 11, 43-51.
- Rong, Y. and Xuefeng, W. (2011). Effects of nitrogen fertilizer and irrigation rate on nitrate present in the profile of a sandy farmland in Northwest China. *Procedia Environmental Sciences* 11, 726-732.
- Roy, B. and Vincke, P. (1981). Multicriteria analysis: survey and new directions. *European Journal of Operational Research* 8(3), 207-218.

- Runkel, R.L. (1998). One-dimensional transport with inflow and storage (OTIS): a solute transport model for streams and rivers: U.S. Geological Survey Water-Resources Investigation Report 98-4018.
- Runkel, R.L. and Broshears, R.E. (1991). One-dimensional transport with inflow and storage (OTIS): a solute transport model for small streams. University of Colorado Center for Advanced Decision Support for Water and Environmental Systems. Final Report.
- Runkel, R.L, McKnight, D.M., and Andrews, E.D. (1998). Analysis of transient storage subject to unsteady flow: diel flow variation in an Antarctic stream. *Journal of the North American Benthological Society* 17(2), 143-154.
- Saaty, R.W. (1987). The Analytic Hierarchy Process- What It Is and How It Is Used. *Mathematical Modeling* 9(3), 161-176.
- Saaty, T.S. (1990). How to make a decision: The Analytic Hierarchy Process. *European Journal of Operational Research* 48, 9-26.
- Sahu, M. and Gu, R.R. (2009). Modeling the effects of riparian buffer zone and contour strips in stream water quality. *Ecological Engineering* 35(8), 1167-1177.
- Saltelli, A., Tarantola, S., and Campolongo, F. (2000). Sensitivity analysis as an ingredient of modeling. *Journal of Statistical Science* 15(4), 377-395.
- Saltelli, A. (2002). Sensitivity analysis from importance assessment. *Journal of Risk Analysis* 22(3), 579-590.
- Shrestha, R.K., Alavalapati, J.R.R., and Kalmbacker, R.S. (2004). Exploring the potential for silvopasture adoption in south-central Florida: an application of SWOT-AHP method. *Agricultural Systems* 81, 185-199.
- Scott, G. R. (1968), Geologic and structure contour map of the La Junta quadrangle, Colorado and Kansas, edited by U. S. G. Survey, Reston, Virginia.
- Sharps, J. A. (1976), Geologic map of the Lamar quadrangle, Colorado and Kansas, edited by U. S. G. Survey, Reston, Virginia.
- Spruill, T.B. (2000). Statistical evaluation of effects of riparian buffers on nitrate and ground water quality. *Journal of Environmental Quality* 29(5), 1523-1538.
- Steele, K., Carmel, Y., Cross, J., and Wilcox, C. (2009). Uses and Misuses of Multicriteria Decision Analysis (MCDA) in Environmental Decision Making. *Risk Analysis* 29(1), 26-33.
- Stemberger, R.S. and Gilbert, J.J. (1985). Body size, food concentration, and population growth in planktonic rotifers. *Ecology* 66(4), 1151-1159.
- Stillings, L.L. and Amacher, M.C. (2010). Kinetics of selenium release in mine waste from the Meade Peak Phosphatic Shale, Phosphoria Formation, Wooley Valley, Idaho, USA. *Chemical Geology* 269, 113-123.
- Sugimura, Y., Suzuki, Y., and Miyake, Y. (1976). The content of selenium and its chemical form in sea water. *Journal of the Oceanographical Society of Japan* 32, 235-241.
- Susfalk, R., Sada, D., Martin, C., Young, M., Gates, T., Rosamond, C., Mihevc, T., Arrowood, T., Shanafield, M., Epstein, B., Fitzgerald, B., Lutz, A., Woodrow, J., Miller, G., and Smith,

- D. (2008). Evaluation of linear anionic polyacrylamide (LA-PAM) application to water delivery canals for seepage reduction. Desert Research Institute.
- Tayfur, G., Tanji, K.K., and Baba, A. (2010). Two-dimensional finite elements model for selenium transport in saturated and unsaturated zones. *Environmental Monitoring and Assessment* 169, 509-518.
- Tiwari, D.N., Loof, R., and Paudyal, G.N. (1999). Environmental-economic decision-making in lowland irrigated agriculture using mutli-criteria analysis techniques. *Agricultural Systems* 60(2), 99-112.
- Tokunaga, T.K., Brown, G.E., Pickering, I.J., Sutton, S.R., and Bajt, S. (1997). Selenium Redox Reactions and Transport between Poned Waters and Sediments. *Environmental Science and Technology* 31, 1419-1425.
- Toledo, R., Engler, A., and Ahumada, V. (2010). Evaluation of Risk Factors in Agriculture: An Application of the Analytic Hierarchy Process (AHP) Methodology. *Chilean Journal of Agricultural Research* 71(1), 114-121.
- Triola, Mario F. (2006). *Elementary Statistics*. Reading, MA: Pearson/Addison-Wesley.
- Tong, S.T.Y. and Naramngam, S. (2007). Modeling the impacts of farming practices on water quality in the Little Miami River Basin. *Journal of Environmental Management* 39, 853-866.
- United States Census Bureau / American FactFinder (2014). Occupation by Sex and Median Earnings. U.S. Census Bureau American Community Survey, Web. 24 September 2016.
- Vaché, K.B., Eilers, J.M., and Santelmann, M.V. (2002). Water quality modeling of alternative agricultural scenarios in the US, corn belt. *Journal of the American Water Resources Association* 38(3) (2002), 773.
- Van Derveer, W.D. and Canton, S.P. (1997). Selenium sediment toxicity thresholds and derivation of water quality criteria for freshwater biota of western streams. *Journal of Environmental Toxicology and Chemistry* 16(6), 1260-1268.
- Van Raij, B., Quaggio, J.A., and Da Silva, N.M. (1986). Extraction of phosphorous, potassium, calcium, and magnesium from soils by an ion-exchange resin procedure. *Communications in Soil and Plant Analysis* 17(5), 547-566.
- Voros, L. and Padisak, J. (1991). Phytoplankton biomass and chlorophyll-*a* in some shallow lakes in central Europe. *Hydrobiologia* 215, 111-119.
- Weres, O., Bowman, H.R., Goldstein, A., Smith, E.C., Tsao, L., and Harnden, W. (1990). The effect of nitrate and organic matter upon mobility of selenium in groundwater and in a water treatment process. *Journal of Water, Air, and Soil Pollution* 49, 251-272.
- White, A.F., Benson, S.M., Yee, A.W., Wollenberg, H.A. Jr., and Flexser, S. (1991). Groundwater contamination at the Kesterson Reservoir, California: geochemical parameters influencing selenium mobility. *Journal of Water Resources Research* 27, 1085-1098.
- Whitehead, P.G., William, R.J., and Lewis, D.R. (1997). Quality simulation along river system (QUASAR): model theory and development. *Journal of The Science of the Total Environment* 194/195, 447-456.

- Ying, X., Guang-Ming, Z., Gui-Qiu, C., Lin, T., Ke-Lin, W., and Dao-You, H. (2007). Combining AHP with GIS in synthetic evaluation of eco-environment quality- A case study of Hunan Province, China. *Ecological Modelling* 209, 97-109.
- Yong, Y.W., Dahab, M.F., and Bogardi, I. (1994). Fuzzy Decision Making in Ground Water Nitrate Risk Management. *Water Resources Bulletin, American Water Resources Association* 30(1). 135-148.
- Zielinski, R. A., S. Asher-Bolinder, and A.L. Meier. (1995). Uraniferous waters of the Arkansas River Valley, Colorado, USA – A function of geology and land-use. *Applied Geochemistry* 10: 133 – 144.
- Zielinski, R.A., S. Asher-Bolinder, A.L. Meier, C.A. Johnson, and B.J. Szabo. (1997). Natural or fertilizer-derived uranium in irrigation drainage: a case study in southeastern Colorado, U.S.A. *Applied Geochemistry* 12: 9-21.
- Zhang, Y. and Moore, J.N. (1997). Reduction potential of selenate in wetland sediment. *Journal of Environmental Quality* 26, 910-916.
- Zhang, D.Q., Tan, S.K., Gersberg, R.M., Zhu, J., Sadreddini, S., and Li, Y. (2012). Nutrient removal in tropical subsurface flow constructed wetlands under batch and continuous flow conditions. *Journal of environmental management* 96(1), 1-6.
- Zuo, K.H., Tuncali, K., and Silverman, S.G. (2003). Correlation and simple linear regression 1. *Radiology* 227(3), 617-628.